"DESIGN AND DEVELOPMENT OF RECONFIGURABLE PLASMA ANTENNA"

A Thesis Submitted in fulfilment of the requirement for the award of the degree of

DOCTOR OF PHILOSOPHY

In

Electronics and Communication Engineering

Submitted by:

GURKIRANDEEP KAUR KAMBOJ
Reg. No: 901706009

Under the supervision of:

Dr. Rana Pratap Yadav
Scientist, IPR, Gandhinagar

Dr. Rajinder Singh Kaler (Co-Guide)
Senior Professor, EIED, TIET, Patiala

ELECTRONICS AND COMMUNICATION ENGINEERING DEPARTMENT
THAPAR INSTITUTE OF ENGINEERING AND TECHNOLOGY (TIET)
PATIALA – 147004 (PUNJAB)

November, 2023

DECLARATION

I, **Gurkirandeep Kaur Kamboj** hereby declare that the work contained in the thesis entitled **"Design and Development of Reconfigurable Plasma Antenna"** in fulfillment of the requirement for the award of degree **"Doctor of Philosophy"** submitted at **Department of Electronics and Communication Engineering, Thapar Institute of Engineering and Technology (TIET), Patiala**, is an authentic record of research work carried out under the supervision of **Dr. Rana Pratap Yadav, Thapar Institute of Engineering and Technology (Past Affiliation)** and **Dr. Rajinder Singh Kaler, Professor, Thapar Institute of Engineering and Technology**. The matter presented in this thesis does not incorporate any material previously published or written by any other person except where due references are made in the text. The results obtained in this thesis have not been submitted in part or full to any other institute or university for the award of degree or diploma.

Gurkirandeep Kaur

Place: CANADA
Date: 2/11/2023

Gurkirandeep Kaur Kamboj
Reg. No 901706009
TIET, Patiala

THESIS CERTIFICATE

This is to certify that the work contained in the thesis entitled "**Design and Development of Reconfigurable Plasma Anetnna**" submitted by **Gurkirandeep Kaur Kamboj (Reg. No. 901706009)** to the **Thapar Institute of Engineering and Technology (TIET), Patiala**, for the award of the degree of **Doctor of Philosophy**, is a bona fide record of the research work done by her under our supervision.The contents of this thesis, in full or in parts, have not been submitted to any other Institute or University for the award of any degree or diploma.

Dr. Rana Pratap Yadav

Dr. Rana Pratap Yadav
Current Affiliation:
Assistant Professor, Homi Bhabha National Institute (HBNI), Mumbai
Scientist officer, Institute for Plasma Research (IPR), Gandhinagar
Past Affiliation:
Thapar Institute of Engineering and Technology, Patiala

Place: GANDHINAGAR
Date: 2/11/2023

Dr. Rajinder Singh Kaler
Professor
Thapar Institute of Engineering and Technology (TIET)
Patiala

Place: PATIALA
Date: 2/11/2023

ACKNOWLEDGEMENTS

This thesis is the culmination of my journey of Ph.D., which was just like climbing a high peak step by step accompanied by encouragement, hardship, trust, and hard work. When I found myself at top experiencing the feeling of fulfillment, I realized though only my name appears on the cover of this dissertation, many people have contributed to accomplishing this huge task. First and foremost, I bow my head humbly in front of Shri Guru Granth Sahib Ji (BABA Ji) for making me capable of completing my Ph.D. Thesis; only with His blessings, I have accomplished this huge task. I could have never done this without his blessings.

I owe a deep debt of gratitude to my institute 'Thapar Institute of Engineering and Technology (TIET), Patiala for giving me an opportunity to complete this work. I would also like to thanks to the Department of Science and Engineering Research Board (SERB), Department of Science and Technology (DST), Government of India and Council of Scientific and Industrial Research (CSIR), Ministry of Science and Technology, Government of India for providing funding support to achieve my research objectives.

I would like to express my sincere gratitude to my thesis supervisors Dr. Rana Pratap Yadav (supervisor) and Dr. Rajinder Singh Kaler (co-supervisor), for their excellent guidance, help and the time they spent throughout my period of association with them. Dr. Rana always encouraged me for everything. He has helped me at each and every point of my research work with patience and enthusiasm. The discussion at every step felt very energetic and full of energy. He ensures that the fire keeps burning, and being there at times when I required motivation and propelling me on the course of this thesis. The positive attitude I learned from him will remain with me forever. I thank him for everything he did for me to make my Ph.D. a success. Again, I want to thank my co-supervisior, Dr. Rajinder Singh Kaler for giving me the right guidance to achieve my objectives and complete my thesis.

I am extremely thankful to my head of department Dr. Alpana Agarwal, for encouraging me throughout my research work. I also thank Dr. O. P. Pandey, Dr. Rajesh Khanna, and Dr. Amanpreet Kaur, being on my Ph.D. committee. Their suggestions and comments have helped me in bringing this thesis to the present shape.

I would like to especially thank my lab colleagues and friends Mr. Abhinav Jain and Mrs. Deepika Singh, for supporting me and helping me in different stages of work. I have learned a lot from them. Also, I would like to thank Ms. Diksha Hooda for being friendly and helpful towards me on various occasions.

My acknowledgement would be incomplete without thanking the biggest source of my strength, my family. I would like to thank my family for standing by me through all the joys and sorrows that life had to offer. Firstly, I would like to thank my better half Mr. Kaminder Singh Brar for having believe in me and supporting me to achieve this task. My heartfelt thanks and life-long gratitude go to my parents Mr. Iqbal Singh and Mrs. Davinder Kaur, who have raised me and wanted me to study more and more and do best in life. They made things seem a lot easier than they were, with their tireless support. A very special thanks to my elder brothers Mr. Gursimarjeet Singh and his wife Mrs. Harsimranjeet Kaur (sister-in-law), my loving nieces Miss. Prabhkirandeep Kaur and Miss. Japleenjot Kaur, and younger brother Mr. Amandeep singh and his wife Mrs. Manmeet Kaur (sister-in-law) for their continuous love, support, and encouragement throughout.

No research is possible without the Library, I take this time to express my gratitude to all the library staff for their services and special thanks to Dr. Shri Ram, who has helped me in solving different issues regarding the Ph.D. thesis work. I would also like to thank Thapar Administration, non-teaching staff of the ECED department, for their kind help. I am grateful to the different authors of the Literature I have gone through, without which it would have been impossible for me to carry out this exciting research. I have tried to express my gratitude to every person who contributed to this work directly or indirectly, there may still be someone hiding behind the veils of my forgetful part of memory.

Last but not the least; I would like to thank all such great souls.

Gurkirandeep Kaur Kamboj
Thapar Institute of Engineering and Technology,
Patiala

ABSTRACT

In this thesis, plasma based reconfigurable antenna and photonic crystal device have been investigated. The first half mainly focused on the design and development of plasma antenna whereas the developed of plasma photonic crystal is presented in second half of the thesis. The research work has been accomplished in many stages which are briefed as follow;

Plasma antenna has been developed and investigated for the analysis of its radiation characteristics for variable plasma properties and operating frequencies. In research work, $30cm$ long plasma column antenna has been experimentally developed at gas pressure, $P_r = 0.030mbar$ and RF power, $P_0 = 60Watts$. The setup is modelled based on the extracted data and simulated for the analysis of resonant frequencies at plasma density $(n_e) = 2.7\times10^{16}m^{-3}$. The radiation patterns at resonant frequencies $112MHz$, $347MHz$ and $409MHz$ have been investigated experimentally which are found in good agreement with simulation outcomes. The study explores that the radiation patterns show significant change for plasma properties which are the function of gas pressure and power and are more similar like a monopolar radiation pattern. The ability to reconfigure the plasma properties electronically provides an option to online control the radiation characteristics of antenna as per the requirement.

Further, an antenna array has been developed by using the classical state of plasma called plasma blobs or striations. This state of plasma inside a column is formed by having critical combination of input parameters where its arrangement is called as collinear array and each blob act as a radiating element. In our experiment, 4 to 6 plasma blobs or striations are formed in $30cm$ long column for gas pressure $P_r = 0.015 - 0.030mbar$ and power $P_0 = 40 - 80Watts$. Based on the experimental data, the modelling and simulations of two plasma based collinear antenna array having 4 and 5 plasma blobs have been done respectively. The resonant frequencies at 4 and 5 plasma blobs based antenna array having plasma densities, $n_e = 2.47 \times 10^{16}m^{-3}$ and $5.85 \times 10^{16}m^{-3}$ have been investigated. The radiation characteristics at resonant frequencies $56MHz, 73MHz, 178MHz$ and $390MHz$ have been experimentally investigated which verify the simulated outcomes. The study explores that the plasma blobs or striations behaving as an antenna array which improves the radiation characteristics in terms of directivity, intensity and beamwidth of radiation in comparison with continues plasma column antenna.

In second half, a reconfigurable one-dimensional Single Column Plasma Photonic Crystal (SC-PPC) has been modelled and investigated its Photonic Bandgaps (PBG). The SC-PPC is a novel structure which is simulated for the first time. In our research, SC-PPC is a glass column containing 6 stationary Standing Plasma Density Patterns (SPDP) called plasma

blobs created at $P_r = 0.035mbar$ and $P_0 = 60Watts$, where its density varies sinusoidally along the column axis. The plasma density of blobs is measured by using the interferomtry setup. The modelling and simulation of SC-PPC is done for the analysis of PBG at variable plasma density ($n_e = 1 \times 10^{16}m^{-3}$, $5 \times 10^{16}m^{-3}$ and $9 \times 10^{16}m^{-3}$), shape and size of blobs etc. The simulation results have been investigated which verifies the reconfigurability of SC-PPC. The additional features of SC-PPC over conventional Plasma Photonic Crystal (PPC) are its small in size, tunable lattice constant, and simple structure that can enable wide application scope in various fields ranging from communication to defence.

Further, a two dimensional reconfigurable photonic bandgap structure using low-pressure fluorescent tubes has been developed. The model consists of square lattice of 3×3 tubes (60cm long) array placed in free space. The dispersion relation of the PPC has been optimized by using mathematical modelling for the variable plasma density. Modelling of PPC incorporates the actual plasma parameters which have been extracted from the experimental setup, where the variable plasma density is created by changing the applied AC potential in the range of 100 - $240V$. The developed PPC is implemented on test bench as per the mathematical modelling outcomes and tested using VNA (Vector Network Analyzer) for investigation of photonic bandgaps in the range of 3 - $7GHz$ for different plasma densities ranging from $0.4 \times 10^{17}m^3$ - $5.3 \times 10^{17}m^3$. The main objective of the work is to conceptualize a reliable plasma-based structure for the development of microwave reflectors, filters, absorbers etc. which can have important applications in the field of radar, satellite and navigation.

LIST OF PAPERS BASED ON THESIS

JOURNAL

P1. G. K. Kamboj, R. P. Yadav and R. S. Kaler, "Development of Reconfigurable Plasma Column Antenna," *IEEE Transactions on Plasma Science*, vol. 49, no. 2, pp. no. 656-662, Feb. 2021.
Doi: 10.1109/TPS.2020.3046615.

P2. G. K. Kamboj, R. P. Yadav and R. S. Kaler, "A Single Column Plasma Photonic Crystal (SC-PPC)," *AIP Physics of Plasmas,* vol. no. 28, pp. no. 053509-(1-8), May 2021.
Doi: 10.1063/5.0030425.

CONFERENCE

P3. G. K. Kamboj, R. P. Yadav, A. Jain and R. S. Kaler, "Design and Development of Capacitively Coupled Plasma Monopole Antenna," 2019 IEEE Canadian Conference of Electrical and Computer Engineering (CCECE), pp. no. 1-4, 2019.
Doi: 10.1109/CCECE.2019.8861549.

ABBREVIATIONS

PA	Plasma Antenna
PC	Photonic Crystal
PPC	Plasma Photonic Crystal
SC-PPC	Single Column Plasma Photonic Crystal
SPDP	Standing Plasma Density Pattern
PBG	Photonic Bandgap
CST	Computer Simulation Technology
MATLAB	MATrix LABoratory
RCS	Radar Cross Section
SW	Surface Wave
PTP	Plasma Transmission Probe
VSWR	Voltage Standing Wave Ratio
AC	Alternating Current
RF	Radio Frequency
NF-FF	Near-Field-Far Field
FDTD	Finite Difference Time Domain
FEM	Finite Element Method
VHF	Very High Frequency
EM	Electromagnetic
VNA	Vector Network Analyser
PVS	Plasma Vacuum System
SWD	Surface Wave Discharge
PEC	Perfect Electric Conductor
OSP	Oscillating Standing Potential
BWFN	First Null Beamwidth
HPBW	Half Null Beamwidth
TMM	Transfer Matrix Method

NOTATIONS

E	Electric Field
H	Magnetic Field
v	Velocity
q	Charge of electron
m_e	Mass of electron
ϵ_0	Permittivity of free space
μ_0	Permeability of free space
J_E	Current density
ρ	Charge density
f	Frequency
f_c	Cut off frequency
σ	Conductivity
ω	Angular frequency
n_e	Plasma density
v_c	Electron neutral collision frequency
ω_p	Plasma angular frequency
σ_p	Conductivity of plasma
ϵ_p	Permittivity of plasma
μ_p	Permeability of plasma
$\alpha(z)$	Attenuation coefficient
$P(z)$	Power flux
a	Inner radius of the tube
r	Radius of the tube
θ	Energy term
μ_b	Bohm velocity
A_{eff}	Effective surface area
ζ_l	Energy loss per electron pair
n_{res}	Characteristics number density
ϵ_g	Dielectric constant of glass tube
P_r	Gas Pressure
P_0	Power value
h_t	Column height
L_0	Characteristics length
β	Propagation constant
k_0	Free space factor
c	Speed of light
G_L	Glass tube length
G_T	Glass tube thickness
P_L	Plasma length
P_D	Plasma diameter

S_H	Sleeve height
S_T	Sleeve thickness
G_{PH}	Ground plate height
G_{PR}	Ground plate radius
R	Far-field region
L	Lenght of antenna
h_b	Height of blob
n_z	Number of blobs
d	Spacing between blobs
ζ_M	Energy by collision
u	Kinetic energy
λ_e	Distance between two successive collisions
n_n	Neutral or atom density
D	Diffusion coefficient
γn_e	Losses of electrons to the side walls
ξn_e	Losses of atoms to the side walls
χn_e^2	Recombination collision between ions and electrons
ηn_n^2	Collision between two atoms
μ	Bifurcation parameter
E_T	Total electric field
φ	Phase difference
ϕ	Progressive phase difference
λ	Wavelength
D_r	Direction of radiation
d_a	Thickness of dielectric layer
d_b	Thickness of plasma layer
Δ	Lattice constant
ϵ_d	Permittivity of dielectric
k	Propagation constant in plasma
W_L	Waveguide length
W_D	Waveguide diameter
G_D	Glass tube inner diameter
A	Plasma blob layer width
B	Air layer width
ϵ_r	Relative permittivity
μ_r	Relative permeability
ϵ_t	permittivity of fluorescent tube
n_t	refractive index of tube
n_r	refractive index of air
k	Bloch wave

List of Tables

List of Figures

Contents

Chapter 1

INTRODUCTION

1.1 Overview

In recent years, plasma based technology is well know and has drawn much attention due to their distinct behaviour and potential advantages over the conventionally used technologies in ranging from RF to microwave applications [1]. A term plasma is a fourth state of matter which is basically a fully or partially ionised gas [9], utilized as a conducting structure in the propagation of EM waves. It is excellently demonstrated that the usage of plasma technology enable an option to electronically change the plasma properties by altering the operating parameters[2, 3]. The ability to reconfigure the physical properties of the plasma provides a wide scope in the development of reconfigurable RF/microwave devices which have innovative range of applications in the field of communication, defence, radar and satellite communication etc.[4]-[6].

In general, RF systems are frequency dependent and it need to be altered with the change of operating frequency. In development of RF/microwave components, plasma can be utilised as a conducting element in-replacement of the metal which are having fixed physical properties and rigidity to change [1, 4]. Applicability of plasma can enable RF components to be reconfigurable in terms of operating frequency and other structure parameters. Utilizing the plasma based reconfigurable components can create a possibility for the development of frequency independent RF/microwave system [7]-[11].

In this context, our thesis is mainly emphasis on the development of experimental model of reconfigurable plasma antenna and plasma photonic crystal devices by replacing the conventional metallic and dielectric mediums with the plasma structure for RF/microwave applications. Also, we demonstrate the reconfigurability of the developed plasma antenna and plasma photonic bandgap using the test setup. The thesis incorporates various investigations on the reconfigurability of the plasma antenna and plasma photonic crystal by developing the experimental setup and its testing.

In a wireless communication system, the antenna device plays a major role for the transmission and reception of electromagnetic waves [6]. Antennas are mostly found in metallic structure with a fixed operating band. Plasma antenna is mainly a plasma column which exploits the reconfigurability of plasma behaviour, shape and size and hence the radiation parameters like directivity, gain, beam angle etc. and bandwidth [26]-[30]. Likewise, the plasma antenna, photonic bandgap is the periodic structure of plasma media and air where

its characteristics can also be reconfigured with the help of changing plasma properties [62]-[68]. Photonic bandgaps are mainly used as a reflector, filter, absorber etc. in real manners. Although, plasma-based devices have a very complicated structure, its application is always in demand in the area of underwater communication, radar, visible light communication systems etc. [74]-[80]

This chapter explores the comprehensive literature review, starting with the concept of plasma fundamental theory. Further, the literature survey is focused on the latest research carried out in the direction of the development of reconfigurable plasma based antenna and photonic crystal devices but still there exist many gaps which have been identified during the literature survey that are presented in next chapter. The literature survey also includes the previous study based on the design and development of the plasma antenna and plasma photonic crystal devices.

1.2 Fundamentals of Plasma

The plasma is the state of matter where its existence was first discovered by Sir William Crookes in 1879 [8]-[10]. In these state, molecules of solid become more energetic due to the rise in temperature and change its state from solid to plasma which is shown in Fig. 1.1. Basically, plasma is an ionised gas containing positive and negative charged particles whose collectively effect is neutral[34]-[35]. It consists free charge carriers where the interaction of particles in plasma is governed by the laws of electromagnetism and thermodynamics.

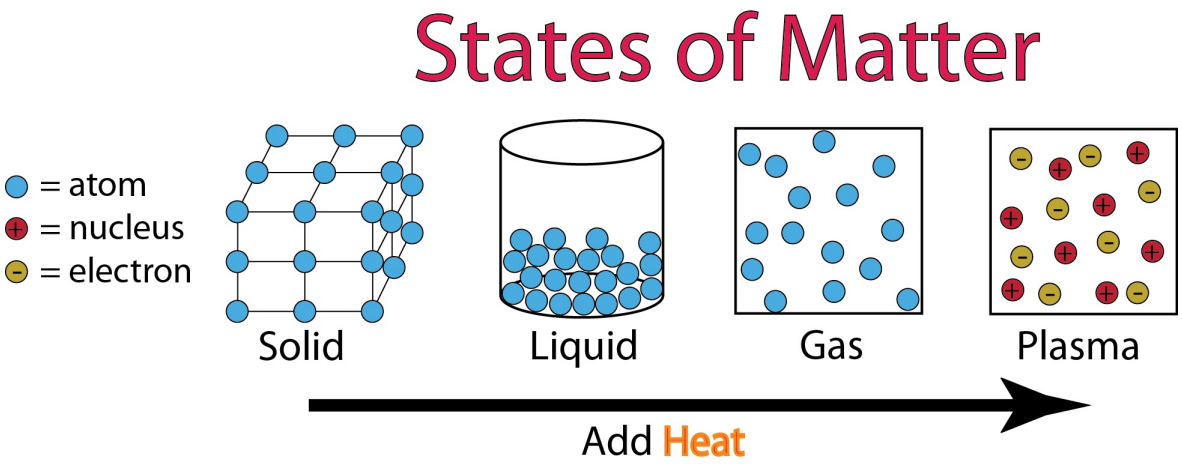

Figure 1.1: Changes of state of matters [60]

The plasma is a Debye dispersive material [11]. It presents some physical properties like plasma conductivity, plasma permittivity, and plasma permeability [18, 21]. The plasma is represented by Drude model which is defined with two main plasma properties i.e. plasma angular frequency and electron-neutral collision frequency [4, 24, 25].

1.2.1 Plasma Conductivity

To obtain the conductivity, let's consider an electron with a charge q and moving with velocity v through an electric E and magnetic fields B, the Lorentz force [22, 60] is expressed as

$$m_e \frac{dv}{dt} = q(E + v \times B) \tag{1.1}$$

where m_e is the mass of electron. In general, the E and B fields are considered as a time varying factor in the free space by $e^{j\omega t}$. Assuming a plane wave is incident on tube where electric field E is in the x-direction and magnetic field B is in the y-direction. Thus, the electric and magnetic fields can be written as [43]

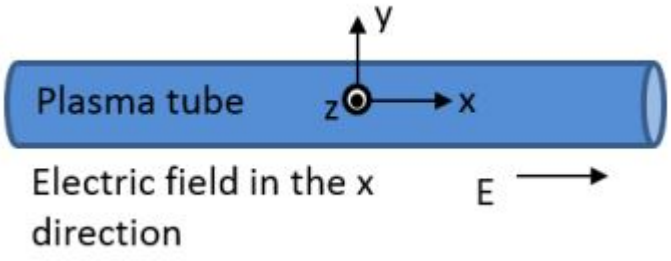

Figure 1.2: E field direction in the plasma [60]

$$E = E_0 e^{j\omega t} a_x \tag{1.2}$$

$$B = B_0 e^{j\omega t} a_y = E_0 c e^{j\omega t} a_y \tag{1.3}$$

where c is the speed of light. By putting the value of E and B in eq. 1.1 and differentiate in Cartesian coordinates and analyse velocity and displacement in x-direction. Assuming the electric current is produced by all the charged particles where the current density vector [41] is written as:

$$J_E = q n_e v a_x \tag{1.4}$$

where $v = \frac{dx}{dt} = \frac{q}{m_e} E_0 \frac{1}{j\omega} e^{j\omega t}$ is the velocity. By putting the value in eq. 1.4 it becomes,

$$J_E = q n_e \left[\frac{q}{m_e} E_0 \frac{1}{j\omega} e^{j\omega t} \right] a_x \tag{1.5}$$

where $J_E = \sigma E$, the conductivity can be formulated as:

$$\sigma E_0 e^{j\omega t} = q n_e \left[\frac{q}{m_e} E_0 \frac{1}{j\omega} e^{j\omega t} \right] \tag{1.6}$$

$$\sigma_p = \sigma = \frac{j n_e q^2}{\omega m_e} \tag{1.7}$$

where term σ_p is the plasma conductivity which is the function of ω, n_e is plasma density, m_e is mass of electron.

1.2.2 Plasma Angular Frequency

Due to the harmonic oscillations of the electrons around the ions, we can assume that the electron density oscillates at the plasma frequency ω_p where the electric field intensity also oscillate at the same plasma frequency [19, 20]. The density of oscillations increases the total charge density ρ which is depends on the volume of current density J. The continuity equation is written as:

$$\nabla.J = -\frac{d\rho}{dt} \tag{1.8}$$

$$\nabla.(\sigma E) = \sigma(\nabla.E) = -\frac{d\rho}{dt} \tag{1.9}$$

$$\frac{jn_eq^2\rho}{\omega_p m_e \epsilon_0} = \frac{d\rho}{dt} \tag{1.10}$$

The plasma angular frequency of oscillation of the free charge density ρ is also ω_p, thus we obtain:

$$\omega_p = \sqrt{\frac{n_eq^2}{m_e\epsilon_0}} \tag{1.11}$$

1.2.3 Plasma Permittivity

Since the plasma is a Debye dispersive medium [28, 32] having complex permittivity which can be calculated by using the conductivity term mentioned in eq. 1.7

$$\nabla \times H = (j\omega\epsilon_0 + \sigma)E \tag{1.12}$$

$$\nabla \times H = j\omega\epsilon_0(1 + \frac{\sigma}{j\omega\epsilon_0})E \tag{1.13}$$

By substituting the conductivity in above eq. 1.12-1.13, the equation becomes,

$$j\omega\epsilon_0(1 - \frac{jn_eq^2}{\omega^2\epsilon_0 m_e})E \tag{1.14}$$

Then, the relative permittivity without collision ($v_m = 0$) is

$$\epsilon_p = (1 - \frac{jn_eq^2}{\omega^2\epsilon_0 m_e}) = (1 - \frac{\omega_p^2}{\omega^2}) \tag{1.15}$$

The plasma frequency is noted by f_p, equal to $\omega_p/2\pi$ and its unit is Hz.

1.3 Plasma Antenna

A plasma antenna is a kind of RF antenna which utilizes plasma element as a conducting element for guiding electromagnetic waves instead of a solid metal conductor that are used in the fundamental metallic antenna [40]-[50]. Basically, plasma is a ionised gas which contains equal numbers of positive and negative charged particles whose collective effect is neutral [8]-[12]. A fully ionized plasma is considered as a good conductor where it can be serve as a transmission line for the guiding of EM waves or as an antenna surface for the radiation [13]-[17]. A common way to develop such antennas is by creating a plasma inside the glass tube by different discharge methods such as RF heating, DC Discharge, microwave signal, fiber optics and laser etc. [53]-[59]. This plasma column structure behaves as a radiating element which permits the electromagnetic waves to radiate in free space. For antenna applications, plasma based antenna can be efficient and have low noise which makes them useful for narrow band high frequency and very high-frequency communications [5, 61].

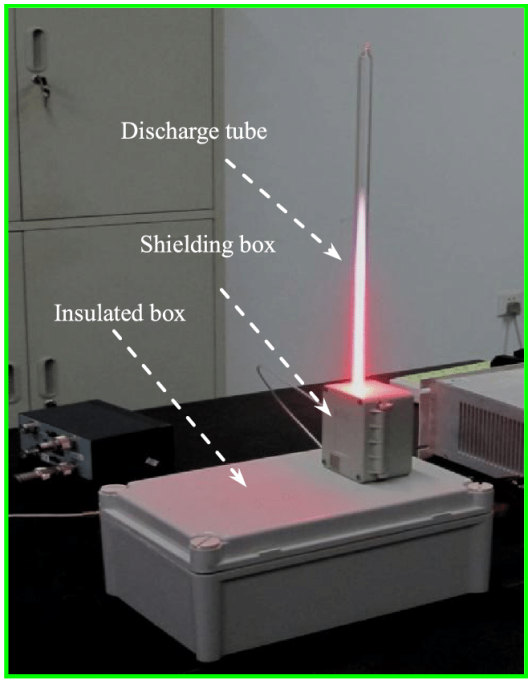

Figure 1.3: Plasma column antenna [19]

1.3.1 Unique Characteristics

Plasma antenna has distinct behaviour which leads to innovative ranges of applications with respect to the conventional antenna technologies. In plasma antenna, plasma element is

created by ionization process and have material properties composed of density and conductivity. These plasma parameters enable antenna to behave differently from metal antenna system and provide numerous key features as listed below:

Stealth behavior: Plasma antenna has the ability to transmit when gas is electrified and become stealth when no excitation is provided to gas for further ionization process. When the antenna is off, no plasma is formed inside tube where it is a transparent tube and act as non-conducting material. When gas is energised, plasma is formed which acts as conducting medium for the applied RF signal [47]-[50]. Therefore, based on the gas ionisation process antenna can be turn on and off electrically instead of mechanically. This property to make antenna stealth has reduced its interference with other nearby antennas which can be helpful in the field of defence [14, 17].

Electrically reconfigurable: Plasma antenna is formed by plasma column which is composed of dielectric properties i.e. plasma permittivity and conductivity. These plasma parameters can be dynamically reconfigurable by altering value of input parameters of the system [16, 40]. With the changing of plasma material parameters, the physical structure of antenna can be electrically reconfigured instead of a mechanical control method that required for the metallic antenna. The findings show that a plasma monopole can be modified and used as a single structure to trans-receive signal at multiple frequencies by changing the plasma parameters such as working pressure, input RF power, discharge tube dimensions, operating frequency etc. [53]-[57]. Therefore, by reconfiguring the plasma properties desired radiation characteristics can be achieved in a single monopole. This property can be utilised to online control the radiation characteristics and antenna performance as per desired [61].

1.4 Plasma Photonic Crystal

Photonic Crystals (PCs) are the devices which have been extensively studied in recent years due to their important applications in the various fields ranging from communication to defence. It has an excellent ability to control the propagation of electromagnetic waves into the dielectric medium [63]-[69]. In general, PCs are the periodic structure of the dielectric materials that produce a range of forbidden frequencies called Photonic Bandgaps (PBGs). The PBG is depending upon the physical properties of the materials, lattice constant, angle of incidence etc [70]-[76]. Due to the fixed physical structure in the conventional PCs, the photonic bandgap is untunable which limits its applicability in the field where tunable bandgaps are required.

In recent years, plasma photonic crystal (PPCs) has drawn much attention due to the numerous advantages over conventional PCs. A PPC is the structure with the periodic arrangement of plasma and dielectric medium of specified thickness [77]-[80]. The schematic

of $1D$ and $2D$ PPC is shown in Fig. 1.4 and 1.5. Plasma is the medium which physical properties like permittivity, conductivity, permeability etc. can be controlled with the plasma parameters such as plasma frequency, plasma density, conductivity, and collision frequency [81]-[85]. This property provides an option to reconfigure the PBG electronically by changing the plasma parameters as per the desired[91]-[94].

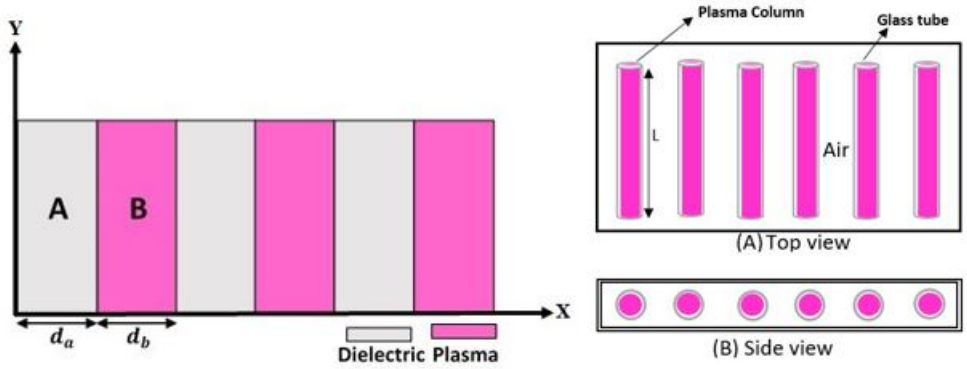

Figure 1.4: 1D plasma photonic crystal

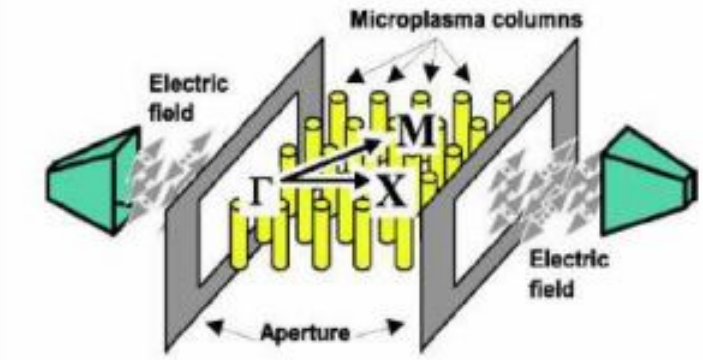

Figure 1.5: 2D plasma photonic crystal [85]

1.5 Literature Survey

To start any project, a detailed research has been done on the plasma based technology to get the knowledge of the remarkable finding that has been already investigated. This section gives overviews based on theoretical and experimental studies related to plasma based antenna and photonic crystal.

1.5.1 Background of Plasma Antenna

Kumar et al. [1]: experiments are carried out for generation of plasma columns that are excited with a surface wave and analyze their field properties i.e., Current distributions along the column, radiated field and power patterns, directivity and also antenna efficiency are investigated. Further, a copper antenna is designed as a reference model where prospective comparison of simulated result with plasma antenna is presented. From experimental results, it is observed that the harmonics components in power content of the plasma antenna show prominent behavior as a reference antenna where only fundamental frequency components exist. However, a bi- spectral analysis is done to give a clear understanding of non-linear interactions in power patterns. The study also explores the radiation pattern of both antennae found similarly. In this, some specific characteristics of the antenna are evaluated that enhance the performance level of the antenna that can be useful in RF-based applications.

Rayner et al. [3]: Experimental design of plasma column antenna filled with argon gas driven by a surface wave generated at 500 MHz and taking gas pressures in the range of 0.03 mb - 0.5 mb. Result outcomes reveal that the increase in antenna's length with an increase of applied power whereas plasma density decreases linearly. In addition to this, noise obtained from plasma is found to be in the range of 10 MHz - 250 MHz which is sufficiently low. Observations from the radiation pattern show linear changes in conductivity and resistance of the plasma which reduces the depth of nulls and consequently increases observed in beam-width of the major lobe.

Ja'afar et al. [4]: Design and development of plasma monopole antenna are done by taking antenna dimension given as L=150mm, r=5.2mm length and radius of plasma column respectively at frequency range 550MHz -600MHz and then taken an aluminum ground plane of radius 40mm. In this project, simulation of the antenna is performed using computer simulation technology (CST) Microwave Studio. Based on this software simulation of the antenna is done to evaluate its performance in terms of average gain, bandwidth, radiation pattern and return losses. Whereas from these observations study shows that plasma antenna has similar characteristics as an equivalent model of metal antenna.

Ja'afar et al. [7]: numerically and experimentally simulate a monopole antenna structure consisting of 12 adjacent fluorescent tubes which involve the combination of argon gas and mercury vapor. These tubes are further electrified and create a plasma inside tubes which acts as a radiating element. In this report, numerical simulation and experimental outcomes in terms of gain, radiation characteristics and S- parameter. are investigated at operating frequency of 4.9 GHz. Findings reveal that plasma monopole antenna are pointed in different three beam shapes i.e. 0°, 90°, and 180° where it can be electrically switchable and provides better gain as 6.691dB which is higher than metallic antenna i.e. is generally 2-3dB. The study explores good agreement in both simulated and experimental outcomes.

Sadeghikia et al. [13]: broadband characteristics can be obtained by increasing the diameter of the plasma tube whereas the depth of minor lobes can also be diminishing as diameter increases. Further study reveals that with a decrease in collision frequency the gain and radar cross-section of the antenna can be increased. To widen the BW there is need to decrease the L/r ratio, where L is the length of plasma antenna and r is the radius of tube i.e. by increasing the radius, BW will increase. Impedance variation becomes less sensitive as a function of frequency as L/r decreases. The plasma conductivity decreases and RCS also reduces with an increase in collision frequency that affects all the characteristics of plasma antennas.

Borg et al. [14]: focused on plasma columns driven by surface waves used as Radio frequency antennas which lead to better noise performance and low radar cross section to be useful for broadcast communications. Experimental setup is created to generate a plasma column inside a tube of length 2430 mm and 38 mm diameter respectively which is driven at 30 MHz operating frequency. Analysis of antenna parameters can be done in terms of current distribution, efficiency and radiation pattern.

Cerri et al. [16]: design a self-consistent model of plasma column antenna fed by the single electrode to evaluate its efficiency and conductivity in plasma. Basically, a new methodological approach is derived to characterize its physical behavior. The plasma antenna's efficiency is found comparable and efficient as a metallic antenna. Whereas results finding reveal that conductivity of plasma is dependent on different antenna properties that affect the antenna losses characteristics and is an important key to establish effective length of plasma column. For conductivity measurements, the experimental model is set up where the plasma column is covered with the waveguide and changes the characteristics of dielectric; reflection coefficient is calculated which is dependent on the conductivity of an inserted portion of the tube in the waveguide. Analysis of S11 parameter gives behavior of reflection coefficient where the dielectric medium i.e. plasma behaves like a lossy metal and used as good conducting material for many antenna applications when sigma is observed to be greater than 100 S/m.

Halili et al. [18]: experimentally fabricated three types of plasma antenna that are containing three different noble gases listed as xenon, neon, and argon with 1 Torr gas pressure by using RF heating technique for ionizing the gas. Here, the performance of every plasma antenna has been calculated to investigate the antenna characteristics in terms of return losses. From design measurements, findings indicate that all noble gases yield return losses below -10dB in the frequency range 3.5GHz - 5.5 GHz which is better than the antenna without formation of plasma in all cases and observed that improvement of 2 to 8 dB is obtained whereas neon gas yield a significant shift of 200MHz in the optimum frequency from original value while measured with plasma state.

Zheng et al. [19]: experimentally designed, developed and fabricated a fluorescent

loop plasma antenna driven by a 220 W A.C power source and RF source. For reference, the metallic antenna was also simulated. Analysis of radiated field, VSWRs and average gains of designed three plasma antennas has been evaluated and compared these results to metal conducting elements that are considered as reference antennas. Findings reveal that the obtained gains from these two designed plasma antennas are observed 6.0dB and 6.7dB decreased in case of antenna driven by AC and RF power source respectively instead of the metal-based antenna.

Zhou et al. [20]: investigate the radiation characteristic of the plasma antenna finite difference time domain technique under two dimensions. Using the FDTD method, initially, the propagation of electromagnetic waves in free space in stretched coordinates is studied and derived update equations from modified Maxwell equations. In advance, propagation of electromagnetic waves in plasma is also studied by using Boltzmann-Maxwell theory. The near-field-far field (NF-FF) transformation is used to obtain radiation characteristics. Whereas results show the influence of electron density on radiation patterns that can change significantly with the variation of the degree of ionization.

Lee et al. [11]: presents the full-wave electromagnetic analysis of simple plasma monopole antenna configurations by using 3-D FDTD algorithm to demonstrate some of their characteristics and evaluates the radiated power, antenna pattern, field distribution, antenna impedance and efficiency of the plasma column antenna using numerical approximation technique. Finding demonstrates that the plasma antenna is found to be efficient and have similar characteristics to conventionally used RF antenna. Furthermore, variation in plasma characteristics provides dynamic reconfiguration in the radiation pattern of the antenna.

Qian et al. [21]: In this, Frequency-dependent FDTD method is used for analyzing return loss characteristics of the rectangular whip antenna. The resonant frequency of the plasma whip antenna is computed for different antenna's length found that frequency 5624 decreases from 1.3 to 1.1 6GHz at L=160mm and resonant frequency increases to 1.3GHz at L=134mm. The further study explores that the effective length and operating frequency of the whip antenna can be adjusted as per requirement by changing the plasma density.

Chao et al. [22]: describes the simulation and analyses a 0.4-m-long plasma column antenna by adopting cylindrical-coordinate FDTD algorithm. The radiation efficiency and input impedance of plasma-based antennas are computed at frequency range 75MHz - 400MHz. Some specific characteristics of the antenna are investigated where plasma antennas behave similarly as of a metallic antenna. When the ratio of f/f_p is observed low then a resonant behavior is obtained in antenna impedance. Whereas, plasma parameters like plasma frequency (f_p) and collision frequency (v_c) is dynamically altered to obtain the reconfigurable radiation pattern of the antenna. Furthemore, changes of collision frequency and ion density produce significant effects on the radiation efficiency of the antenna.

Luo et al. [23]: presented FDTD simulation of a simple cylinder plasma monopole antenna of dimension 300mm as length and 4mm as the radius of the antenna. For the FDTD method, the near-field far-field transformation is used to compute the radiated electric and magnetic field of the plasma monopole antenna in the far-field zone. Further, the pattern is reconfiguring for the variable dielectric permittivity and sinusoidal signal frequency. From simulation results, observed that radiation intensity of antenna is a function of the permittivity of the dielectric medium where the radiation intensity increases as the value of dielectric permittivity increases and reaches to a maximum value when permittivity is equal to 4.5. Afterward, the radiation intensity decreases as the still value of permittivity rises. Whereas, at permittivity reaches a value equal to 7 the magnitude of ration intensity goes to broaden. Later on, the radiation is investigated for variable operating frequency ranging from 50-500 MHz by taking other parameters constant throughout the analysis i.e. permittivity = 4.5, plasma frequency = 20GHz, collision frequency = 10GHz.

Zali et al. [24]: proposed a monopole plasma antenna with a parabolic reflector of cylindrical dimension located at the back section of the antenna to reflect the focused signal that is received from the transmitter and then sent back for improving directivity and gain of the antenna. Plasma monopole antenna of configuration 310 mm antenna height and 12 mm of diameter respectively is placed at the center location of a parabolic reflector and studied the difference on antenna's average gain for both antennas and the performance is calculated terms involves return loss characteristics and radiated pattern throughout numerical simulations. From the result, it observed that the applicability of the reflector significantly increases the average gain ranging from 2.54 dB-7.19 dB and yield return losses below than -10dB at frequency 4.0 GHz - 4.7 GHz. This property makes the antenna acceptable for indoor wireless transmission applications.

Darvish et al. [25]: investigate a basic theory of the plasma material and then a design of a Plasma antenna at VHF band based on these theories is presented in detail. The plasma antenna simulation process can be done with help of computer-aided software i.e. CST Microwave Studio Suite. In order to validate the outcomes obtained from the designed plasma antenna, an experimental fabrication is performed to develop a proposed antenna model. Results from experimentally implemented antennas show a good agreement with the simulation results which has been obtained based on the proposed design of plasma antenna.

1.5.2 Background of Plasma Photonic Crystal

Tan et al. [63]: investigated the effect of plasma density on one dimensional PPC structure. The modelling of PPC structure involves the 5 plasma columns where its PBG has been analysed over the range of $1 - 14GHz$. The finding reveals that the bandgaps are the function of plasma properties which can be tuned by varying the parameters like as, plasma density, plasma permittivity, plasma frequency etc. The with variation in permittivity of

structure the bandgaps are shifted from lower frequency to higher frequency.

Zhang et al. [62]: investigated the transmission characteristics of $1D$ plasma photonic crystals (PPCs). The PPC structure having 5 plasma tubes has been developed initially and analysed for PBG structure over the range of microwave signal upto 14GHz. The developed setup of PPC verify the reconfiguribility of PBG for variable plasma density and lattice constant. The developed setup is further modelled and simulated for the PBG. The simulation outcomes found in good agreement with experimentally analysed PBG of 1D PPC. The study state that the structure of PPCs can be utilised as band-stop filter to control the propagation of microwave signal.

Mittal et al. [71]: presented the modelling of 1D magnetised plasma photonic crystal where the effect of extra ordinary modes of plasma on the photonic bandgaps has been investigated. The modelling of PPC is done by using TMM (Transfer Matrix Method) where the dispersion relation has been analysed for the variable plasma parameters, angle of incidence, magnetic field, structure dimensions etc. over the frequency range of $1 - 140GHz$. The study explore that due to the presence of magnetic field, trapped oscillation are introduced in PBG which can be controlled by changing the magnetic field and plasma properties.

Guo et al. [74]: presented the modelling of 1D photonic crystal doped with plasma and investigated the effect of angle of incidence on photonic bandgaps. The study stated that for smaller value of lattice constant in comparison to the incident wavelength which converted the dielectric properties of plasma into complex and plasma become an-isotropic medium. The dispersion relation of PPC is evaluated for lattice constant by using two techniques i.e. TMM and effective medium approximation. The finding shows that the lattics constant reconfigure the PBG structure.

Qi et al. [67]: investigated the Properties of EM waves with normal and oblique incidence of 1D plasma layers with sinusoidal densities. Wave transmittance as a function of wave frequency exhibits photonic band gaps characteristic of photonic crystals. In periodic photonic crystal, increasing in the collision frequency lead to greater absorption of the wave whereas the increase in the modulation factor widen the photonic bandgap width. Also increasing in incidence angle able to relocate the location of the gap. The study reveals that if defect layer is introduced by incorporating a plasma layer, a defect mode may appear within the gap whereas the collision frequency, periodic number,and modulation factor has significantly effect the magnitude of the defect mode. The incidence angle enables the frequency to be tuned. Defect layer thickness affects both frequency and number of defect modes. These results may provide theoretical guidance in designing tunable narrow-band filters.

Wang et al. [73]: developed 2D PPC structure using gaseous plasma column. The investigation of photonic bandgaps has been analysed for variable plasma density and lattice

constant. The developed model includes a array of 7×7 of plasma column placed with the lattice of $2.8cm$ in free space. The applied current to the tube which is varied to change the plasma density inside the tube and transmission parameters are analysed for potential $0 - 240V$. The study reveals that with the variation in density, PBG is shifting to higher frequency and similar fashion is observed for the lattice constant. This developed setup of PPC is considered as bandgap filter which can be useful in the field of optical communication.

Jafari et al. [70]: examined the band structures of two types of photonic crystals (PCs). The first is a one-dimensional metamaterial photonic crystal (1D MMPC) composed of double-layered units for which both layers of each unit are dielectric. The second type is a very similar one-dimensional plasma photonic crystal (1D PPC) also composed of double-layered units in which the first layer is a dielectric material but the second is a plasma layer. This study compares the band structures of the 1D MMPC with specific optical characteristics of the 1D PPC using the Fresnel coefficients method and also compares the results of this method with the results of the transfer matrix method. It is concluded that the dependency of the electric permittivity of the plasma layer on the incident field frequency causes differences in the band structures in 1DMMPC and 1DPPC for both TE and TM polarizations and their gaps reside in different frequencies

Goldstein et al. [52]: presented the study related gto the formation of plasma blob or striation inside the column. A bifurcation theory has been developed to explain the generation of blobs inside column for the critical combination of power and gas pressure value. The study stated that the plasma mode become unstable when critical value of bifurcation is increased and the generation of blobs appears.

Howlader et al. [80]: investigated the plasma density of the column by using interferometry technique. The density is evaluated from the attenuation and phase shift of the wave passing through the plasma medium which is calculated using refractive index parameters. The setup of interferometry involves the transmitting and receiving antenna close to the plasma where its transmission characteristics are analysed by VNA. This technique approximate the plasma density and collision frequency of the column which is simpler than other available options.

1.5.3 Perspective Comparison of the Advantages and Disadvantages of Existing Literature

A detailed comparison of the advantages and disadvantages of the literature review of plasma antenna and plasma photonic crystal are mentioned in below Table 1.1 and Table 1.2

Author	Advantages	Disadvantages
R. Kumar	Design and developed plasma system, Compared with conventional antenna	Complexity, Interference and Noise
Rayner	Antenna parameter exploration, Experimental setup for radiation characteristics	Narrow frequency range (10-250MHz)
Ja'afar	Simulated plasma monopole, Broadband frequency range	No experiment validation
Sadeghikia	Broadband characteristics, reduction of Minor Lobes, Gain and Radar Cross-Section, Impedance stability	Complex design and experimental challenges, Sensitivity to collision frequency
Borg	Better noise performance, Low Radar Cross-Section (RCS), Experimental setup	Limited frequency range
Cerri	Efficiency comparable to metallic antenna, Experimental model for conductivity measurements, Dielectric characterization	Complexity of the Model, Resource-Intensive experimentation
Halili	Improved return losses, Significant frequency shift, Comparative analysis using variable noble gases	Gas dependency and pressure control
Zheng	Novel plasma antenna design, Experimental validation, Broadband frequency	Decreased Gain, no comparison with reference antenna
Zhou	Numerical modeling, Variation of ionization, Near-Field to Far-Field transformation	Theoretical analysis
lee	Numerical analysis, Radiation characteristics reconfigurability, Efficiency similar to traditional antenna	no experimental verification
Qian	Effective length adjustment, Resonant frequency control, Frequency range analysis	Complex numerical analysis, No practical implication
Chao	Reconfigurable radiation pattern, Effect of plasma parameters	Numerical method complexitity
Drvish	experimental and simulation design, reconfigurability due to plasma properties	complex theoretical analysis
Zali	Improved directivity and gain, Focused signal reception, Acceptable for indoor wireless transmission	limited frequency band, less reconfigurability

Table 1.1: Comparision of advantages and disadvantages of each paper of plasma antenna

Tan	Plasma density impact, Tunable bandgaps, Frequency shift, Frequency-Selective devices	simulation outcomes
Zhang	Reconfigurability, band stop filter 1-14GHz, Propagation control	Limited frequency range
Mittal	Broad frequency range, Trapped oscillations, Transfer matrix method	complex Numerical Analysis,
Guo	Numerical analysis with two techniques, reconfigure PBG	no Practical implementation
Qi	simulation analysis of PPC, variation in collision frequency, widen frequency band, narrow band filter	defect layer introduced in the gap of plasma structure
Wang	Two Dimensional PPC experimental setup, variable potential 0-240V produce variable density, reconfigurable PBG	fixed lattice constant
Jafari	Variable plasma photonic crystal design, Reconfigurable PBG, Numerical analysis	no experimental validation

Table 1.2: Comparision of advantages and disadvantages of each paper of plasma photonic crystal

1.6 Proposed Model

The detailed description of the proposed experimental model of plasma-based antenna and photonic bandgap device are presented in the subsection below.

1.6.1 Plasma Antenna

Schematic of the model of plasma antenna using the plasma column is shown in Fig. 1.6. A model can be categorized into three parts: plasma column and vacuum system, RF signal source and radiation measurement which are explained here.

Plasma column and vacuum system

The setup involves RF generator, vacuum and gas dosing system, argon gas cylinder, power meter, glass tube, KF vacuum assembly, capacitive sleeves etc. The detail description of the components is given below:

- ***Discharge tube:*** The glass tube is used to enclose the gas and form plasma inside the tube. The tube with different material properties and variant in sizes is easily available such as soda lime tubes, Pyrex tubes, borosilicate tube etc.

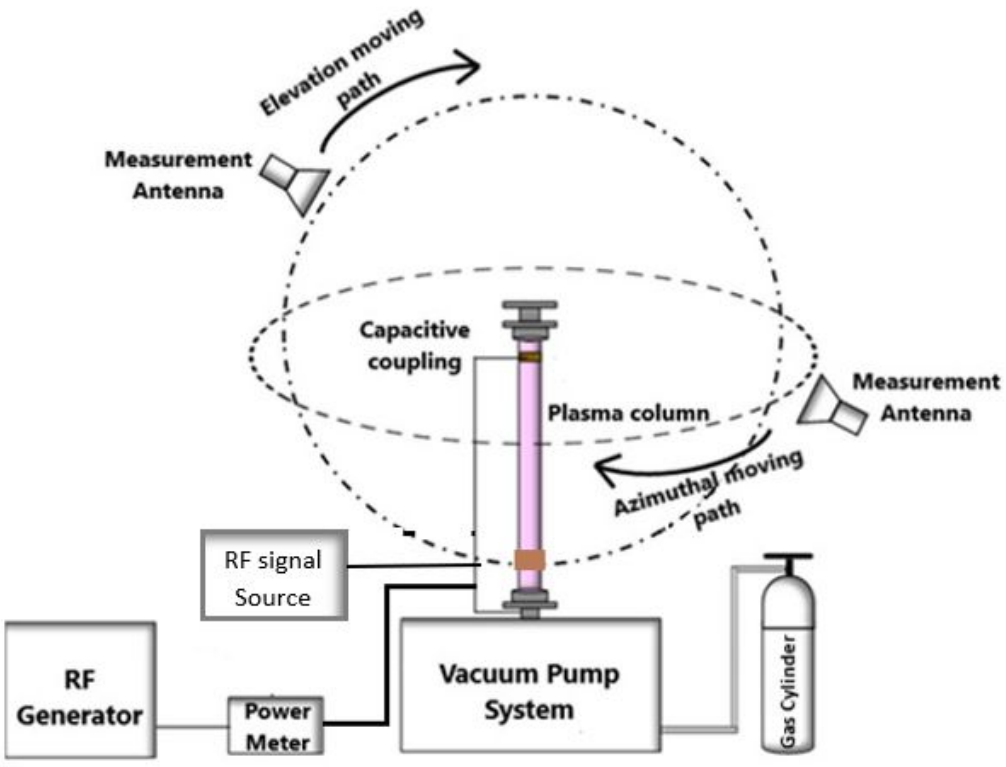

Figure 1.6: Schematic of complete proposed layout of plasma antenna system

- ***Vacuum and gas system:*** The vacuum system plays a crucial role in the generation of plasma column. The system involves combined system of a rotatory pump, Pirani and penning gauge and gas feeding. It is basically used to evacuation process to create vacuum inside the tube. This vacuum pressure inside the glass tube is measured using Pirani and Penning gauges. The neutral fill gas is injected into the glass tube using a needle valve to maintain the required operating working pressure.
- ***RF generator source and power meter:*** A RF generator plays an important role for the generation of plasma as it is utilised as a power source for the ionisation of gas. The RF power is applied to the glass tube via power meter. A power meter is used to control the forward and backward power in between the RF generator and glass tube.

The formation of plasma involves two major processes i.e., evacuation and ionization of gas inside the tube. To perform these processes, the vacuum system and RF generator plays an important role. The vacuum system is a combined setup of rotatory pump, gas dosing valve, Pirani and penning gauge etc. whereas RF generator is stable and continuous wave RF power source using transmitting tube filament and produces few Watts. For the initial evacuation process, one end of the glass tube is mounted on a vacuum system and the other end enclosed by KF assembly. The vacuum is created inside the tube by vacuum pump and then low-pressure argon gas is fed via gas dosing valve. After gas feeding, the tube is energized by an RF generator via. power meter to ionize the argon gas inside it. The power meter is used to control the power delivered to the tube. Once the gas is ionised, a plasma column is formed which acts as a conducting medium for the propagation of signals.

RF signal source:

After the plasma formation stage, the RF source signal is connected to the column for signal transmission. The signal source system consists of signal generator, stub tuner, capacitive sleeve etc. The RF signal generator is utilized to produce RF signal and delivered to the plasma column via. stub tuner and capacitive sleeve. The stub tuners are used to provide matching between the signal generator and plasma column for the proper delivery of the signal.

Radiation measurement system:

This system is utilised to measure the radiation from the antenna by using a combined setup of RF probe, spectrum analyser, computer etc. In the setup, the RF probe is connected to the spectrum analyzer which captures the radiation magnitude in the real-time domain and programmed to present the measured data with polar plot coordinates in elevation and azimuthal plane.

1.6.2 One-dimensional Plasma Photonic Crystal Bandgap Device

Schematic of proposed model of $1D$ Plasma Photonic Crystal (PPC) bandgap device is shown in Fig. 1.7. The PPC structure is the periodic arrangement of plasma and air medium having a thickness of d_a and d_b respectively, with the periodicity Δ. Generally, $1D$-PPC is designed by utilising multiple plasma columns placed in the air in one direction for the bandgaps analysis. Our proposed model of PPC involves the plasma column having plasma blobs aligned along the tube direction. A plasma blob is the critical state of plasma which can be achieved by varying the plasma properties electronically. A plasma column with plasma blobs is the periodic arrangement of plasma and air medium which acts as a bandgap device.

For bandgap analysis, an EM wave is incident at one end of the plasma column which propagates through the plasma blobs and air inside the column and received the passed wave at another end of the column. The transmission of wave through PPC structure depends on the dielectric properties of the plasma and air medium. Based on the given dielectric parameters of both medium, bandgap appears in transmission spectra which can be tuned by changing them.

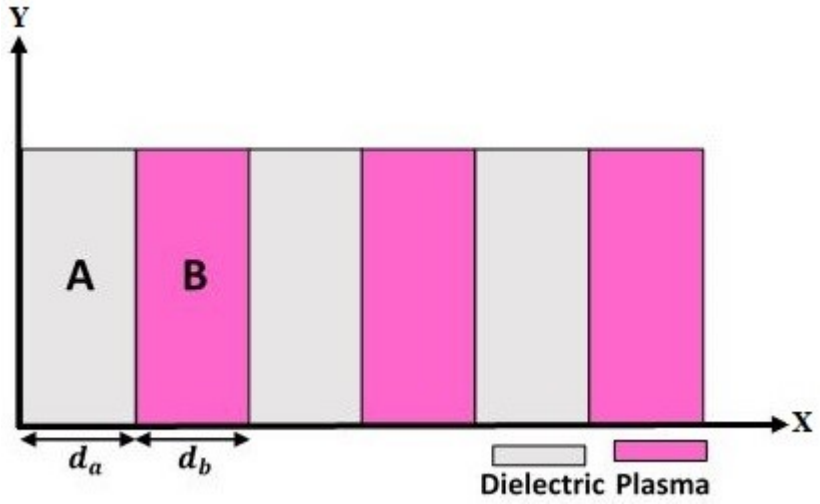

Figure 1.7: Schematic of general 1D plasma based photonic crystal bandgap

1.6.3 Two-dimensional Plasma Photonic Crystal using Fluorescent Tubes

Schematic of the prposed model of the $2D$ plasma based photonic crystal is shown in Fig. 1.8. The setup consists fluorescent tubes, voltage supply, Vector Network Analyser (VNA),

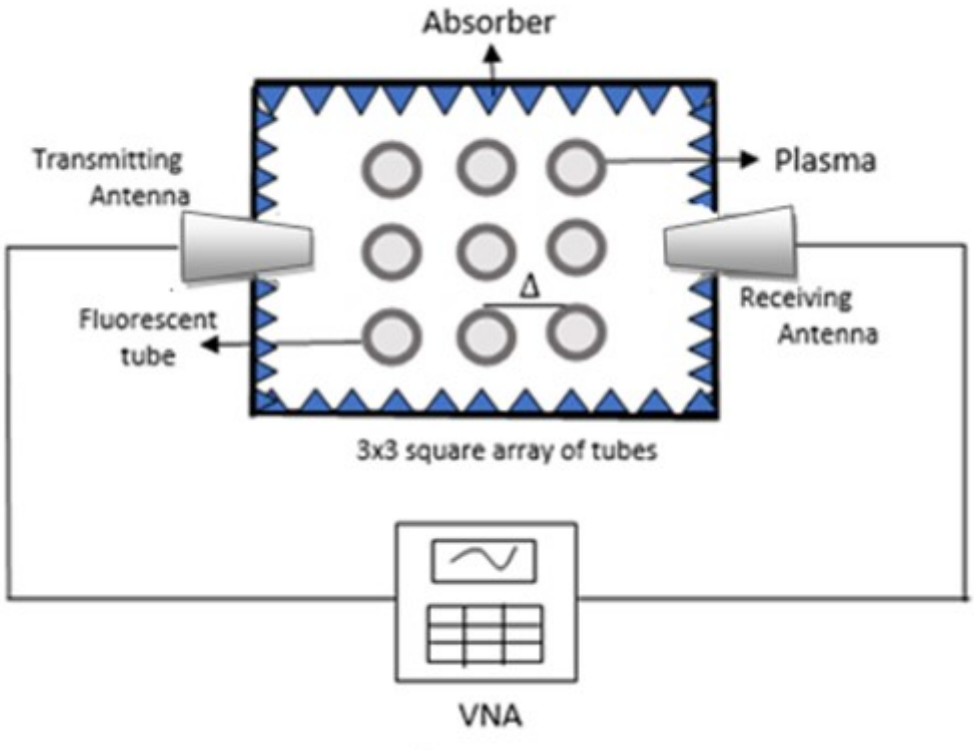

Figure 1.8: Schematic of complete proposed layout of plasma based photonic bandgap system

transmitting and receiving antenna, absorbers etc. In $2D$ PPC setup, plasma tubes are arranged periodically with the lattice constant in air. The two antennas are placed across the both ends of the setup for transmission and reception of the signal passing through plasma tubes. The setup is surrounded by absorbers to absorb the signal and eliminates the interference of unwanted noise signals. The tubes are connected with variable voltage meter for the discharging and glowing process. The transmission parameters are captured by using VNA which is connected to both antennas through port 1 and port 2.

1.7 Organisation of Thesis

This thesis deals with the design and development of plasma based reconfigurable antenna system and passband device which involves several stages to achieve the research objectives. The experimental setup of both devices involves various components which have been procured initially and then integrated components for in house fabrication. The developed setup of plasma antenna and bandgap devices are tested for variable plasma and operating parameters to analyze its reconfigurability in terms of radiation characteristics and photonic bandgaps.

- ***Chapter 1*** deals with the introduction and literature survey of plasma column antenna and plasma photonic crystal, fundamental of plasma theory, its limitations, challenges, and the structure of the thesis is also discussed in this chapter.
- ***Chapter 2*** deals with research gaps and motivation of doing present research work, objectives, methodology to achieve the goals are elaborated in this chapter.
- ***Chapter 3*** deals with the design and development of a reconfigurable plasma column antenna using continuous state of plasma. Simulation, fabrication and test results have been presented in this chapter.
- ***Chapter 4*** deals with the design and development of plasma based collinear antenna arrays using standing plasma density pattern called blobs or striations. Simulation, fabrication and test results have been presented in this chapter.
- ***Chapter 5*** deals with the design and development of single column plasma photonic crystal having standing plasma density pattern. Modelling and simulation has been presented for the analysis for photonic bandgap for variable plasma parameter in this chapter.
- ***Chapter 6*** deals with the design and development of a reconfigurable plasma based photonic bandgap structure using fluorescent tubes array to reconfigure the bandgap structures. Theoretical modelling and implementation of PPC for the investigation of photonic bandgaps have been presented in this chapter.
- ***Chapter 7*** provides the conclusion of the thesis and also discusses the future work that could be taken up to extend the results of this effort.

Chapter 2

RESEARCH GAPS, OBJECTIVES AND METHODOLOGY

2.1 Research Gaps

Development of plasma-based reconfigurable RF/microwave components is a research interest because of its innovative range of applications. Plasma is fully or partially ionised gas where its physical properties can be electronically reconfigured. This property of tunability enables a wide scope for the development of reconfigurable RF/microwave components like plasma antenna, plasma photonic crystal, plasma based RF absorbers, filter etc, which may have many important applications in the field of wireless communication, radar technology, defense, homeland security etc. In general, RF systems are frequency dependent and it need to be altered with the change of operating frequency. In development of RF/microwave components, plasma can be utilised as a guiding structure in-replacement of the metal which are having fixed physical properties and rigidity to change. Application plasma can enable RF components to be reconfigurable in terms of operating frequency and other operating parameters. Utilizing the plasma based reconfigurable components can create a possibility for the development of frequency independent RF/microwave system. In this context, this thesis presents the development of reconfigurable Plasma Antenna (PA) and Plasma Photonic Crystal (PPC). These are the components of the RF/microwave system whereas its reconfigurability will provide a wide range of application scope. The research gaps, which are basically highlighting our contribution in current literature are mentioned as follow,

- First half of the thesis incorporates the development of plasma antenna setup which mainly utilizes a plasma column and a signal source to feed antenna via. capacitive coupling. The coupling of RF signal in plasma antenna is mainly depends on the plasma parameters like plasma density, degree of ionisation, shape and size etc. which decides the operating frequency range of the antenna. Signal coupling in a plasma column is an important part of our investigation which have not been presented earlier. To investigate the operating band, we have analysed the plasma antenna using theoretical modelling and verify it with experimental outcomes. Our analysis results data about RF coupling in plasma column for different plasma parameters.

- The reconfigurability in radiation patterns of the PA has been realised by exploiting the classical state of the plasma in a column called plasma striations. It presents a sinusoidal variation of plasma density along the column which appears like plasma blobs. We have applied signal to the plasma antenna in desired frequency band and investigated its radiation patterns. It is found reconfigurablility in patterns with plasma

density pattern (nos. of blobs) which mainly depends on gas pressure and ionisation energy. It is comprehensively presented in the thesis for the first time.

- The next half of the thesis is mainly devoted for the development of reconfigurable plasma photonic crystal bandgap device. The PPCs have an excellent ability to control the propagation of electromagnetic waves and introduces the various forbidden frequency ranges for the EM waves called photonic bandgaps. PBG can be reconfigured with the plasma parameters. This thesis conceptualises the Single Column Plasma Photonic Crystal (SC-PPC) for the very first time where we have investigated the reconfiguribility in PBG for the various plasma parameters. In addition to this, a fluorescent tube based 2D plasma photonic crystal has been also developed to demonstrate the tunability of PBG with plasma density.

Work presented in the thesis has been accomplished in several steps which is defined in terms of various thesis objectives.

2.2 Objectives

The thesis objectives are outlined as,

- Theoretical modelling of plasma antenna and passband by using computational electromagnetic method i.e., Finite Difference Time Domain method (FDTD).
- Development of experimental setup of plasma antenna and passband which includes plasma column, vacuum system, RF supply, and radiation measurement system.
- Investigation of radiation characteristics of plasma antenna with various operating parameters.
- Analysis of the reconfigurability of the plasma antenna and passband in contrast to the various plasma parameter and shapes of the plasma column.
- Development of various research data and techniques in reference to the reconfigurability of plasma antenna.

2.3 Methodology

In order to achieve the outlined research objectives, we have worked in several stages. These stages involves the modelling, designing, simulation, fabrication and testing of the plasma antenna and passband device called photonic crystal. The work done in each stages have been explicitly discussed as follow,

- To begin the research work, we made a review on earlier work to obtain knowledge about similar plasma devices and its physics. A comprehensive review based on the available literature is given in chapter-1. After receiving the sufficient data from literature, the experimental model of plasma antenna is planned. Detail discussion about the experimental setup is given chapter-3. We have extracted the plasma related data using experimental setup which has been utilized in modelling and simulation of plasma antenna which has been presented in ***Chapter 3***. It mainly covers the ***first, second and third research objectives*** of the dissertation.

- The reconfigurability in radiation patterns of the plasma antenna have been discussed in ***Chapter 4***. This chapter mainly describes the collinear patterns of the plasma structure which radiation patterns are found reconfigurable with plasma parameters. This chapter covers the ***fourth and fifth objectives*** mentioned in the thesis.

- This part of thesis is mainly devoted on the development of Plasma Photonic Crystal (PPC) as a passband structure where we have developed $1D$ and $2D$ PPC. The details about the development of PPC is mentioned in ***Chapter 5 and chapter 6***. In ***Chapter 5*** explore the idea of $1D$ Single Column Plasma Photonic Crystal (SC-PPC). Here, modelling and simulation of $1D$ SC-PPC is presented. The ***chapter 6*** development of a $2D$ PPC using fluorescent tubes and its reconfigurability with plasma density is discussed. These chapters covers the ***first, second, third, fourth and fifth objectives*** which are mentioned in the thesis.

- Additionally, this chapter also incorporates the detail about the design and development of the interferometer which has been utilised for the plasma diagnostic during the analysis and development of PPC. The work has been executed as per the proposed objectives and published in reputed journals in the area of plasma sciences and plasma physics.

Chapter 3

DESIGN AND DEVELOPMENT OF RECONFIGURABLE PLASMA ANTENNA

3.1 Overview

This chapter deals with the design and development of Radio-Frequency (RF) reconfigurable plasma antenna. Basically, plasma column is a glass tube filled with ionised Nobel gas at low pressure which behave as a conducting antenna element. The experimental setup of plasma antenna has been developed, which includes plasma and vacuum system, RF signal source along with the matching network, and an automated radiation measurement system to measure the radiation parameters. The radiation characteristics of the plasma antenna mainly depend upon the plasma parameters like length of plasma and plasma density. These plasma properties are the function of operating input parameters i.e. gas pressure and RF power. The data from experimental setup is utilised to model the plasma column antenna using software where its transmission parameters have been investigated to evaluate antenna resonant frequencies. The radiation patterns of antenna have been measured for the variable plasma parameters and tuned resonant frequencies where the experimental results is verified with the simulated outcomes.

3.2 Experimental Setup

The proposed design of experimental setup of plasma column formation is presented in Fig. 3.1. The formation of plasma column involves two major tasks i.e. evacuation process and ionization of gas. To accomplished this process, a combined setup of RF generator, vacuum system and gas dosing valve is required. The detailed description of each component and its working has been described below

3.2.1 *Vacuum and Gas Dosing System:*

The vacuum and gas dosing system is basically used for the evacuation process and filling of gas inside the glass tube. It is a combined setup of rotary pump, gas dosing valve and Pirani and penning gauges. The rotary pump is a type of vacuum pump which is capable to produce pressure up to $10^{-6}bar$. A Pirani and penning gauge is used to measure the

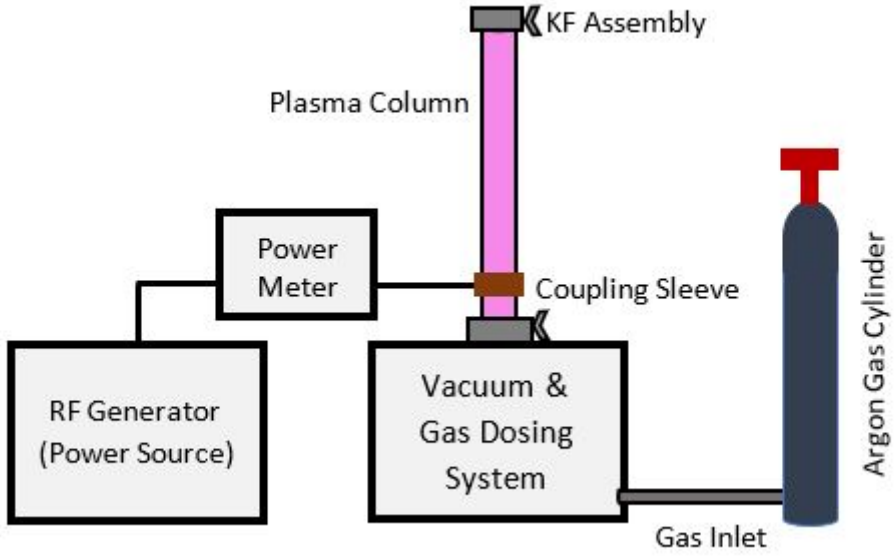

Figure 3.1: Schematic of experimental setup of plasma column formation

vacuum pressure inside the mounted glass column which is controlled by pump needle valve and able to produce up to $120mbar$. A gas dosing system involves the gas filling process via gas inlet which is controlled by gas inlet valve. Argon gas cylinder is utilised and connected to the vacuum gas inlet system.

3.2.2 *RF Generator and Power Meter:*

A RF generator plays an important role for the generation of plasma as it is utilised as a power source for the ionisation of gas. The vacuum tube-based RF generator is utilised for the plasma generation experiments. It operates at $13.56MHz$ and able to produce RF power upto $100Watts$. The RF power is applied to the glass tube via power meter. A BIRDTHRU-LINE power meter $(2-30MHz, 500Watts)$ is used to control the forward and backward power in between the RF generator and glass tube.

3.2.3 *Glass Column and its Assembly:*

A $300mm$ long borosilicate glass tube of $30mm$ outer diameter with wall thickness of $2mm$ is utilised. The both ends of the tube are sealed with $KF-25$ vacuum sealing kit which involves flanges, O-ring, clamps and adapters. A capacitive sleeve is mounted on the one side of the tube. A capacitive coupler provides the required electromagnetic field distribution in the wave excitation region to excite a surface wave. A capacitive coupler of material copper with width of $35mm$ is placed with the gap of $10mm$ from the top of the tube sealing. The

N-type coaxial wire is connected between the power meter and tube. The inner conductor of the wire is attached to capacitive coupler sleeve and outer conductor is shielded with grounding.

3.2.4 *Developed Experimental Setup for Plasma Column:*

Based on the selected components mentioned in proposed model as shown in Fig. 3.1, an experimental setup for the plasma column formation has been developed in High Power RF Lab (HPRFL). The photograph of the developed system is presented in Fig. 3.2.

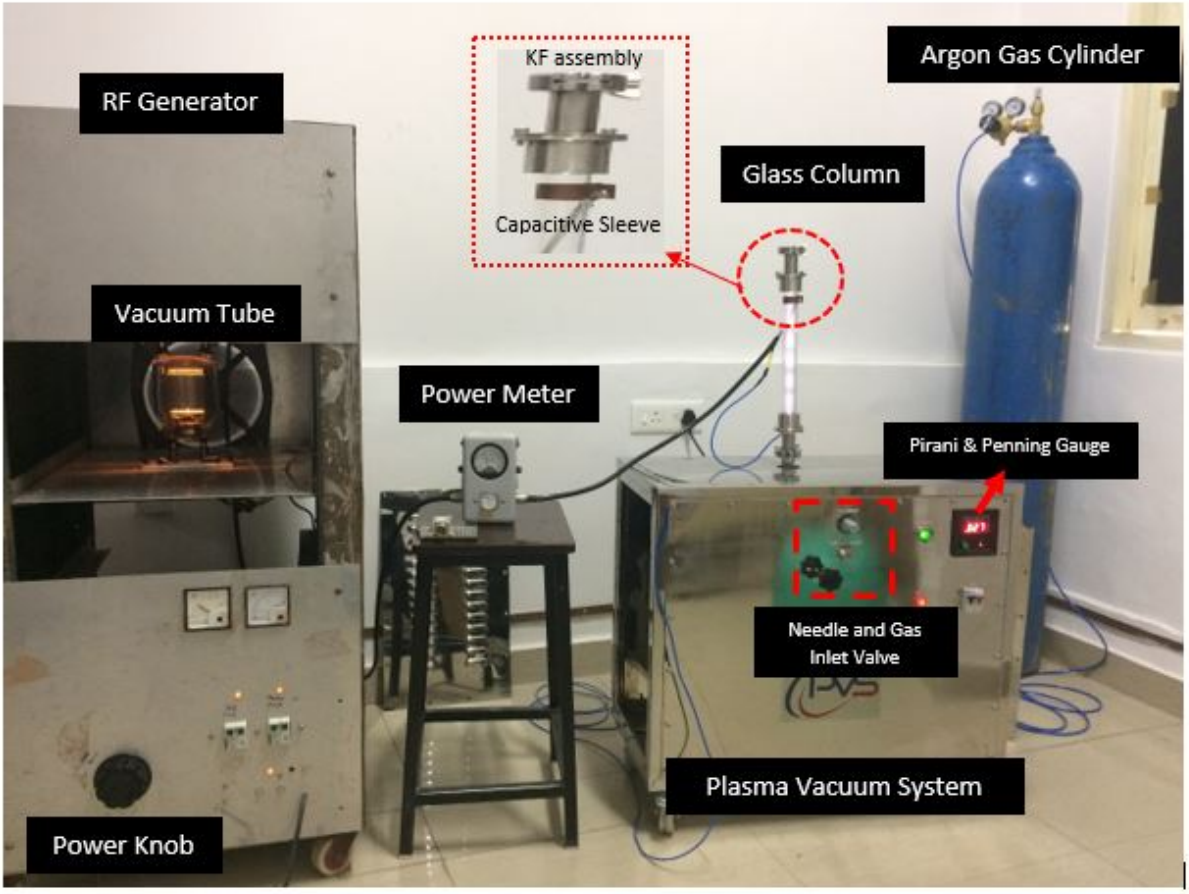

Figure 3.2: Developed experimental setup of the plasma column formation

To generate the plasma column, one end of the $30cm$ long glass column is mounted on the vacuum and gas dosing system where it's another end is sealed with $KF-25$ vacuum assembly. The PVS (Plasma Vacuum System) system initially evacuated the glass column up to the pressure $0.005mbar$. After that, the gas is feeding into the glass column via gas inlet which is connected to the argon gas cylinder. The pressure of gas can be controlled by using gas valve and visible on the Pirani and penning gauge. Once the gas pressure is maintained inside the glass column, RF power is then applied to the tube via power meter

which basically control the forward and backward power. The RF power is applied to the tube through capacitive sleeve. The initial breakdown occurs at the gap and then discharge the argon gas inside the tube and formed a surface wave plasma column. The detail of formation of plasma column and its discharge mechanism is discussed in section 3.3.

3.3 Plasma Column and its Parametric Analysis

A process of the establishment of a fully developed plasma column and the analysis of properties of plasma formation are given below in subsection,

3.3.1 Plasma Column by Surface Wave Discharge

The generation of plasma column using Surface Wave Discharge (SWD) is well known technique from decades and various theoretical and experimental studies are presented by researchers [34]. In the SWD, an electromagnetic surface waves travel along the interference between the plasma and glass tube boundary. A surface wave discharge is accomplished by using a compact wave launcher which is placed on glass tube of few mm in diameter filled with low gas pressure up to the range of $10^{-5}Torr$ and high frequency power source [35]-[39].

In our experiment setup, a plasma column is formed by using surface wave launcher which involves the high-power source up to $100Watts$, capacitive sleeve of thickness of few mm and glass tube of radius $15mm$ which is describe in above section 3.2. For initial breakdown, power is applied to the gas filled tube via capacitive sleeve where the capacitive discharge is occurred at the gap between the sleeve. In the capacitive discharges [39], a surface wave is travelled along the plasma column by using a capacitive coupling, an intense electric field is induced between the ground and a capacitive sleeve. Due to the induced electric field, atoms of the neutral argon gas is ionised which release an electrons and ions. The free electron, ions and charged particles accelerate and make collisions and emit the energy in the form of light. Basically, EM wave is excited which moves along the interface of these two media and the discharge build-up goes on until the plasma column is fully filled in the glass tube.

The surface wave discharge parameters depend on the power absorbed per unit length and discharge conditions like tube dimension, material, operational frequency, input power, working pressure, gas, wall material of tube etc. The discharges which are sustained by surface wave belong to the general category of Traveling Wave Discharge (TWDs) [51, 52, 96]. Because of their specific mechanism of energy transfer from the electromagnetic field to the plasma. A high frequency discharge is created in a glass tube from the field of electromagnetic wave which is propagating along the axis. The wave is launched at position $z = 0$ and travel in the axial $z - direction$. As the wave travel, the power flux decreases with increasing in axial length of plasma. The plasma column ends at $z = L$, where power

drops below the level require to sustain the plasma. The power dissipated per unit length of the plasma column varies along the axis of the tube. The analysis of a given travelling wave discharge in a segment z to $z+dz$ is the same as that for uniform discharge, assuming axial, radial inhomogeneity in density and step-wise ionization process. The axial distribution of the electric field $E(z)$ gives the attenuation constant of the surface wave [35] which is expressed as,

$$\Lambda(z) = -ln\frac{E(z)}{E(0)} = \int_0^z \alpha(z)dz \tag{3.1}$$

where $\alpha(z)$ is the attenuation coefficient. For collision-less plasma or low collisions ($v_m << \omega$) and non-uniform radial density profile rather than to non-linear effects [41], the axial distribution $\Lambda(z)$ can be written as

$$\Lambda(z) = \frac{v_m}{2\alpha\omega_p}\int_0^z \frac{\omega_p}{\omega_p(z)} \times \frac{d[\beta(z)\alpha]}{d[\frac{\omega}{\omega_p(z)}]}dz \tag{3.2}$$

where v_m is the electron neutral collision frequency and ω_p denotes the plasma frequency. Integral part of eq. 3.2. depends on the local dispersion properties of plasma in the column which is calculated by considering the axial density distribution. The attenuation of wave is due to the damping of the wave power into the plasma. A power flux, $P(z)$ of the wave propagating along the discharge over the distance z to $z+dz$, can be expressed as, [3]

$$\alpha(z) = -\frac{1}{2}\frac{1}{P(z)}\frac{dP(z)}{dz} \tag{3.3}$$

where dz is the power absorbed in the plasma per unit volume along axial distance. The power deposited per unit length of the discharge over the distance z to $z+dz$ is then,

$$\Lambda(z) = -\frac{dP(z)}{dz} = 2\alpha(z)P(z) \tag{3.4}$$

The power loss in the plasma under steady state condition can be expressed as

$$2\alpha(n)P(z)\Delta z = 2\pi\int_0^a \sigma(n)E^2(r)rdr\Delta z \tag{3.5}$$

where n is the electron density, a is the inner radius of the tube, $\sigma(n)$ denotes the plasma conductivity, and $E(r)$ is the average total electric field strength of the wave. Under the given discharge conditions, the attenuation coefficient depends only on the cross-sectional average electron density n which varies with z. When the field frequency is exceeded, all the power absorbed by the plasma is intercepted by the electrons. The power per unit length lost by the electrons through collisions of all kinds, and gained by heavy particles can be expressed as,

$$\Gamma(n)\Delta z = \pi a^2 n\theta\Delta z \tag{3.6}$$

where θ is the energy term. Taking into the account of above well-established facts of

surface wave produced plasma column, we can measure the length of plasma column and its plasma density with the applied input power and given pressure which is discussed in below subsection.

3.3.2 Plasma Density

A plasma density of the column is measured by considering a power balance equation according to the analysis mentioned by M. Moisan [39]. The power absorbed per unit length by the plasma from the surface wave at any position along the axis (z) of the column i.e. $\Lambda(z)$ is balanced with power per unit length lost $\Gamma(z)$ to the walls from plasma by the movement of electron-ion pairs at the Bohm velocity (u_B). Under steady state condition, the power balance equation is $\Lambda(z) = \Gamma(z)$, is written as [96],

$$\Lambda(z) = -\frac{dP(z)}{dz} = \alpha(z)P(z) \tag{3.7}$$

For given radius, r of glass tube, the $\Gamma(z)$ is given as,

$$\Gamma(z) = u_B A_{eff} \zeta_l n(z) \tag{3.8}$$

$$\alpha(z)P(z) = \pi r^2 n\theta \tag{3.9}$$

Where A_{eff} is the effective surface area per unit length of the column. ζ_l is the energy loss per electron pair, r is the radius of the tube, θ is power loss by electron. The attenuation coefficient can be calculated from the dispersion characteristics of the surface wave, for losses via collision. Based on the calculation [3], $\alpha = \alpha(n)$, function of plasma density and its analytical approximation is written as,

$$\alpha(n) = \frac{C v_m}{n - n_{res}} \tag{3.10}$$

The constant C has fixed value for the given experiment.

$$n_{res} = \frac{\epsilon_0 m}{e^2}\omega^2(1 + \epsilon_g) \tag{3.11}$$

The n_{res} is the characteristics number density at a plasma frequency (ω_p) corresponding to the operating angular frequency (ω). m and e are the mass and charge of electron. ϵ_0 is the free space permittivity, ϵ_g is the dielectric constant of glass tube. if the column is excited at base of the column ($z = 0$) with the power P_0 and density is $n_e > n_{res}$, than [44, 3]

$$n_e = A(p)\sqrt{P_0} \tag{3.12}$$

$$A(p) = \sqrt{\frac{2Cv_m}{K(p)}} \tag{3.13}$$

where $K(p) = u_B(p)A_{eff(p)}e\zeta_l(p)$ is the function of pressure and u_B and ζ_l are the function of electron temperature for the given geometry. The value of $A(p)$ is constant for given gas pressure.

3.3.3 Plasma Column Length

A plasma inside the column is formed by surface wave discharge method. A length of the plasma depends on the height of the column (h_t) and potential applied to the column $P(z)$. The variation in density with distance along the column is expressed by [3, 44],

$$P(z) = \frac{K}{2Cv_m} n(n - n_{res)} \tag{3.14}$$

Differentiating the eq. (1.14) with respect to z, we get

$$\frac{dP}{dz} = -2\alpha P = -Kn \tag{3.15}$$

$$\frac{1}{n}\frac{dn}{dz} = -\frac{2Cv_m}{2n - n_{res}} \tag{3.16}$$

At the top of the column $z = h_t$ and $n = n_{res}$ where n_{res} is the minimum value of n for which the wave propagates. With boundary conditions, eq. (3.16) at any positions of z,

$$\frac{n(z)}{n_{res}} - \frac{1}{2} ln(\frac{n(z)}{n_{res}}) = 1 + \frac{h_t - z}{L_0} \tag{3.17}$$

Where $L_0 = \frac{n_{res}}{Cv_m}$ is the characteristics length. In most experiment, $\frac{n}{n_{res}} >> ln(\frac{n}{n_{res}})$

$$\frac{n}{n_{res}} = 1 + \frac{h_t - z}{L_0} \tag{3.18}$$

From eq. 3.18, it is indicated that the plasma density decreases in an approximately linearly along the column which directly reduces the length of plasma. So, surface wave does not propagate below the $n < n_{res}$, the $n = n_{res}$ defines the top end of the column. If the column is excited at the base where $z = 0$ and $n = n_e$, then the height of plasma column is defined as,

$$h_t = \frac{n_e L_0}{n_{res}} - L_0 \tag{3.19}$$

By putting the value of n_0, in eq. (3.19), we get

$$h_t = B(p)\sqrt{P_0} \tag{3.20}$$

$$B(p) = \sqrt{\frac{2}{CK(p)v_m}} \tag{3.21}$$

In our experiment, the variable plasma profile is formed inside the column by applying RF power in the range of $(P_0) = 10 - 100Watts$ and gas pressure in the range between $(P_r) = 0.025 - 0.055mbar$. As per the well described fundamental theory of plasma, its length and density can be controlled by varying the input parameters i.e. RF power, gas pressure, column length, column diameter etc. Based on the formulations given in eq. 3.21 and 3.13, plasma column length and its density are dependent on variable $B(p)$ and $A(p)$ which are the function of gas pressure. The plot of the slope of $B(p)$ is evaluated from the global model [3] by considering the parameters as $C = 5\times10^9 m^{-4}$, $K(p) = 2.7\times10^{14} m^2 W^{-1}$, $v_m = 10^9 Hz$ for given gas pressure range $0.025mbar - 0.055mbar$, which is presented in Fig. 3.3.

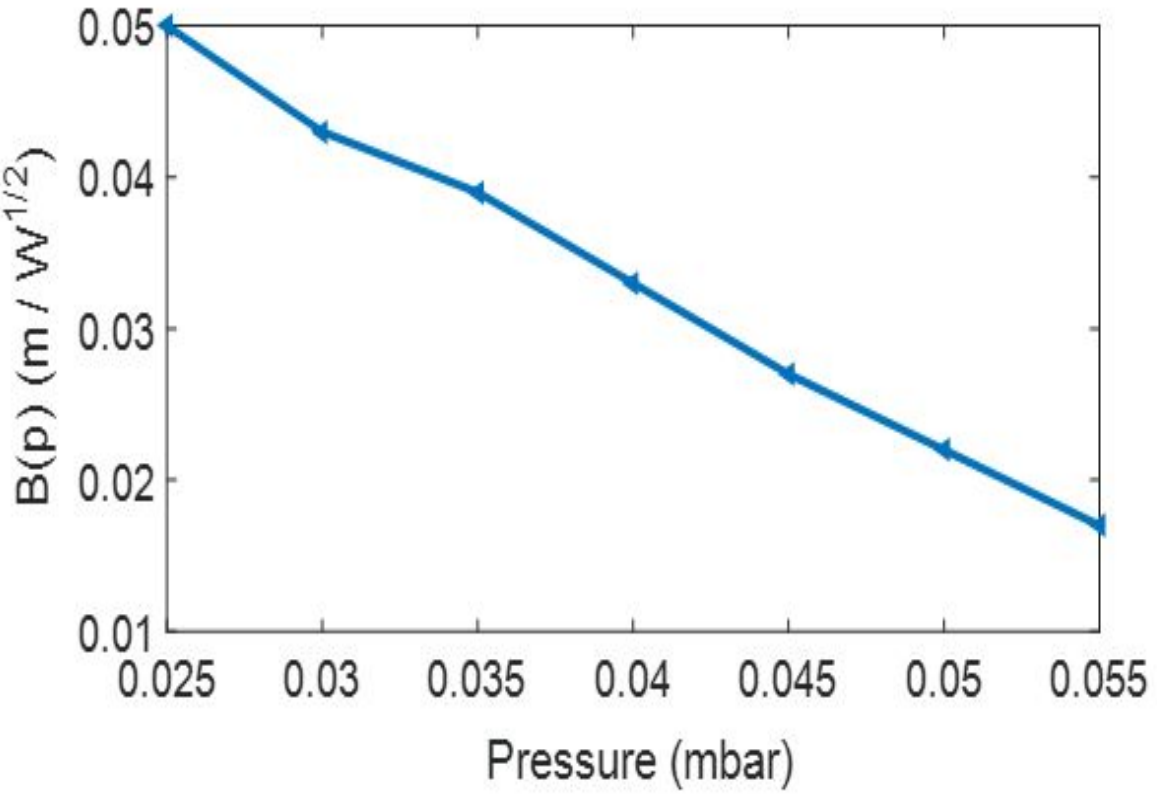

Figure 3.3: Slope of $B(p)(m/W^{1/2})$ for variable gas pressure $(mbar)$ predicted from theoretical global model

From the given figure, it can be seen that the slope of $B(p)$ is linearly decreasing with the increase of gas pressure which significantly influence the length of the plasma inside the column. For instance, at $P_r = 0.025mbar$, the value of $B(p) = 5.0cm/W^{1/2}$ whereas reaches to its minimum value $1.9cm/W^{1/2}$ when pressure is $0.055mbar$. The Fig. 3.4 presents the variation in height of plasma inside the column with respect to applied RF power for variable $B(p)$ values at given working pressure.

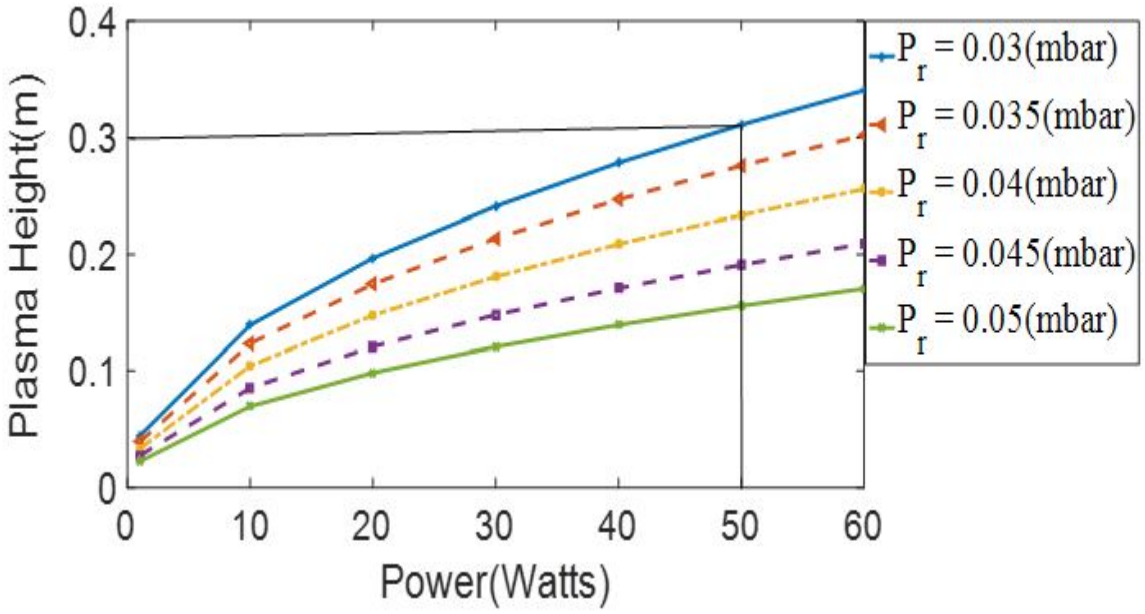

Figure 3.4: Height of SWD plasma column is function of power level at different pressure

From investigated outcomes, it can be observed that the height of plasma increases linearly proportional to the square root of input power. For instance, at pressure $0.03mbar - 0.05mbar$, the value of $B(p) = 4.4 - 2.8cm/W^{1/2}$ and column length is increasing from $0.15m$ to $0.3m$ for RF power $10Watts$ to $50Watts$. The factor affecting the antenna length is the electron collision frequency (v_m) which is a linear function of gas pressure. As the pressure increases, the collision frequency increases which minimise the value of $B(p)$ and lower the plasma height.

For plasma density evaluation, we have developed $0.3m$ long plasma that is formed by setting gas pressure $0.30mbar$ inside the column and applied $50Watts$ to the column via capacitive sleeve. A density of plasma column is mainly depending on the applied RF power and gas pressure which can be calculated by using eq. 3.13. For $0.3m$ long plasma, the value of variable $A(p)$ is $0.016 \times 10^{16} m^{-3} W^{1/2}$ for parameters $C = 5 \times 10^9 m^{-4}$, $K(p) = 2.7 \times 10^{14} m^2 W^{-1}$, $v_m = 10^9 Hz$. Based on the calculated value of variable $A(p)$, the plasma density (n_e) of the column is estimated along the axial length of column for applied power which is shown in Fig. 3.5.

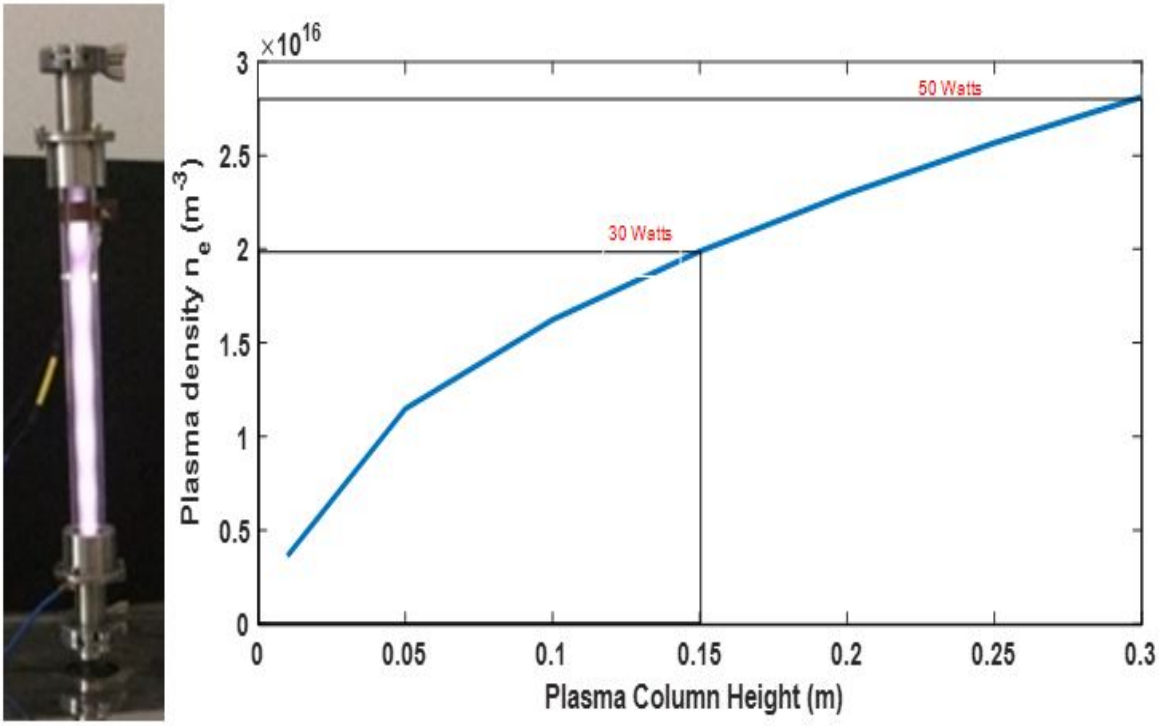

Figure 3.5: Plasma density of developed $0.3m$ long plasma column at $0.03mbar$ and $50Watts$.

3.3.4 Plasma Permittivity and Conductivity

A cold plasma is a Debye dispersive media with a relative permittivity $\epsilon_p(\omega)$, permeability $\mu_p(\omega)$ and non-zero conductivity $\sigma_p(\omega)$ which are given as

$$\epsilon_p(\omega) = 1 - \frac{\omega_p^2}{\omega(\omega - i\upsilon_m)} \tag{3.22}$$

$$\sigma_p(\omega) = \frac{\epsilon_0 \omega_p^2}{\omega^2 + \upsilon_m^2} \tag{3.23}$$

$$\mu_p(\omega) = 1 \tag{3.24}$$

Where ω is angular wave frequency, $\omega_p = \sqrt{\frac{n_e e^2}{m_0}}$ is an angular plasma frequency, υ_m is collision frequency, n_e is plasma density, e is an electron charge, m is a mass of electron and ϵ_0 is a free space permittivity. Based on the n_e profile, the permittivity and conductivity can be varied as per the requirement. The value of $\epsilon_p(\omega) = -1.207$ for $13.56MHz$ frequency. A plasma column is aligned along the z direction, where the propagation of signal follows the EM wave equation i.e. [14, 17],

$$E(z) = E_0 e^{-\beta z} \tag{3.25}$$

where $\beta = jk_0\sqrt{\epsilon_p\mu_p}$, is the propagation constant which depends on the free space factor, $k_0 = \sqrt{\epsilon_0\mu_0}$. Based on the value of plasma permittivity and permeability, the propagation constant can be written as,

$$\beta = jk_0\sqrt{1 - \frac{\omega_p^2}{\omega(\omega - iv_m)}} \tag{3.26}$$

For collision less plasma, $v_m = 0$,

$$\beta = jk_0\sqrt{1 - \frac{\omega_p^2}{\omega^2}} \tag{3.27}$$

The propagation of wave into the plasma depends on the value of propagation constant. If $\omega > \omega_p$, the permittivity of plasma become less than unity, plasma medium behaves as dielectric where the value of β will be imaginary and wave will be propagated through the plasma with the dispersion relation [24, 29], i.e.

$$\omega^2 = \omega_p^2 + \beta^2 c^2 \tag{3.28}$$

where c is the speed of light. If $\omega < \omega_p$, permittivity become negative, plasma behave as waveguide and β is real where wave is an evanescent wave which do not allow to propagate through plasma medium. The plasma medium is bounded by the positive dielectric, then surface wave is propagating through the plasma dielectric interface with the transverse evanescent field on both sides with the dispersion relation as:

$$\frac{K_p I_0 K_p a}{\epsilon_p I_1 K_p a} + \frac{K_p K_0 K_0 a}{k_1 K_0 a} \tag{3.29}$$

where $K_p = (\beta^2 - \omega^2\epsilon_p/c^2)^{1/2}$, $K_0 = (\beta^2 - \omega^2/c^2)^{1/2}$, a is a plasma column radius and $K$and I are the Bessel function.

The developed setup of plasma column is further analysed for antenna characteristics which is accomplished by modelling and simulation approach and explained in next section 3.4.

3.4 Modelling and Simulation of Plasma Antenna

A plasma column antenna is modelled and simulated by using $3D$ electromagnetic simulation software i.e. CST (Computer Simulation Technology) microwave studio. The CST utilizes the finite element method (FEM) for the electromagnetic simulation. It discretizes the problem space into discrete elements and solved Maxwell's equations to analyse the transport properties of the designed model. A process of designing a plasma column antenna model in software is presented by flow chart which is shown in Fig. 3.6.

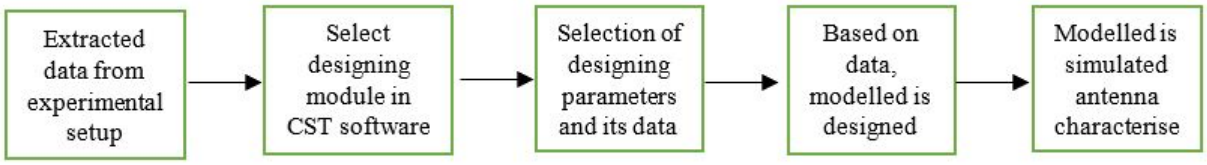

Figure 3.6: Flow chart of designing plasma column antenna

In CST software, plasma antenna is designed using Drude module which is basically depend on the plasma properties i.e. plasma frequency (ω_p) and collision frequency (v_m). The designing parameters of plasma column antenna is extracted from the experimental setup. A list of designing parameters and its values are shown in the Table 3.1. Based on the measured data in Table 3.1, the designed model of plasma column antenna is shown in Fig. 3.7

Table 3.1: Parameters for simulated model of plasma antenna

Parameters	Single(cm)
Glass Tube Length G_L	30
Glass Tube Thickness G_T	0.2
Plasma Length P_L	30
Plasma Diameter P_D	1.3
Plasma Density n_e	2.74×10^{10}
Sleeve Height S_H	3
Sleeve Thickness S_T	0.02
Ground Plate Height G_{PH}	3
Ground Plate Radius G_{PR}	6

The figure presents the front and top view of plasma column antenna. A plasma is enclosed in glass tube in the z direction where the capacitive sleeve is used for transmission of wave. A metallic ground plate is used at the bottom of tube to provide an infinite ground plane for plasma antenna. The PEC (perfect electric conductor) boundary has been assigned to the simulation space. A discrete port is assigned between the ground plate and capacitive sleeve which is shown by zoomed version. A plasma column antenna is simulated for the analysis of transmission parameters (S-parameters) in the range of $1 - 500MHz$. The plot of S_{11} parameter is shown in Fig. 3.8.

From figure, it can be observed that the designed plasma column antenna is resonating at three different frequencies, i.e. $112MHz$, $347MHz$, $409MHz$. At these resonant frequencies, return loss characteristics are $-30.53dB$, $-23.73dB$ and $-31.99dB$ respectively. The resonant frequency of plasma column antenna is the function of plasma properties which can be reconfigured as per desired. The simulated radiation patterns on these resonant frequencies are presented in Fig. 3.9.

It can be observed that the plasma column antenna radiation patterns are more similar

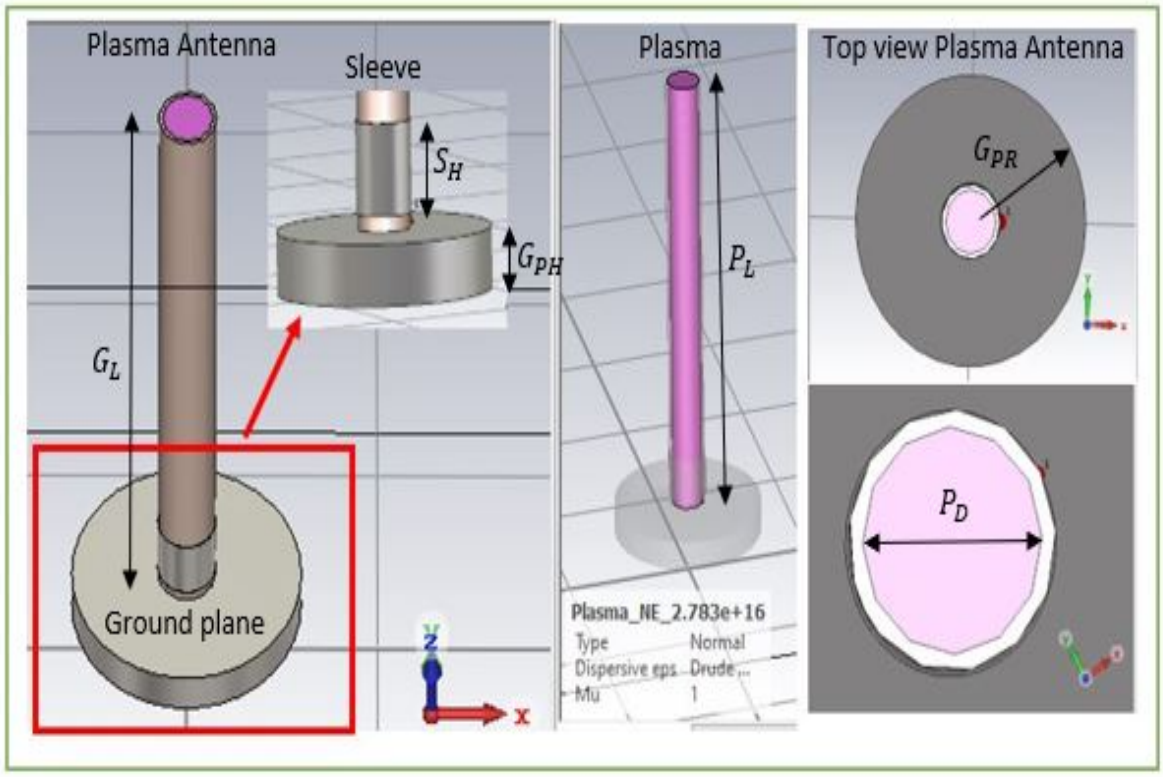

Figure 3.7: Designing Model of plasma column antenna (a) front view of plasma column antenna (b) plasma medium inside glass tube (c) top view of plasma column antenna

like a monopolar radiation pattern. It changes in a similar fashion with the change of frequency which can be realised in metallic antenna [6]. In general, the beamwidth of antenna is significantly influenced by the increase in operating frequency. Basically, with the increases of frequency, an effective electrical length of antenna increases that improves its gain and directivity. A similar observation has been made herewith, at frequency $112MHz$, the beamwidth of the pattern is wider and it became narrower as the frequency increases to $347MHz$ which is clearly shown in Fig. 3.9.

In the same, radiation pattern of antenna gets intended to form multiple lobes at frequency $409MHz$ and appears resultantly wider as compared to the lower frequencies $112MHz$ and $347MHz$. In this investigation, we found the developed plasma antenna behaves like a plasma monopole at tuned frequency. The tuning of antenna can be made by changing input power and pressure which leads to change in plasma density. Moreover, plasma antenna has added advantages over metallic antenna, that its height can be varied by altering the plasma parameters. Based on the simulation outcomes, the developed plasma column antenna is tested for these resonant frequencies which is described in next section.

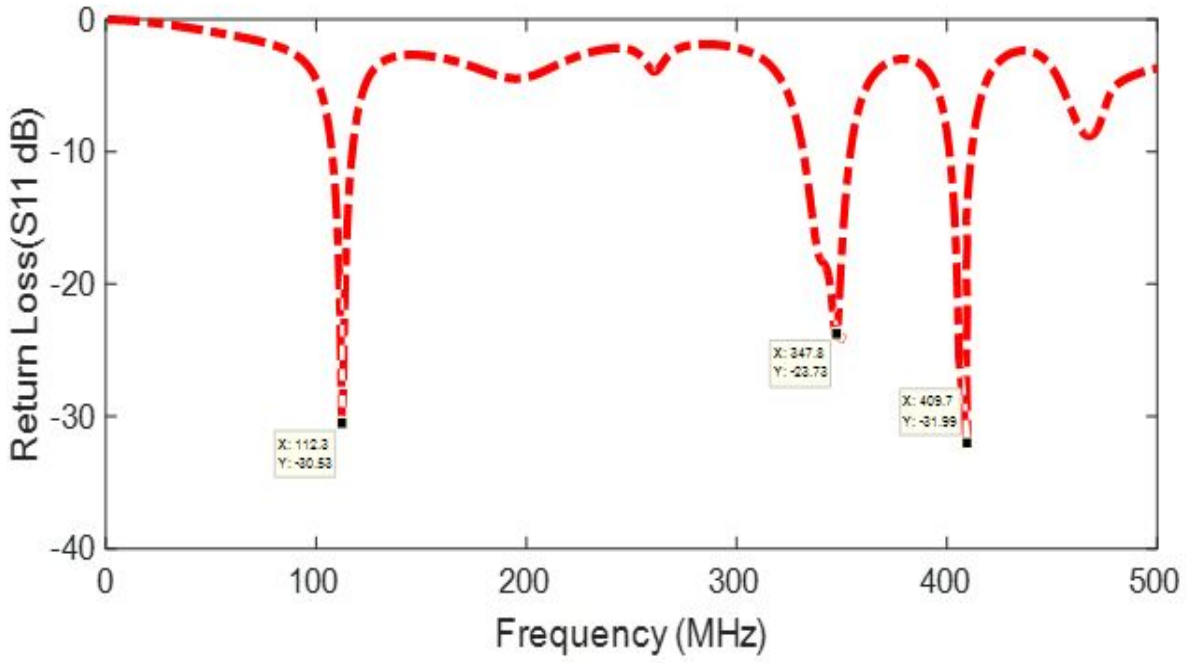

Figure 3.8: S_{11} parameter of plasma column antenna for frequency upto $500Mhz$

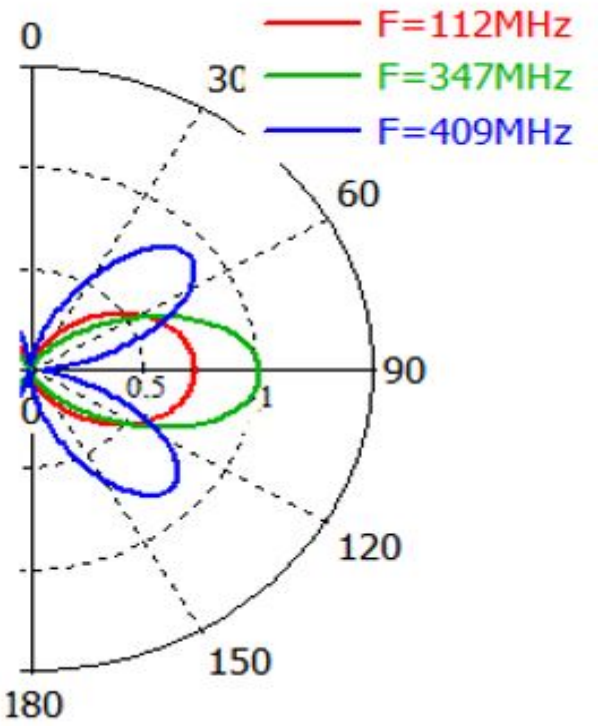

Figure 3.9: Polar plot of plasma column antenna at three resonant frequency $112MHz$, $347MHz$ and $409MHz$.

3.5 Experimental Setup of Plasma Antenna

The schematic of the plasma column antenna is shown in Fig. 3.10 whereas the photographs of the developed experimental setup are shown in Fig. 3.11 and Fig. 3.12. The developed setup is mainly classified into three parts i.e. plasma and vacuum setup, RF signal source and automated radiation measurement system which are briefly described as follow,

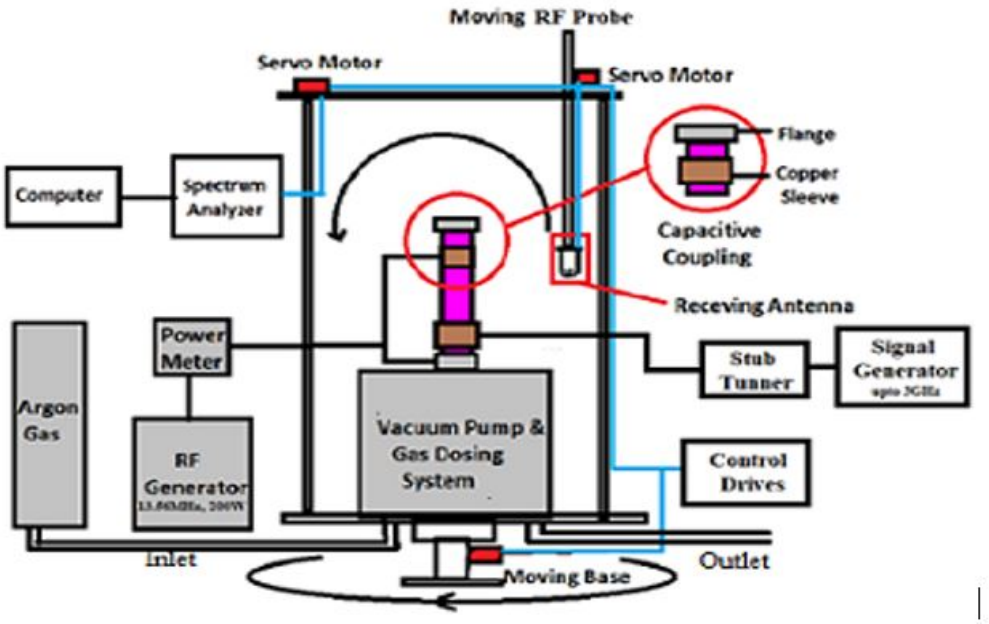

Figure 3.10: Schematic of plasma column antenna

3.5.1 Plasma and Vacuum System

The plasma and vacuum setup mainly consist of $13.56MHz$, $100Watts$ RF generator, power meter, glass column (tube), vacuum system, argon gas supply, etc. which are used to generate the RF plasma inside a column. The dimension of the column is selected as, $0.3m$ long with $0.03m$ outer diameter which is mounted on a vacuum system and sealed at the top with $KF-25$ assembly for evacuation. The volume of glass tube $159.5cm^3$. The vacuum system consists of a rotatory pump, gas dosing valve, and Pirani and penning gauges which are capable to produce vacuum up to $0.005mbar$. Argon gas is supplied in the tube with controlled pressure the range $0.01mbar$ to $0.05mbar$. A $30cm$ long plasma column antenna is developed by having the combination of power $50Watts$ and gas pressure $0.03mbar$ which is shown in Fig. 3.11 and also explained in section 3.3.

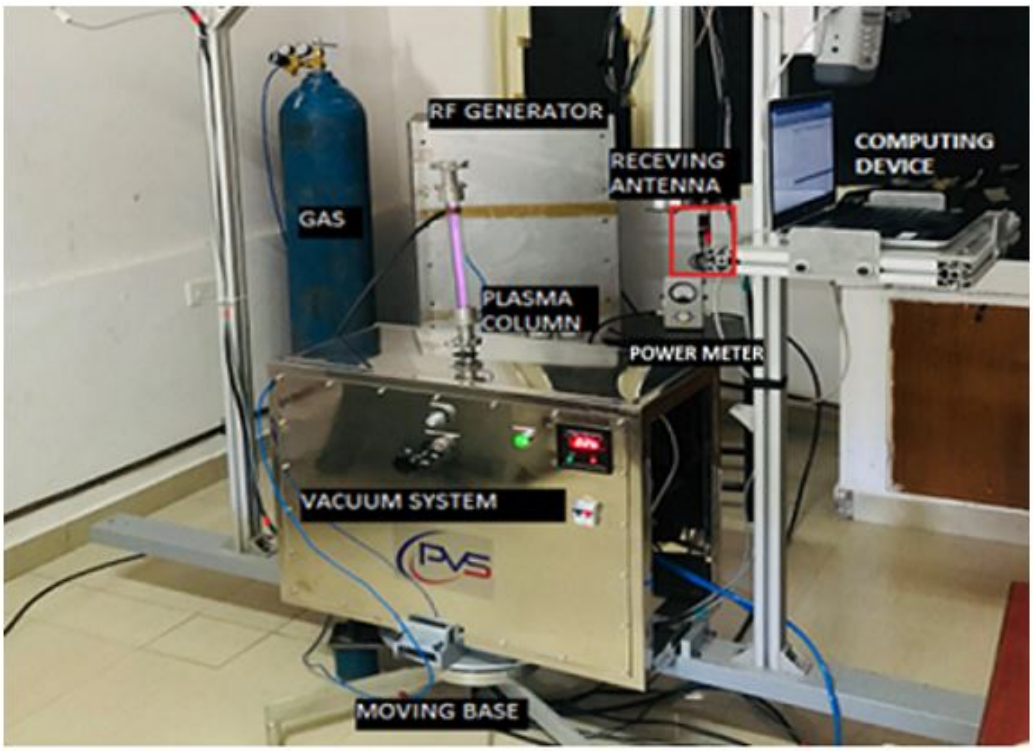

Figure 3.11: Experimental setup of plasma column antenna with automated radiation measurement system

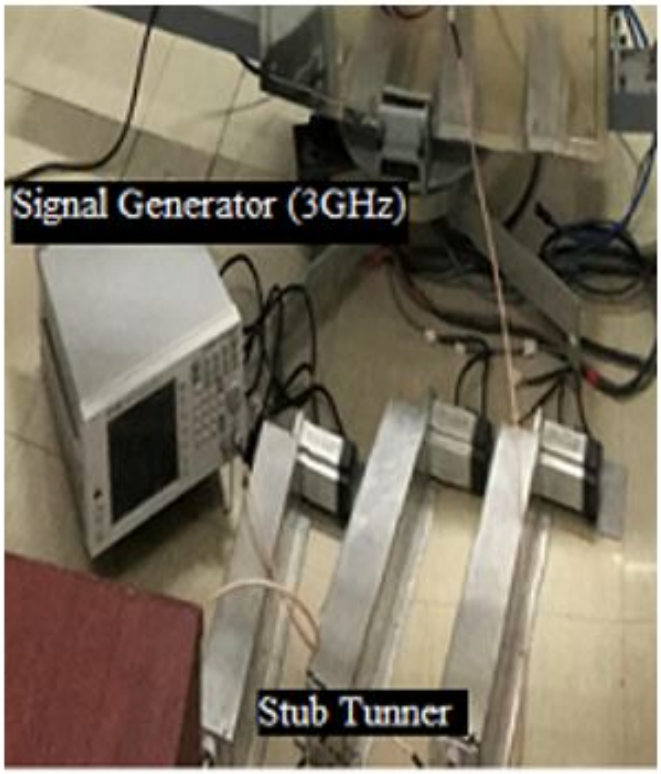

Figure 3.12: RF signal source

3.5.2 Automated Radiation Measurement System

To test the radiation characteristics of the plasma column antenna in the far-field region, a customized automated radiation measurement system has been developed. The RF probe is connected to the spectrum analyser which captures the radiation magnitude in the real-time domain. It has been programmed to present the measured data with polar plot coordinates in elevation and azimuthal plane. In elevation plane, the measurement probe moves in semi-circular space with angle $0^0 < \theta < 180^0$ degree whereas in the azimuthal plane it rotates, $0^0 < \phi < 360^0$ with the precision of 1-degree angle. The photograph of the developed system of plasma antenna and automated radiation measurement system is shown in Fig. 3.11.

3.5.3 RF Signal Source

Plasma is a good conductive medium that can serve as a guiding structure for the propagation of electromagnetic waves. The RF signal of the range up to $500MHz$ is fed to the plasma column via. another capacitive sleeve. The RF signal source setup includes a signal generator up to $3GHz$ and stub tuners as a matching network which is shown in Fig. 3.12. The stub tuners are used to provide matching between the signal generator and plasma column for the proper delivery of the signal.

3.6 Measurement and Test Results

3.6.1 Experimental Results

The developed experimental setup of plasma column antenna is tested for the investigation of radiation patterns at different plasma properties and resonant frequencies. To measure the radiation characteristics, an automated radiation measurement system is utilised. A testing procedure is beginning with the formation of plasma column at the combined combination of power ($50Watts$) and gas pressure ($0.03mbar$). Once the plasma inside the glass tube is created and become stable with density profile density $2.7 \times 10^{16} m^{-3}$, RF signal of $112MHz$ is applied to the glass tube via. capacitive sleeve from the signal generator. Further, the radiation from the antenna is measured by the reference antenna which is connected to the moving probe of the automated system. The reference antenna is in far field region ($R < 2\pi/L$) and rotate in azimuthal plane with the precision of 1 degree. Similar steps are followed for other resonant frequencies, i.e. $347MHz$ and $409MHz$. The captured radiation patterns in elevation and azimuthal plane at these frequencies are shown in Fig. 3.13 and Fig. 3.14.

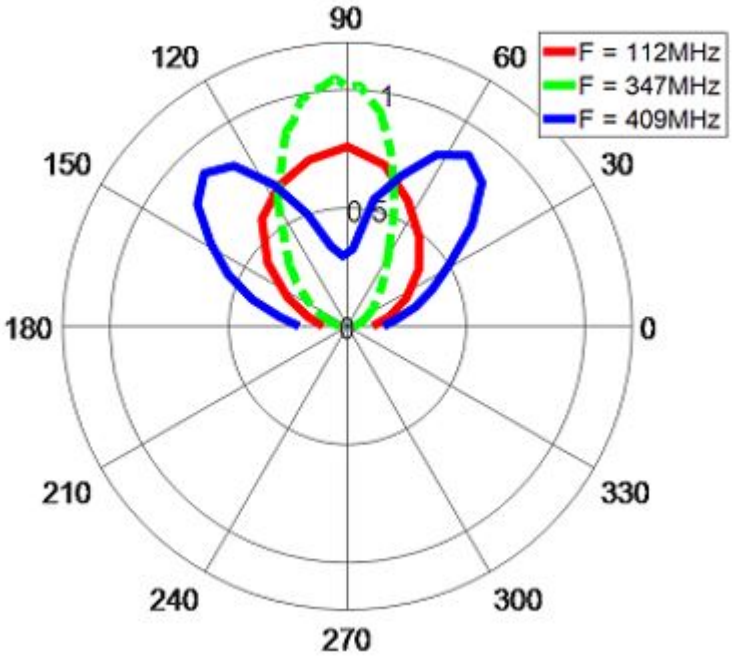

Figure 3.13: Elevation Polar plot patterns of plasma column antenna for three different resonant frequencies

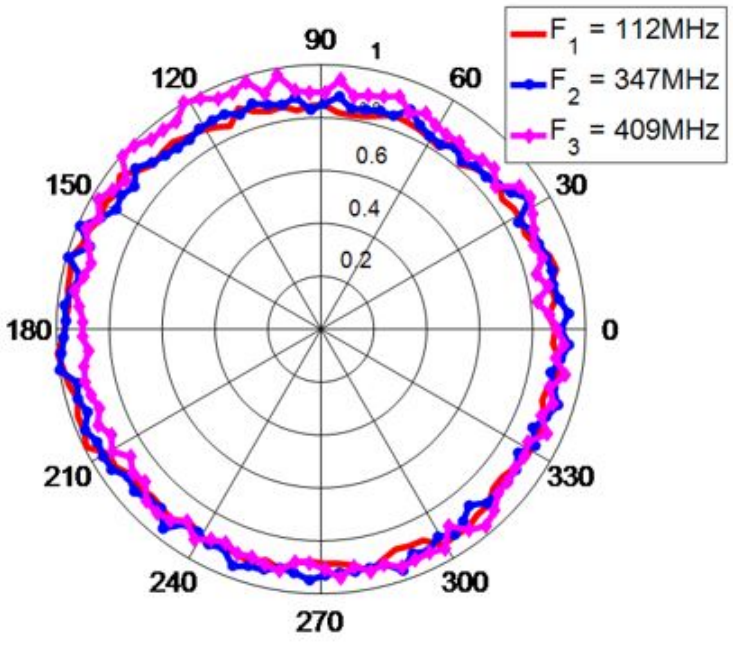

Figure 3.14: Azimuthal Polar plot pattern of plasma column antenna for three different resonant frequencies

3.6.2 Comparison of Experimental and Simulation Outcomes

The polar plots of plasma column antenna at these resonant frequencies with perspective comparison with simulation results for $0.3m$ long plasma column is shown in Fig. 3.15. It can

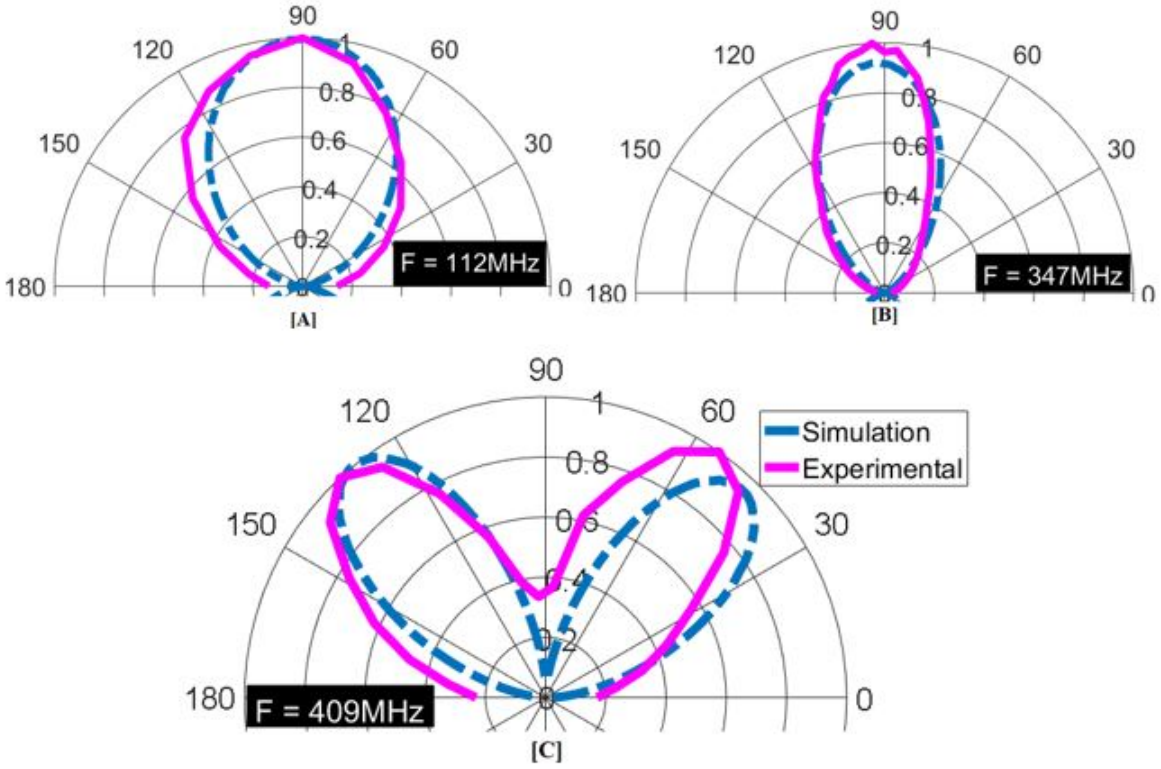

Figure 3.15: Perspective comparison of experimental and simulation results for single length plasma column antenna $(a)112MHz(b)347MHz(c)409MHz$

be observed that the radiation pattern of antenna changes in a similar manner as obtained from simulation outcomes. At frequency $112MHz$, beamwidth of antenna is wider and measured 58 degrees. As the frequency increases to $347MHz$, the beamwidth changes and reduced by 17 degrees. At $409MHz$, the lobing in the beamwidth of antenna appears. The finding reveals that the plasma antenna behaves as a monopolar antenna where its radiation characteristics can be controlled by plasma properties. The experimental outcomes verify the simulation outcomes and found in good agreement.

3.6.3 Experimental Results for Variable RF Power and Gas Pressure

In advance, other experiments have also been performed to investigate the plasma column antenna radiation characteristics for variable RF power and gas pressure values. The plots of captured radiation patterns in elevation plane are shown in Fig. 3.16 for variable gas pressure at constant applied RF power i.e. $50Watts$ and $60Watts$ respectively. The azimuthal polar patterns are shown in Fig. 3.17.

From captured patterns, it is observed that the direction of radiation and beamwidth of

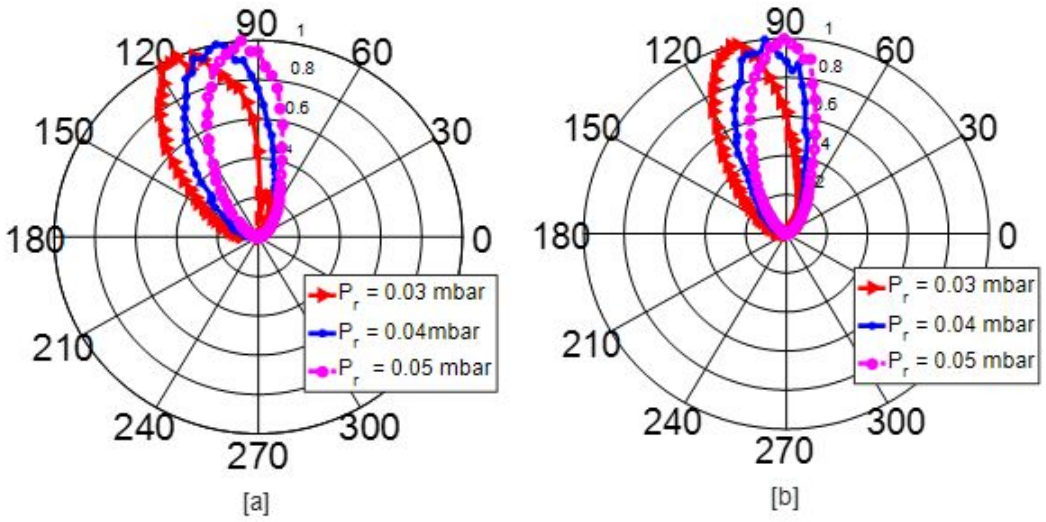

Figure 3.16: Elevation polar plot pattern of single structure plasma monopole at $L = 0.3ma) Power = 50Wattsb) Power = 60Watts$

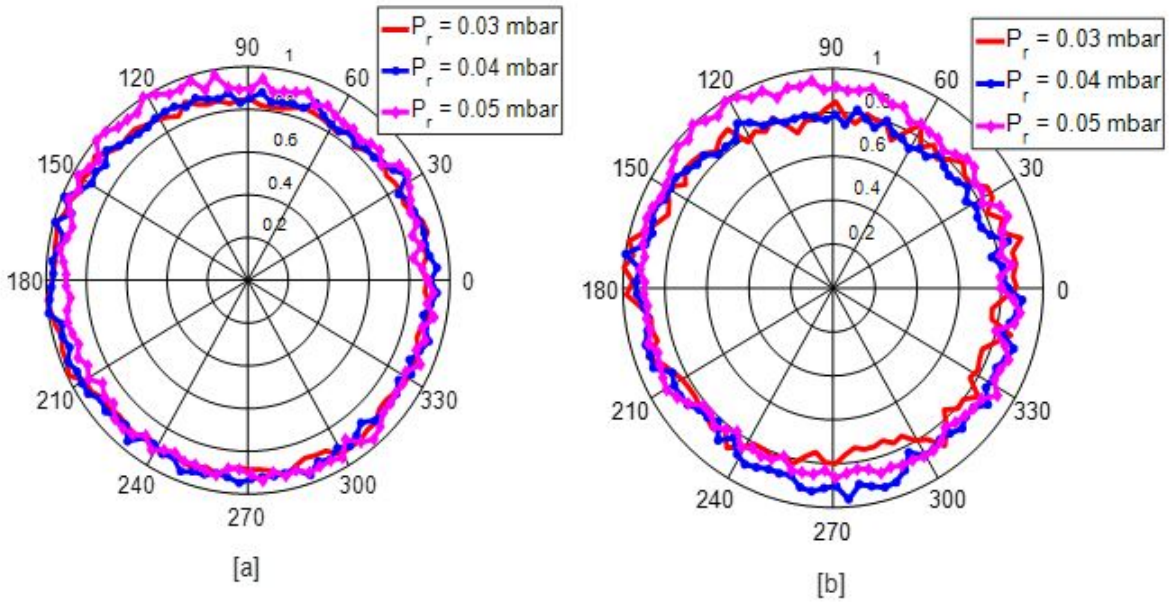

Figure 3.17: Azimuthal polar plot pattern of single structure plasma monopole at $L = 0.3ma) Power = 50Wattsb) Power = 60Watts$

patterns changes with the increase in gas pressure and RF power values. For instance, at $P_r = 0.03mbar$ the direction of radiation of the main lobe is towards the angle $\theta_1 = 115^0$ $(50Watts)$ and $\theta_2 = 110^0$ $(60Watts)$ whereas at $P_r = 0.05mbar$, it is shifted to the end fire side and the direction of the main lobe towards the angle, $\theta_1 = 98^0$, $\theta_2 = 90^0$ respectively. The study explores that the radiation patterns of the antenna are the function of input parameters can be reconfigured as per desired.

Summary

In this chapter, radiation characteristics of plasma column antenna have been investigated for variable plasma properties and resonant frequencies. For radiation measurement, an automated radiation measuring system is fabricated which represents a novel technique to evaluate the radiation parameter of the antenna. The investigated study reveals that the radiation patterns show significant change for plasma properties like plasma density, plasma frequency, and plasma length, etc. which are the function of input parameters such as gas pressure, RF power, and drive frequency. It can be evident from investigated outcomes that the radiation intensity shifted its direction with the increase in the values of input parameters. The study reveals that this property provides an option to online control the radiation characteristics as per requirement and has a potential applications in the field of wireless communication, radar technology, defense etc.

Chapter 4

DESIGN AND DEVELOPMENT OF PLASMA BASED COLLINEAR ANTENNA ARRAY

4.1 Overview

This chapter mainly describes the design and development of a reconfigurable collinear antenna array based on the plasma column. A plasma antenna array simply presents a classical state of plasma in a column where plasma blobs or striations are formed by having the critical combination of input parameters i.e. gas pressure and input RF power. In particular, plasma blobs or striations are aligned in such a way that its arrangement is called as collinear array where each blob acts as a radiating element. Based on the experimental data, modelling and simulations of plasma-based collinear antenna array have been done using the CST software. The radiation characteristics have been investigated for variable plasma properties like plasma density, number of blobs and size, plasma frequency and input operating parameters. Experimental results are presented in comparison with simulated outcomes. The work is summarised in the last of this chapter which emphasis on the novel findings of the work for the wide range of its applicability.

4.2 Experimental Setup of Plasma Blobs Column

The schematic of experimental setup of plasma blobs in a column is shown in Fig. 4.1. It includes a combined setup of RF generator, vacuum and gas dosing system, power meter, gas cylinder, glass column and its assembly etc. Basically, the same setup is considered for plasma blobs formation which has been used to form plasma antenna. The detailed description of each component of the setup is mentioned in section 3.2. However, in the formation of plasma blobs in a column, a continuous state of plasma inside the column is transformed into the plasma blobs or striations by having critical combinations of applied input parameters i.e. RF power and gas pressure. The developed plasma blobs inside a column is called classical state of plasma. It's alignment is along the axis of the column which are arranged in a collinear manner. The photograph of developed experimental setup of plasma blobs inside a column is shown in Fig. 4.2.

It can be observed that the plasma blobs of certain height are formed for critical combination of applied RF power and gas pressure. The developed plasma blobs inside a column

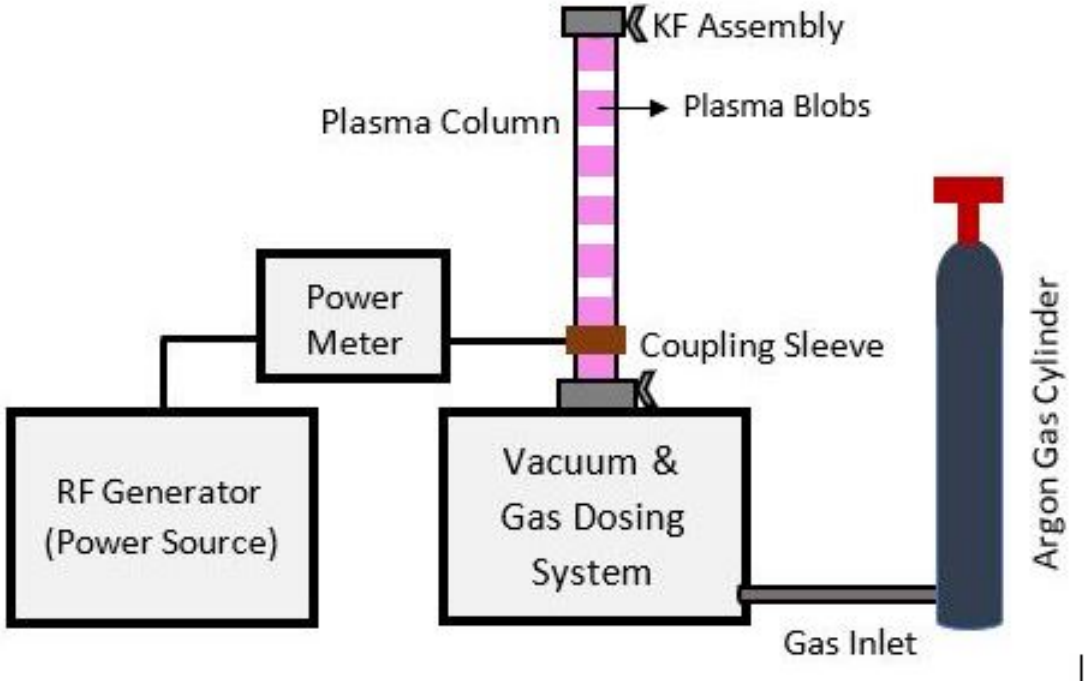

Figure 4.1: Schematic of experimental setup of plasma blobs column

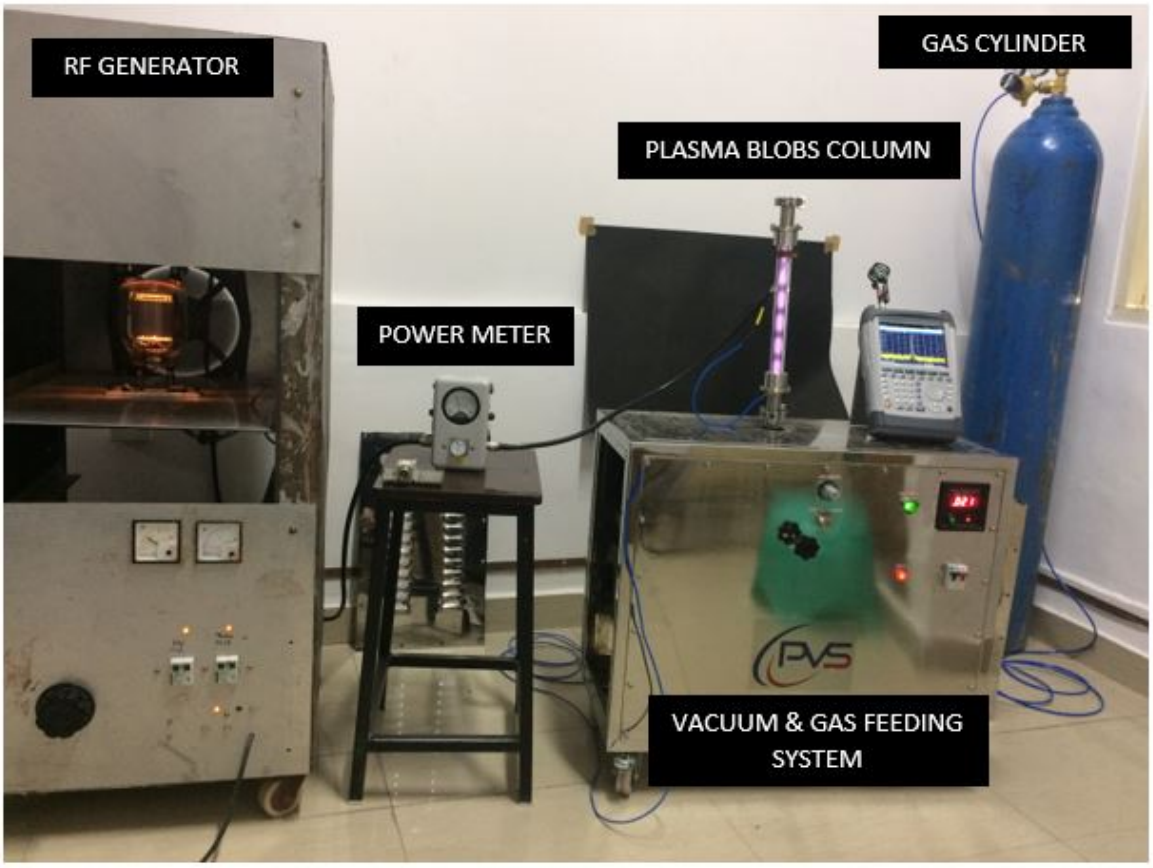

Figure 4.2: Photograph of developed experimental setup of plasma blobs column

are in stationary state. In figure, it is evident that 5 plasma blobs are formed inside the $30cm$ long glass tube for given external parameters i.e. RF power $P_0 = 60Watts$ and gas pressure $P_r = 0.015mbar$ at $13.56MHz$ operating frequency. In particular, plasma blobs are the sinusoidal variation of plasma density called as Standing Plasma Density Pattern (SPDP) which are the function of RF power and gas pressure. The SPDP can be changed by varying of these parameters. In our experiment, finite number of SPDP are formed in a column by controlling of these input parameters. The photograph of developed standing plasma density patterns in a column is shown in Fig. 4.3.

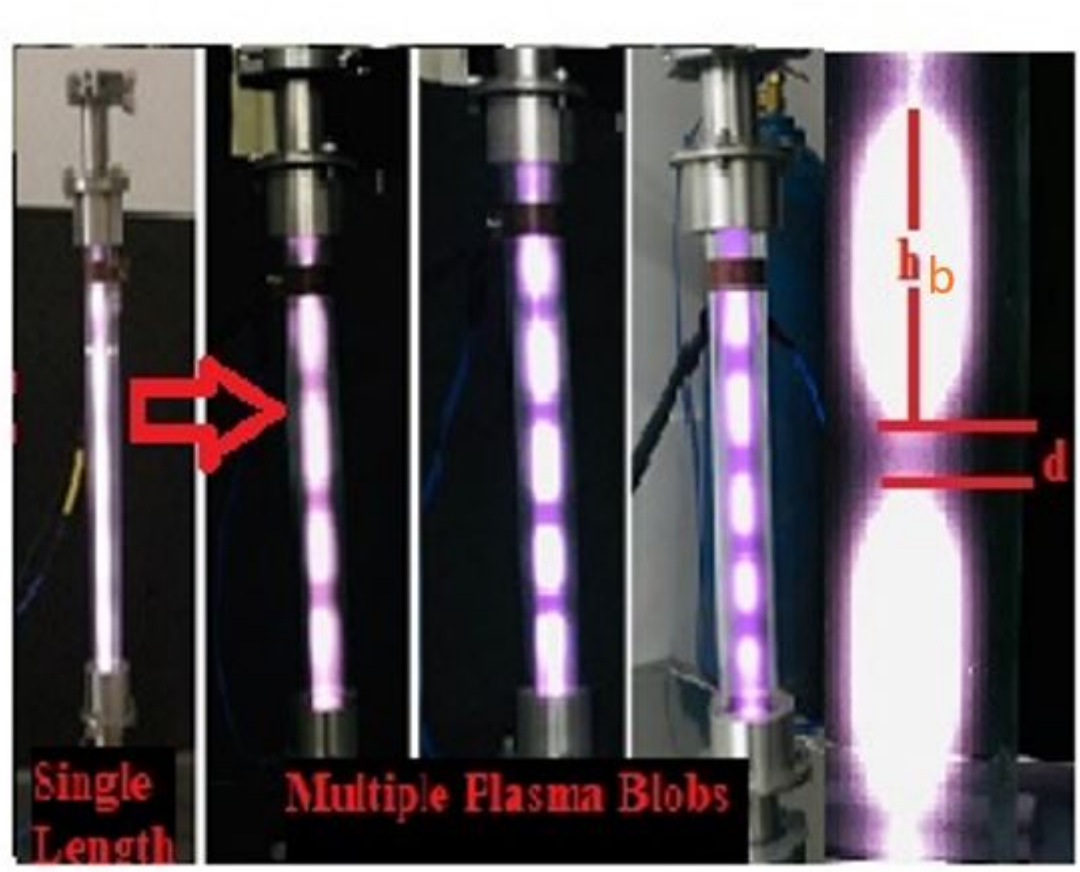

Figure 4.3: Photograph of developed three different SPDP in a column

In Fig. 4.3, three glass columns are presented in which 4 to 6 standing plasma density patterns are formed at the gas pressure range $(0.020 - 0.050mbar)$ and input RF power range $(55 - 80Watts)$ where its height is calculated from the given formula;

$$h_b = \frac{L(z) - (n_z - 1)d}{n_z} \tag{4.1}$$

where h_b is the height of the blob, n_z is the number of plasma blobs, d is spacing between two blobs which are marked in Fig. 4.3. A $L(z)$ is the length of the column which is equal to h_t. The measured data of developed plasma blobs are shown in Table 4.1.

Table 4.1: Gas and pressure values for experimentally developed blobs in 30cm long column

Gas(mbar)	Power(Watts)	Blobs size(cm)
0.020-0.025	75-80	4blobs ($h_b = 5, d = 3.3$)
0.030-0.035	65-75	5blobs ($h_b = 4.5, d = 2.4$)
0.040-0.050	55-65	6blobs ($h_b = 3.5, d = 1.8$)

From measured data, it can be analysed that to form 4 number of plasma blobs, gas pressure is required to be low for high value of applied RF power. Whereas in case of 6 blobs, gas pressure should be high for low value of applied power. It is observed that for less number of blobs in a column, the height and spacing between the blobs is more and it reduced with the increases of blobs number inside the column.

4.3 Formation of Plasma Blobs Column and its Analysis

The Standing Plasma Density Pattern (SPDP) is generated at considerably low gas pressure and high-power input as compared to the continuous state of plasma. In our experiment, 4 to 6 nos. of plasma blobs have been formed by tuning the RF power and gas pressure at different values in the range of $40 - 80 Watts$ and $0.015 - 0.045 mbar$ respectively. The photograph of developed plasma blobs is shown in Fig. 4.3 and corresponding physical parameters are given in Table 4.1.

The physical mechanism of the blobs formation can be understood with the help of two-step ionization theory [42]. By this theory, applied energy, $\zeta_i(11.56eV)$ initially pulls the atom into the meta-stable state, where an additional collision by an electron provides subsequent energy, $\zeta_M(4.2eV)$, required for the ionization of the meta-stable atom. At low pressure, the numbers of atoms are subsequently less where electrons attain sufficient kinetic energy (u) after being injected from the position of the electrode at $x = 0$ and achieved a threshold energy level, ζ_i after a mean free path, λ_e (is a distance between two successive collisions)[83]. These electrons experience inelastic collisions and lose their energies obtained from the electric field to the atoms and produce slow electrons after the mean free path. These accelerating and de-accelerating electrons produce an Oscillating Standing Potential (OSP) profile with spatial period of λ_e along the column axis with the interaction of alternating electrodes. The OSP modulates the plasma density which results a sinusoidal SPDP and appears as bright and dark plasma blobs along the column axis. These dark and bright regions represent the density minima and maxima respectively.

For the analytical explanation of the SPDP formation (plasma blobs or striations), the Goldstein bifurcation theory [52] can be referred. Based on the theory of bifurcation, a set of nonlinear equations that have stationary state and become unstable when a bifurcation parameter exceeds its critical value is required to develop.

The diffusion equations for a meta-stable atoms and electron is solved as a meta-stable atoms providing two-step ionization [42], which are responsible to excite the weak instability in a plasma column. For transverse bifurcation, solved diffusion equations for an electron and meta-stable atoms along the axial direction (x-axis) can be written as,

$$\frac{\partial n_e}{\partial t} - D_x \frac{\partial^2 n_e}{\partial x^2} = S(n_e, n_n) \tag{4.2}$$

$$\frac{\partial n_e}{\partial t} - \alpha D_x \frac{\partial^2 n_e}{\partial x^2} = R(n_e, n_n) \tag{4.3}$$

where the term n_e and n_n are the plasma density and neutral density. The term S and R are the rate of creation of electrons and atoms, respectively whereas D is the diffusion coefficient for the electrons and ions. The term α is the ratio of the atom to that of the ions. According to the discharge mechanism S and R can be written as

$$S(n_e, n_n) = n_n S_2 n_e + \eta R^2 + \chi n_e^2 + S_3 n_e - \gamma n_e - \zeta n_e \tag{4.4}$$

$$R(n_e, n_n) = S_1(n_e) - \Gamma n_n S_2(n_e) - \xi n_e - 2\eta n_n^2 \tag{4.5}$$

The destruction of atoms by electron is represented by the term $n_n S_2 n_e$. The destroyed atoms are becoming ions which is presented as $\Gamma n_n S_2(n_e)$. The term $S_1(n_e)$ presents the rate per unit volume for formation of atoms by electron collision by the background ions. The terms γn_e and ξn_e are the losses of electrons and atoms by radial diffusion to the side walls of the column, respectively. The term ηn_n^2 is the collision between two atoms whereas χn_e^2 is the recombination collision between ions and electrons. The term $S_3 n_e$ presents the direct ionization of the ground state atoms by the electron collisions. The Boundary condition at the plasma edges as, $x = 0$ and L where L is the length of the plasma column. The boundary conditions can be assumed as

$$n_e(x = 0, t) = n_e(x = L, t) = n_{e0} - n_e^{'}(x, t) \tag{4.6}$$

$$n_n(x = 0, t) = n_n(x = L, t) = n_{n0} - n_n^{'}(x, t) \tag{4.7}$$

where $n_e^{'}(x, t)$ and $n_n^{'}(x, t)$ are the perturbation terms in a plasma and neutral densities, respectively. The linear stability analysis is carried out by putting an eq. 4.6 and eq. 4.7 in an eq. 4.2 and eq. 4.3, and linearization to obtain

$$\frac{\partial n_e}{\partial t} = \frac{\partial S}{\partial t} n_e^{'} + \frac{\partial S}{\partial t} n_n^{'} + D_x \frac{\partial^2 n_e}{\partial x^2} \tag{4.8}$$

$$\frac{\partial n_e}{\partial t} = \frac{\partial R}{\partial t} n_e^{'} + \frac{\partial R}{\partial t} n_n^{'} + \alpha D_x \frac{\partial^2 n_e}{\partial x^2} \tag{4.9}$$

$$n_e^{'}(x,t) = N_{e_n}^{'} e^{\lambda_n \tau} sin \frac{n\pi x}{L} \tag{4.10}$$

$$n_n^{'}(x,t) = N_{n_n}^{'} e^{\lambda_n \tau} sin \frac{n\pi x}{L} \tag{4.11}$$

$$\begin{bmatrix} \lambda_n + S_{n_e} - D\frac{n^2\pi^2}{L^2} & S_{n_n} \\ R_{n_e} & \lambda_n + R_{n_n} - \alpha D\frac{n^2\pi^2}{L^2} \end{bmatrix} \begin{bmatrix} N_{e_n}^{'} \\ N_{n_n}^{'} \end{bmatrix} = 0 \tag{4.12}$$

$$\lambda_n^2 = \lambda_n \left[S_{n_e} + R_{n_e} - (1+\alpha) D \frac{n^2\pi^2}{L^2} \right] + \left(S_{n_e} - D\frac{n^2\pi^2}{L^2} \right) \left(R_{n_n} - \alpha D \frac{n^2\pi^2}{L^2} \right) - S_{n_n} R_{n_e} = 0 \tag{4.13}$$

$$\lambda_n^2 - \lambda_n H_n + I_n = 0 \tag{4.14}$$

$$H_n = R_{n_n} + S_{n_e} - (1+\alpha) n^2 (\frac{1}{\mu}) \tag{4.15}$$

$$I_n = \frac{n^4}{\mu^2} - (R_{n_n} + S_{n_e}) \frac{n^2}{\mu} + S_{n_e} R_{n_n} - S_{n_n} R_{n_e} \tag{4.16}$$

where μ is the bifurcation parameter which are the function of length of plasma column and diffusion constant, D. The bifurcation parameter can be written as,

$$\mu = \frac{L^2}{D\pi^2} \tag{4.17}$$

$$L = B(p) \sqrt{\frac{P}{V_m}} \tag{4.18}$$

where, $B(p) = \sqrt{\frac{2}{CK(p)}}$, $K(p)$ is the function of given gas pressure, the energy lost per electron ions pair due to collision ($\zeta_L = \zeta_c + 2T_e + \zeta_i + \zeta_m$)[27], v_m is an electron neutral collision and C is constant, P is the applied power or power absorbed.

$$\mu = \frac{(B(p)\sqrt{\frac{P}{V_m}})^2}{D\pi^2} \tag{4.19}$$

$$A = \frac{(B(p))^2}{D\pi^2} \tag{4.20}$$

$$\mu = A\frac{P}{v_m} \tag{4.21}$$

Hence it can be seen from eq. 4.21 that bifurcation parameter is the depending on the terms i.e. applied power and working gas pressure. According to the theory and observations, at certain combinations of input power and working pressure μ becomes μ_c (critical value for bifurcation) where plasma column bifurcates in a transverse axis, hence

$$\mu_c = A\frac{P_c}{v_{m_c}} \tag{4.22}$$

$$\frac{\mu}{\mu_c} = \frac{P}{P_c}\frac{v_m}{v_{m_c}} \tag{4.23}$$

It is clearly evident from eq. 4.23 that $\mu > \mu_c$ for all the values of $P > P_c$ and $v_m > v_{m_c}$. Hence, as soon as the value of bifurcation parameter μ increases from its critical value μ_c, stable modes become unstable which means plasma column bifurcates in stationary blobs.

4.4 Modelling and Simulation of Plasma Antenna having SPDP

In this section, plasma antenna having its classical state called SPDP is modelled and simulated using CST microwave studio. It uses FEM technology to discretizes the problem space and solved Maxwell's equations to analyze the transport properties of the model. In CST software, Drude module is considered to design the plasma antenna. In software, two model of plasma antenna having 4 and 5 blobs are modelled and simulated. The designing parameters which are utilised in Drude module are extracted from the experimental setup of plasma antenna array. The photograph of designed plasma antenna array is shown in Fig. 4.4 whereas its list of designing parameters are given in Table 4.2.

The designed modelled of both plasma antennas array are simulated for the transmission parameters. For analysis, discrete port is assigned to plasma antenna at one end whereas at bottom PEC (perfect electric conductor) plate is acting as infinite ground. The simulation outcomes are presented in terms of transmission S parameters upto operating frequency $500MHz$. The perspective comparison of S_{21} parameters of both plasma antenna array is shown in Fig. 4.5.

From S_{21}-parameter, it can be observed that the four different resonant frequencies are obtained for both plasma antenna. The plasma antenna with 4 blobs resonant at frequency $56MHz$ whereas in case of 5 blobs, it resonant at three frequencies i.e. $73MHz$, $178MHz$ and $390MHz$ respectively. At theses resonant frequencies, the return loss characteristics

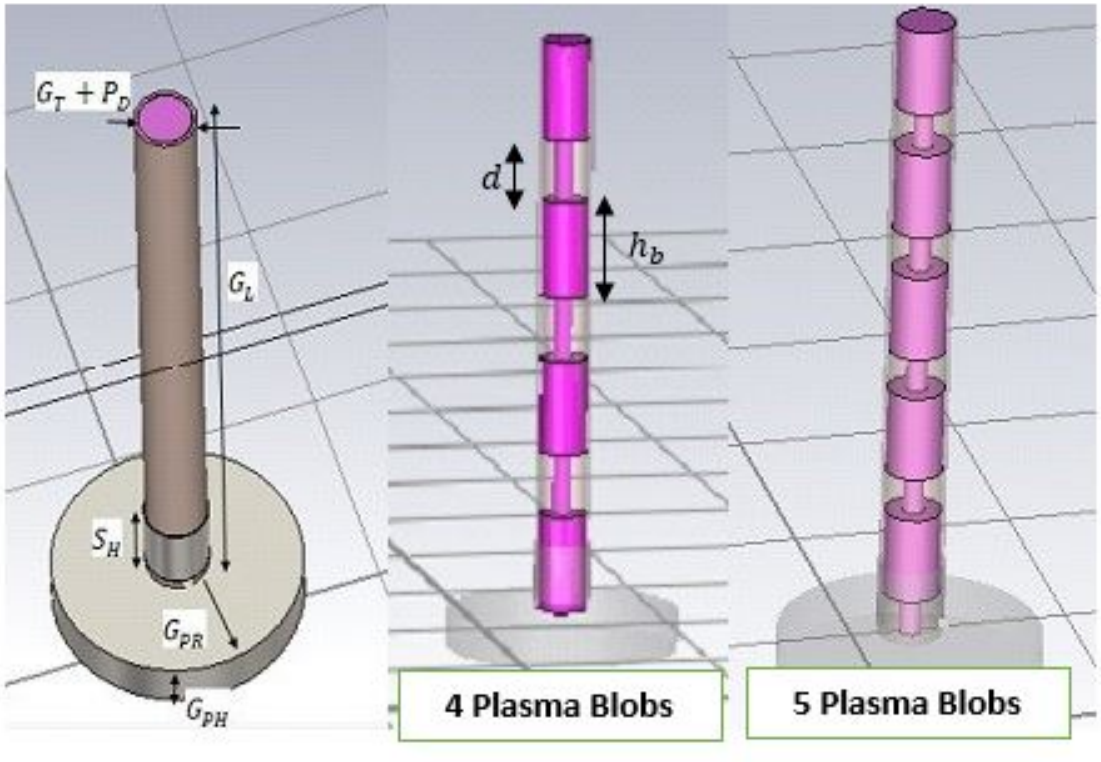

Figure 4.4: Simulation model of plasma antenna array having 4 and 5 blobs (SPDP)

Table 4.2: Parameters for simulated model of plasma antenna with 4 Blobs and 5 Blobs.

Parameters	4 Blobs(cm)	5 Blobs(cm)
Glass Tube Length, G_L	30	30
Glass Tube Thickness, G_T	0.2	0.2
Plasma blobs height, h_b	5	4.5
Plasma blobs spacing, d	3.3	2.4
Plasma Diameter, P_D	1.3	1.3
Plasma Density, n_e	$2.47\text{x}10^{10}$	$5.85\text{x}10^{10}$
Sleeve Height, S_H	3	3
Sleeve Thickness, S_T	0.02	0.02
Ground Plate Height, G_{PH}	3	3
Ground Plate Radius, G_{PR}	6	6

are $-30.67dB$, $-15.12dB$, $-22.44dB$, $-10.76dB$ respectively. These obtained resonant frequencies are the operating frequency of antenna which can be reconfigured by changing the plasma parameters.

Further, both plasma antenna array are simulated for the analysis of radiation patterns at the evaluated resonant frequencies. The simulated polar plot of both antenna is presented in Fig. 4.6. The radiation pattern of the antenna is analysed for the case of the multiple stationary blobs i.e. 4 and 5 respectively. These striations are observed as a collinear array arrangement where the blobs parameters mainly decide the radiation characteristics. It can

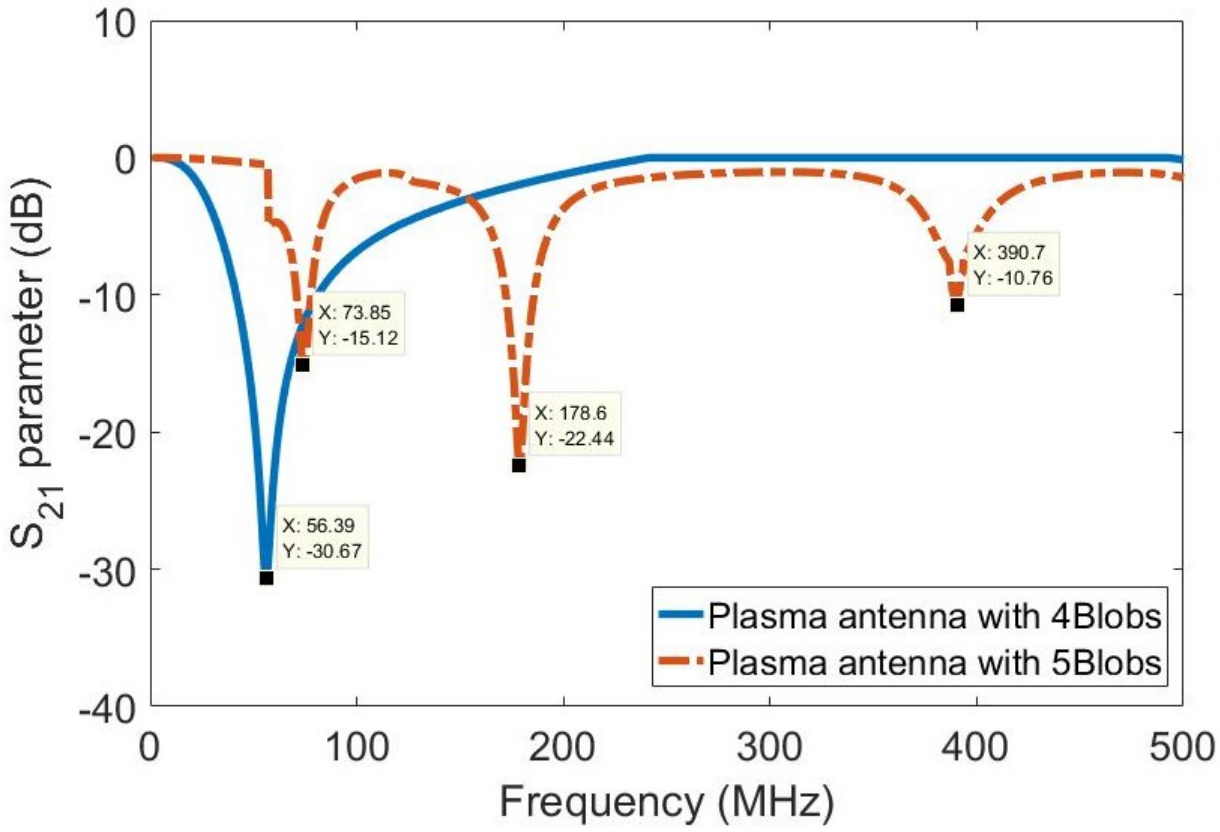

Figure 4.5: S_{21} parameters of plasma antenna having 4 and 5 blobs

be seen that the radiation pattern of plasma antenna changes as the frequency increases. At $56MHz$, the beamwidth and gain of the radiation is less which become more as the frequency approaches to $178MHz$. It can also be observed that at frequency $390MHz$ the direction of beamwidth is changed from broadside to endfire. In this investigation, the study explores that the incorporation of plasma blobs in a column acts as an antenna array [42] which improves the overall gain and also enable an option of beam steering as compared to the continuous plasma antenna which is mentioned in previous chapter.

Further, a theoretical analysis has also been presented which explains the obtained results explicitly. The schematic of the N element plasma based collinear antenna array is shown in Fig. 4.7. Here, each of the blob of height h_b is placed along the axis with uniform spacing, d between the blobs. The total electric field radiated from N-elements of the array with uniform spacing and progressive phase difference between the elements are,

$$E_T = E_{\theta_1} + E_{\theta_2} + E_{\theta_3} + ... + E_{\theta_N} \tag{4.24}$$

$$E_T = E_0 e^{0j\phi} + E_0 e^{j(\phi_2 + kdcos\theta)} + ... + E_0 e^{j(\phi_N + (N-1)kdcos\theta)} \tag{4.25}$$

where

$$E_0 = I_0 \frac{e^{-jkr}}{4\pi r}, E_T = E_0(A.F) \tag{4.26}$$

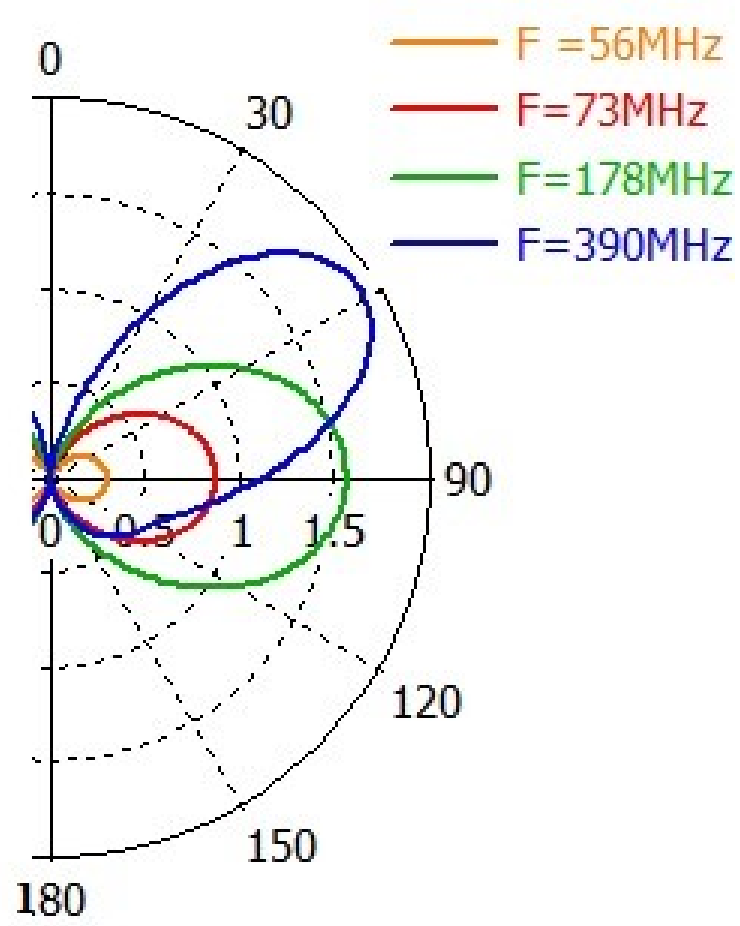

Figure 4.6: Polar plot of radiation patterns of plasma antenna at resonant frequencies

The Array factor is

$$A.F = (1 + e^{j\varphi} + e^{2j\varphi} + ... + e^{(N-1)j\varphi} \tag{4.27}$$

$$A.F = \frac{Sin\frac{N\varphi}{2}}{Nsin\frac{\varphi}{2}} \tag{4.28}$$

Where $\varphi = kdcos\theta + \phi$, the phase difference of the field, k is wave vector, ϕ is a progressive phase difference between two blobs. The direction of maximum radiation is defined as follows,

$$\theta_N = \cos^{-1}\frac{\lambda\phi}{2\pi d} \tag{4.29}$$

$$\phi = kd, wherek = jk_0\sqrt{1 - \frac{\omega_p^2}{\omega^2}} \tag{4.30}$$

The progressive phase changes due to the distinct plasma density profile of plasma blobs along the column. The First Null beamwidth of broadside antenna with collinear arrangement antenna,

$$\text{BWFN} = \frac{2\text{m}\lambda}{\text{nd}} = \frac{2\text{m}\lambda}{\text{L}} \tag{4.31}$$

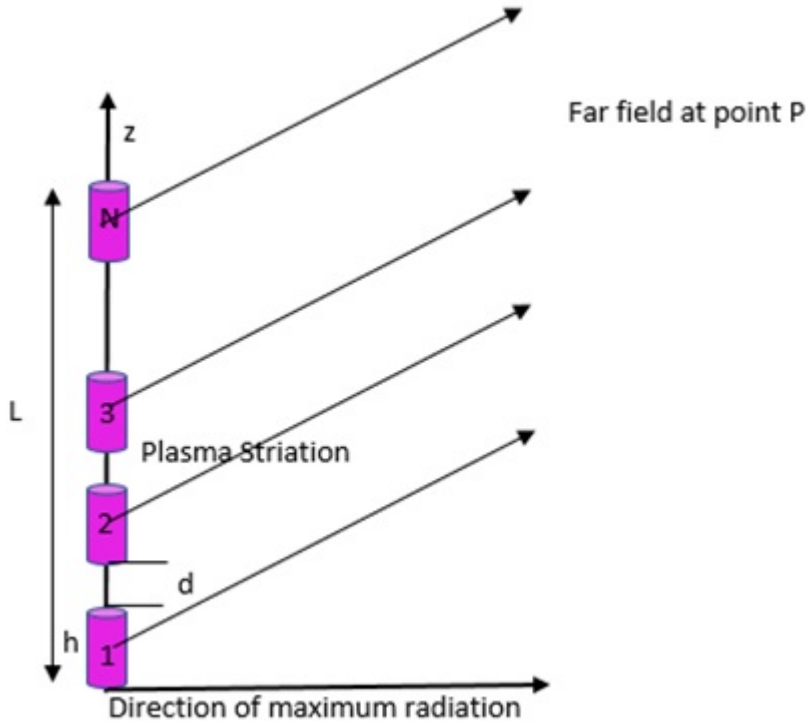

Figure 4.7: Schematic of the N-element plasma antenna array

$$\text{HPBW} = \frac{\text{BWFN}}{2} \tag{4.32}$$

$$D_r = \frac{2L}{\lambda} \tag{4.33}$$

By considering the above eq. 4.29-4.33 of beamwidth and direction of maximum radiation, it can be analysed that the beamwidth and direction of radiation can be controlled by a number of blobs and spacing between the blobs. The parameters n and d are the functions of plasma properties that can be altered by changing the value of input power and gas pressure.

In our case of blobs, the spacing between the blobs is smaller for lower frequency which provides a wider polar pattern and directive towards the 90 degrees. As the frequency increases, the effective length of antenna become larger that increases the spacing parameters d between the blobs which significantly narrow the beamwidth of antenna which is clearly interpreted from Fig. 4.6. This similar effect can be seen in metallic antenna array [6] where the beamwidth of antenna becomes narrow with the increases in number of elements and spacing between the elements. Moreover, the shifting effect in main lobe of antenna array appears is due to the progressive phase difference between the plasma blobs. The value of ϕ is depended on the plasma parameters and operating frequency that can be varied to introduce

the phase between the blobs and significantly influence the radiation parameters of plasma antenna which can be clearly seen in investigated outcomes. The study explores that the maximum radiation direction of plasma antenna array can be reconfigured by changing the array parameters like element spacing, number of elements and progressive phase difference, etc. by controlling plasma properties that are the function of input operating parameters. This property introduced a reconfigurability feature in plasma antenna where its radiation characteristics are reconfigured as per requirement. Based on the simulation outcomes, the developed plasma antenna array is tested for these resonant frequencies which is described in next section.

4.5 Measured and Testing Results

4.5.1 Experimental Results

The developed experimental setup of plasma based collinear antenna array is tested for the investigation of radiation pattern at different plasma properties and resonant frequencies. To measure the radiation characteristics, same setup of an automated radiation measurement system is utilised which is explained in Chapter 3. A testing procedure is beginning with the formation of plasma column having stationary standing plasma density pattern called plasma blobs (striations) at the critical combination of power ($75Watts$) and gas pressure ($0.025mbar$). Once the 4 plasma blobs inside the glass tube is created and become stable with density profile $2.47 \times 10^{16}m^3$, than RF signal of $56MHz$ frequency is applied to the glass tube via. capacitive sleeve from the signal generator. The radiation from the antenna is measured by the reference antenna which is connected to the moving probe of the automated system. The reference antenna is in far-field region ($R < 2\pi/L$) and rotate in azimuthal plane with the precision of 1 degree. Further, 5 plasma blobs inside column are formed by varying input parameters and having plasma density profile $5.85 \times 10^{16}m^3$. Similar approach is used to capture its radiation patterns at resonant frequencies i.e. $73MHz$, $178MHz$ and $390MHz$. The captured radiation patterns in elevation plane at these frequencies are shown in Fig. 4.8.

4.5.2 Comparison of Experimental and Simulation Outcomes

The perspective comparison of experimental results with simulation outcomes of plasma antenna array at these resonant frequencies for $0.3m$ long plasma column are shown in Fig. 4.9. It can be observed that the radiation patterns of antenna changes in a similar manner as obtained from simulation outcomes. At frequency $73MHz$, beamwidth of antenna is wider and measured 54 degrees. As the frequency increases to $178MHz$, the beamwidth changes

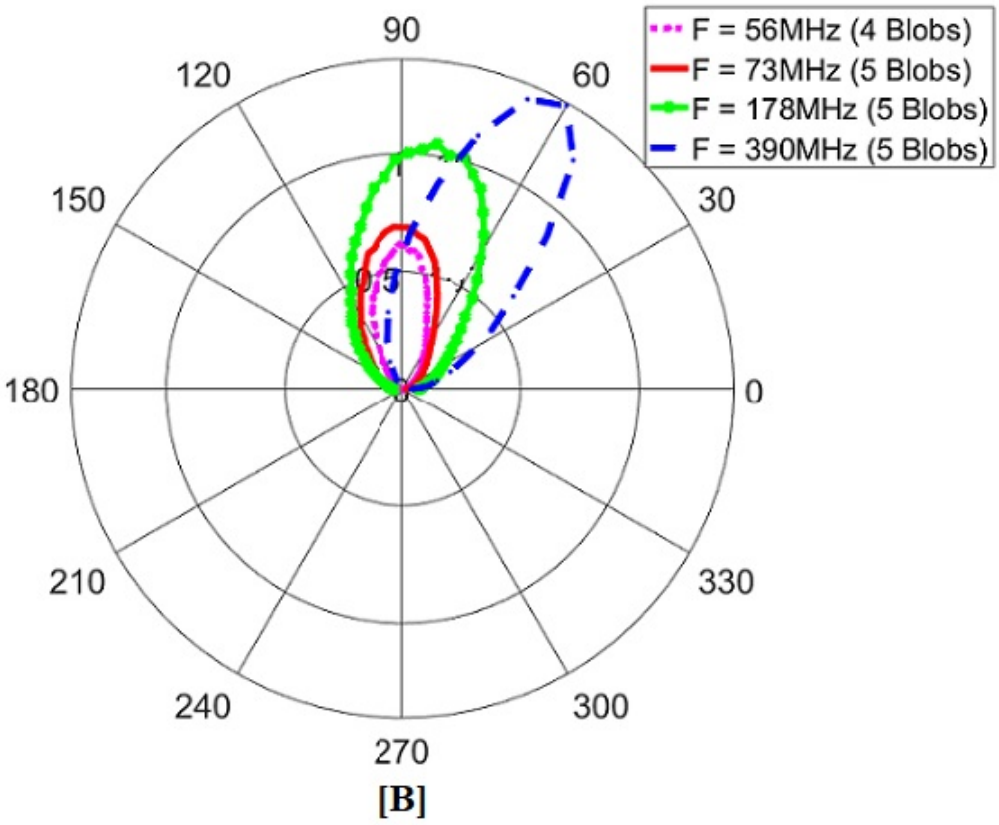

Figure 4.8: Polar plot of radiation patterns of plasma antenna array at resonant frequencies

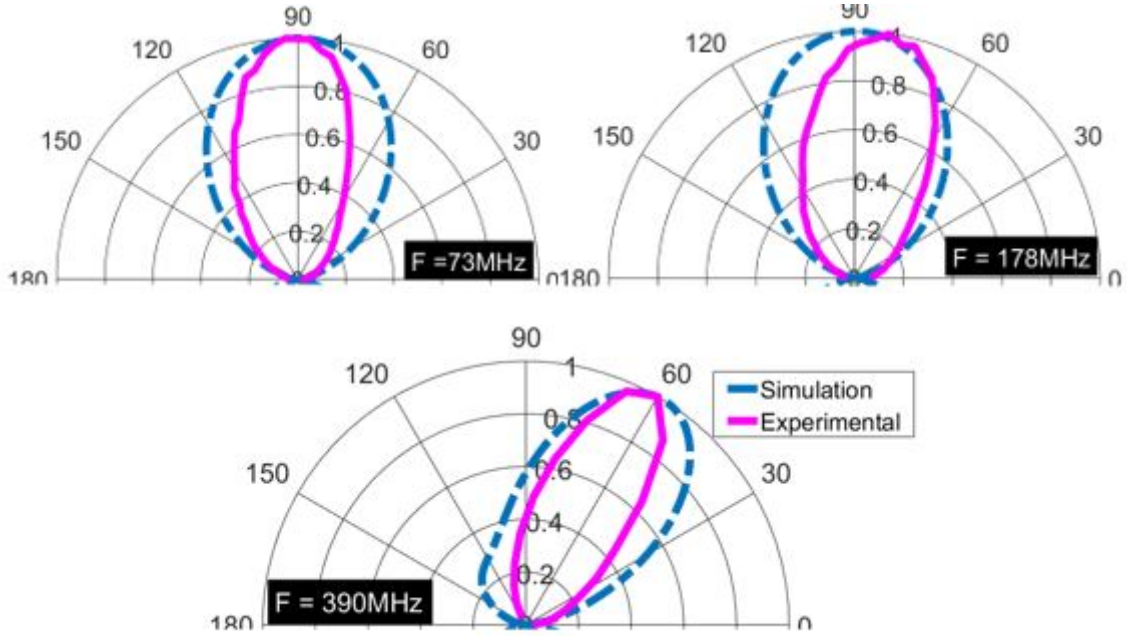

Figure 4.9: Perspective comparison of experimental and simulation results for plasma antenna array (a)$73MHz$ (b)$178MHz$ (c)$390MHz$

which is reduced by 15 degrees with slight shift in direction of radiation. At $390MHz$, the beamwidth of antenna become narrower and also shifts toward the endfire. The finding

reveals that the plasma antenna array behaves as a metallic antenna array where its radiation characteristics can be controlled by plasma properties. The experimental outcomes verify the simulation outcomes and found in good agreement.

Summary

This chapter evaluates the radiation characteristics of a plasma column for its classical state called plasma striations. These are the state of sustained radiating arrays of blobs, where the radiation pattern is mainly dominated by the blobs parameters. Therefore, the antenna can be electrically reconfigured with plasma parameters without changes in the physical size of plasma column. This feature has useful applications in the field of defense, homeland security, long-distance communication. The presented work utilizes an experimental setup of plasma antenna which incorporates plasma and vacuum system, RF signal source and automated radiation measurement system. The developed experimental setup is capable to tune the plasma parameters and operating frequency of the antenna as per desired where the inbuilt radiation measurement system captures the radiation in different planes. The created experimental setup is a useful development for the study of plasma devices like plasma antenna, plasma photonic crystal, plasma-based frequency selective surface etc.

Chapter 5

DESIGN AND DEVELOPMENT OF SINGLE COLUMN PLASMA PHOTONIC CRYSTAL USING PLASMA BLOBS

5.1 Overview

This chapter mainly conceptualises a reconfigurable one-dimensional Single Column Plasma Photonic Crystal (SC-PPC). The SC-PPC is a glass column containing stationary Standing Plasma Density Patterns (SPDP) called plasma blobs, where its density varies sinusoidally along the column axis. It appears like a collinear array of the plasma blobs which are produced by having the critical combination of input RF power and gas pressure in a column. The numbers of blobs and plasma density can be controlled by RF power and gas pressure. The value of plasma density is measured for the different nos. of plasma blobs formation by using the experimental setup of interometry. The measured data has been utilized in the modelling of SC-PPC. The SC-PPC is simulated for the analysis of Photonic Bandgap (PBG) with various plasma parameters like plasma density, shape and size of blobs etc. The additional features of modelled SC-PPC over conventional PPC are its small in size, tunable lattice constant, and simple structure that can enable wide application scope in various fields ranging from communication to defence.

5.2 Experimental Setup

This chapter presents a novel structure of plasma photonic crystal with a single column, called SC-PPC. Generally, plasma photonic crystal are the structure having periodic arrangement of dielectric layer A and plasma layer B with the thickness of d_a and d_b respectively. The relative permittivity of layers A and B are taken as ϵ_d and ϵ_p. Its periodicity, $\triangle = d_a + d_b$, also known as the lattice constant. The schematic of $1D$ PPC is shown in Fig. 5.1.

In our experiment, this periodic structure of PPC has been formed by considering the single column containing stationary standing plasma density patterns. The schematic of experimental model of SC-PPC is shown in Fig. 5.2.

The SPDP in a column is the classical state of plasma which is created by using the same experimental setup presented in Chapter 4. The detailed description of the components and

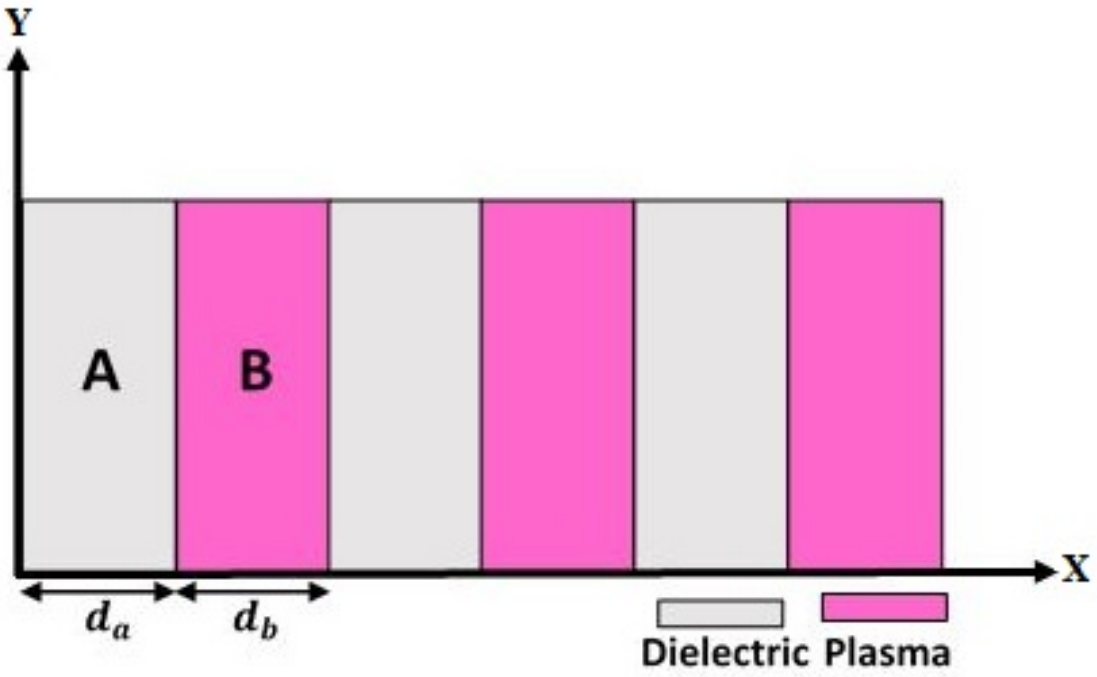

Figure 5.1: Schematic of $1D$ Plasma Photonic Crystal (PPC) with dielectric and plasma medium

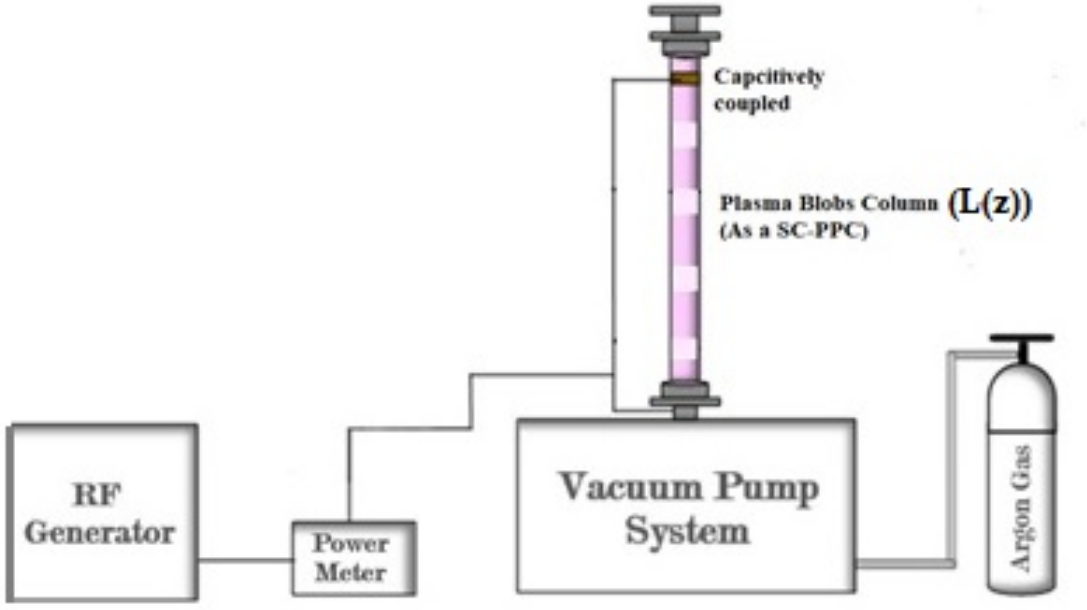

Figure 5.2: Schematic of SC-PPC experimental setup

fundamental theory to form SPDP in a single column has been already discussed in section 4.2 and 4.3. This classical state of plasma is generated at considerably low gas pressure and high-power input as compared to the continuous state of plasma. In our experiment, 4 to 6 nos. of plasma blobs have been formed by tuning the RF power and gas pressure at different values in the range of $40 - 80 Watts$ and $0.015 - 0.045 mbar$ respectively. The photograph

of developed plasma blobs is shown in Fig. 5.3 and corresponding its physical parameters are given in Table 5.1.

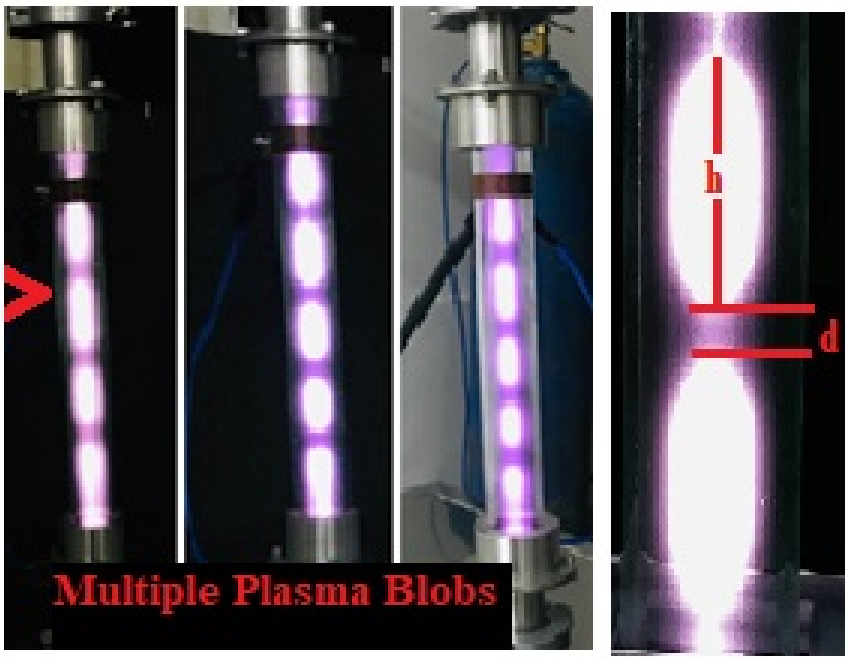

Figure 5.3: Experimentally produced SPDP with 4 to 6 plasma blobs in a single column for critical values of RF power and gas pressure

Table 5.1: Physical parameters of experimentally developed SPDP with 4 to 6 plasma blobs in 30cm long column.

Gas pressure (P_r) ($mbar$)	RF Power (P_0) ($Watts$)	Blobs size (cm)
0.015-0.025	75-80	4blobs(h = 5, d= 3.3)
0.025-0.035	65-75	5blobs (h = 4.5, d =2.4)
0.035-0.045	55-65	6blobs (h = 3.5, d = 1.8)

This developed SPDP is considered as a SC-PPC periodic structure of plasma and air medium which is utilised to investigate the photonic bandgaps characteristics (PBG). For PBG analysis, an experimental data of developed SC-PPC are extracted by using interferometry technique which is explained in subsection below.

5.2.1 Interferometry Setup

An interferometry setup is developed for the measurement of plasma density of blobs inside a column which is shown in Fig. 5.4. The setup includes two Vivaldi antennae having operating bandwidth $2.4GHz - 18GHz$ and antenna beamwidth 30°. In setup, both antennas

are wired up with Vector Network Analyzer (VNA) and placed in horizontal polarization across the column to transmit and receive signal. The distance between the both antenna is $3.0cm$. A VNA (RS ZVH8) is the device which is capable to capture the transmission parameters upto the $8GHz$. The interferometer resolution mainly depends on the antenna beamwidth and the distance between the antenna. The resolution of the interferometer is greater than $3.5cm$ which is the lowest blob height. Therefore, it is unable to correctly measure the density in gap between blobs, $d \leq 3$. However, it is capable to measure the blob density without any interference by the nearby blobs.

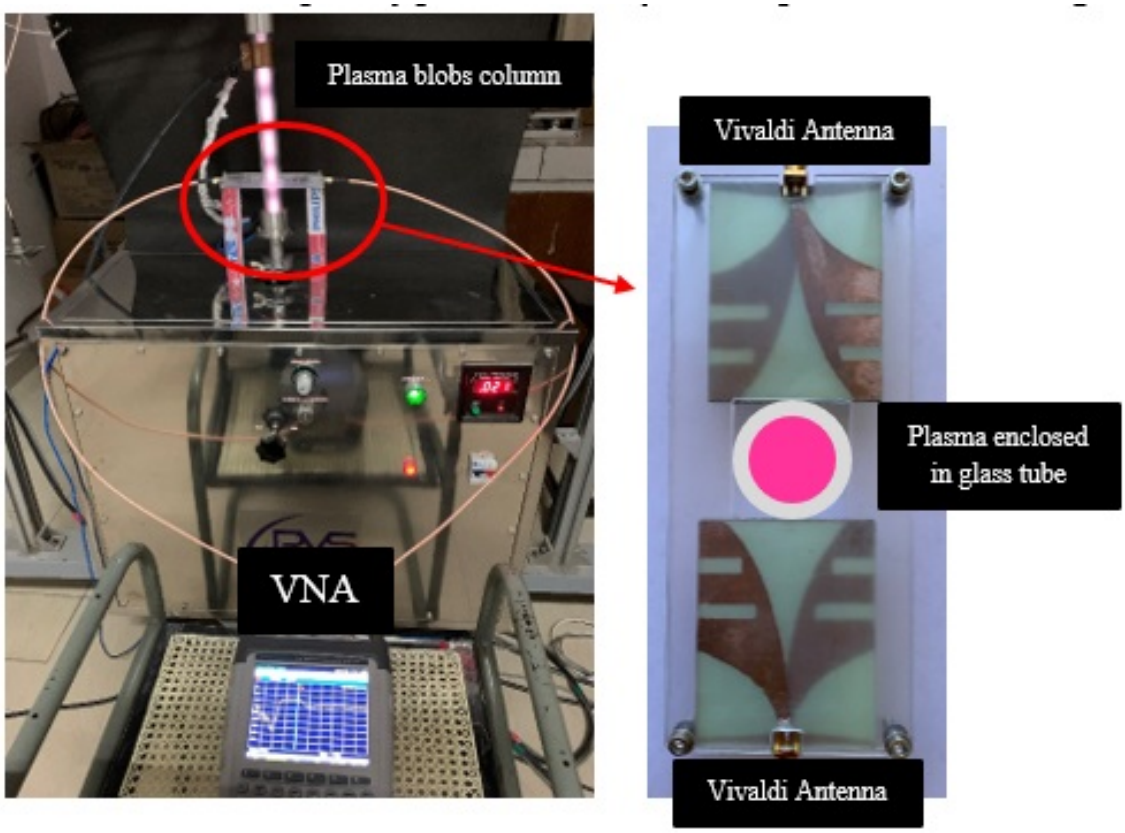

Figure 5.4: Interferometry setup for the measurement of plasma density of the blob.

To evaluate the plasma density of blob, column of having six blobs is formed at given pressure ($P_r = 0.040mbar$) and RF power ($P_0 = 60Watts$). The transmission S-parameters (with phase and magnitude) upto the range of $1-8GHz$ are captured 50 times with a delay of $10s$ by using the VNA. Based on the captured data of S_{21}-parameter, plasma density has been calculated for all 50 samples using a standard interferometer technique as mentioned in the earlier study by Howlader[80]. An isotropic and un-magnetized plasma having refractive index $\mu = \mu - j\chi$, can be written as,

$$\mu = \left[\frac{1}{2}\left(1 - \frac{\omega_p^2}{\omega^2 + v_m^2}\right) + \frac{1}{2}\left[\left(1 - \frac{\omega_p^2}{\omega^2 + v_m^2}\right)^2 + \frac{v_m^2}{\omega^2}\left(1 - \frac{\omega_p^2}{\omega^2 + v_m^2}\right)^2\right]^{1/2}\right]^{1/2} \tag{5.1}$$

$$\chi = \left[-\frac{1}{2}\left(1 - \frac{\omega_p^2}{\omega^2 + v_m^2}\right) + \frac{1}{2}\left[\left(1 - \frac{\omega_p^2}{\omega^2 + v_m^2}\right)^2 + \frac{v_m^2}{\omega^2}\left(1 - \frac{\omega_p^2}{\omega^2 + v_m^2}\right)^2\right]^{1/2}\right]^{1/2} \tag{5.2}$$

where ω and ω_p are the angular wave frequencies in the medium air and plasma, v_m is the electron-neutral collision frequency. The term $k = \alpha + i/\delta$ is the propagation constant in the plasma where $\alpha = (\omega/c)\mu$. The skin depth, δ is given as $(1/\delta) = (\omega/c)\chi$. The signal propagating in the plasma can be written as,

$$E(z,t) = Re(E_0 e^{j(\omega t - kz)}) \tag{5.3}$$

Attenuation of an EM wave in the plasma can be written as

$$\alpha(dB) = 10log_{10}(E/E_0)^2 = 10log_{10}(e^{-2d/\delta}) \tag{5.4}$$

$$\alpha(dB) = 10log_{10}(e^{-2d\omega/c}) = f(n_e, v_m, \omega, d)$$

The phase change of the propagating wave at distance d in the plasma is $\phi = (\omega/c)\mu d$ and in free space is $\phi_f = (2\pi/\lambda)d$. The phase shift arises due to the EM wave propagating in the plasma and free space can be written as,

$$\Delta\phi = \phi - \phi_f = ((\omega/c)\mu - 2\pi/\lambda)d = g(n_e, v_m, \omega, d) \tag{5.5}$$

From above eq. 5.4 and 5.5, it is seen that attenuation and phase shift (α and $\Delta\phi$) are the function of plasma parameters (n_e and v_m), and the incident wave parameters (ω and d). The value of ω and d are constant for a specific signal and experimental configuration. By experimentally measured the phase shift and attenuation of signal in plasma, the value of plasma density and collision frequency can be calculated by using the eq. 5.4 and 5.5.

The plot shown in Fig. 5.5 presents the plasma density of blob formed at $60Watts$ and $0.040mbar$ vs samples where its average gives the plasma density number, $n_e = 9 \times 10^{16} m^{-3}$. The measured plasma density number is also verified with our theoretical calculation by using density formulation which are presented in Chapter 3. The plasma density can be estimated using the formula $n_e = A(p)\sqrt{P_0}$ which is linearly dependent on the variable $A(p)$ and RF power applied to a column for the formation of plasma. $A(p)$ is the constant parameter whose value is dependent on the gas pressure (P_r). The plot shown in Fig. 5.6 presents the theoretical calculation for the plasma density at variable values of applied RF power (P_0) to the column at fixed gas pressure $P_r = 0.040mbar$. The extracted data of blobs in terms of plasma density, lattice constant, nos. and size of blobs etc. is utilised to model the SC-PPC using software for the analysis of PBG which is explained in next section.

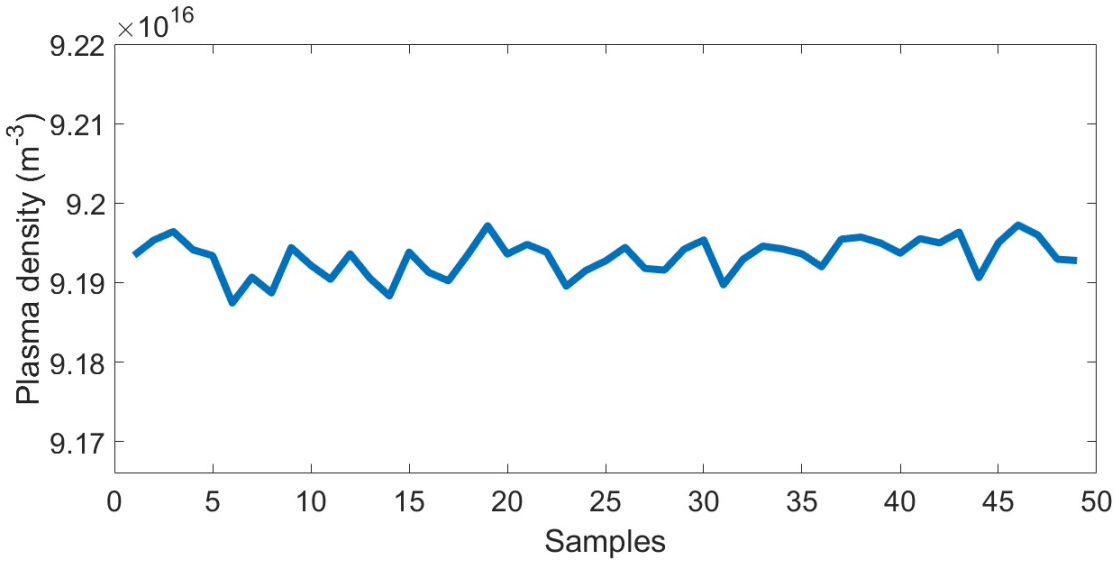

Figure 5.5: Measured plasma density of SPDP with 6 blobs vs 50 samples at $60 Watts$ and $0.040 mbar$

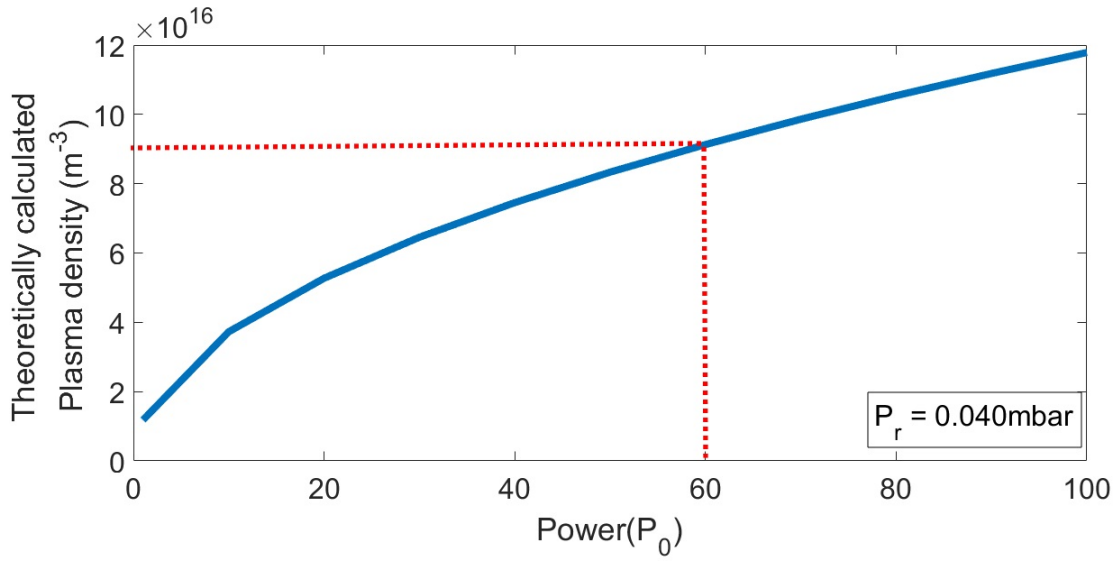

Figure 5.6: Theoretically calculated plasma density of plasma column for power $60 Watts$ and $0.040 mbar$ for 6 plasma blobs

5.3 Modelling and Simulation of SC-PPC

Based on the experimental data given in Table 5.1, SC-PPC has been modelled and simulated using $3D$ electromagnetic simulation software, CST microwave studio. The CST utilises the Finite Element Method (FEM) for the electromagnetic simulation. It discretizes the problem space into discrete elements and solved Maxwell's equations to analyze the transport properties of the model. Fig. 5.7 shows the front and side view of SC-PPC with detailed dimensional parameters of the model in tabulated form.

The SC-PPC model is a circular metallic waveguide containing the glass column with a plasma standing density pattern. The layers A and B highlight the plasma blob and air. The thickness dimension of layer A and B are taken from the experimental data i.e. $d_a = 3.5cm$ (plasma blob, h_b) and $d_b = 1.8cm$ (air, d) respectively. In the 1D SC-PPC structure, the lattice constant (Δ) is the sum of the thickness of layer A and B, $\Delta = d_a + d_b = 5.3cm$. In the simulation, plasma blobs are modelled by using Drude model parameters like plasma frequency (ω_p) and collision frequency (v_m) which are calculated based on the given input in terms of plasma density and nos. of blobs along with its physical dimensions by CST itself and explained in subsection below. The model is approximated by selecting the hexahedral meshing with cell size and resolution of $0.2mm$. The waveguide ports are assigned to both ends of the circular waveguide which are named port-1 and port-2 respectively. The Perfect Electric Conductor (PEC) has been assigned beyond the simulation space which provides an equivalent to metallic enclosure at the outer surface of SC-PPC. Simulation analyses transmission characteristics of SC-PPC in the fundamental transverse electric mode, TE_{11} mode.

5.3.1 Plasma Medium and its Fundamental Parameters

Plasma is a Debye dispersive medium with a relative permittivity $\varepsilon_p(\omega)$, permeability $\mu_p(\omega)$ and non-zero conductivity $\sigma_p(\omega)$, which are given in eq. 5.6 and eq. 5.7[9, 10],

$$\epsilon_p(\omega) = 1 - \frac{\omega_p^2}{\omega^2 + v_m^2} \tag{5.6}$$

$$\sigma_p(\omega) = \frac{\epsilon_0 \omega_p^2}{\omega^2 + v_m^2} \tag{5.7}$$

where $\omega and \omega_p = \sqrt{n_e e^2/m\epsilon_0}$ are the angular frequency and plasma frequency respectively, e is an electron charge, and m is a mass of an electron. The permeability of cold plasma is $\mu_p(\omega)$ which is 1. It can be seen from eq. 5.6 that the permittivity of the plasma medium can be adjusted by changing the wave frequency and plasma parameters (ω_p, v_m).

With the help of simulation software CST, the calculated plasma parameters ω_p is $5.7 \times 10^9 rad/sec$, $1.2 \times 10^{10} rad/sec$, and $1.6 \times 10^{10} rad/sec$ whereas v_m is $3.7 \times 10^7 Hz$, $1.6 \times 10^8 Hz$, and $2.9 \times 10^8 Hz$ for three values of densities of $n_e = 1 \times 10^{16} m^{-3}$, $n_e = 5 \times 10^{16} m^{-3}$, and $n_e = 9 \times 10^{16} m^{-3}$ respectively. The obtained collision frequencies are very low as compared to operating frequencies and plasma frequencies which has negligible effect on the plasma permittivity and also on PBG [63, 84, 95]. For the same reason, the effect of collision frequency is not taken into account in the analysis of PBG.

The relation between the plasma permittivity and incident frequency as well as the plasma density is shown in Fig. 5.8. It presents the frequency vs permittivity plot for

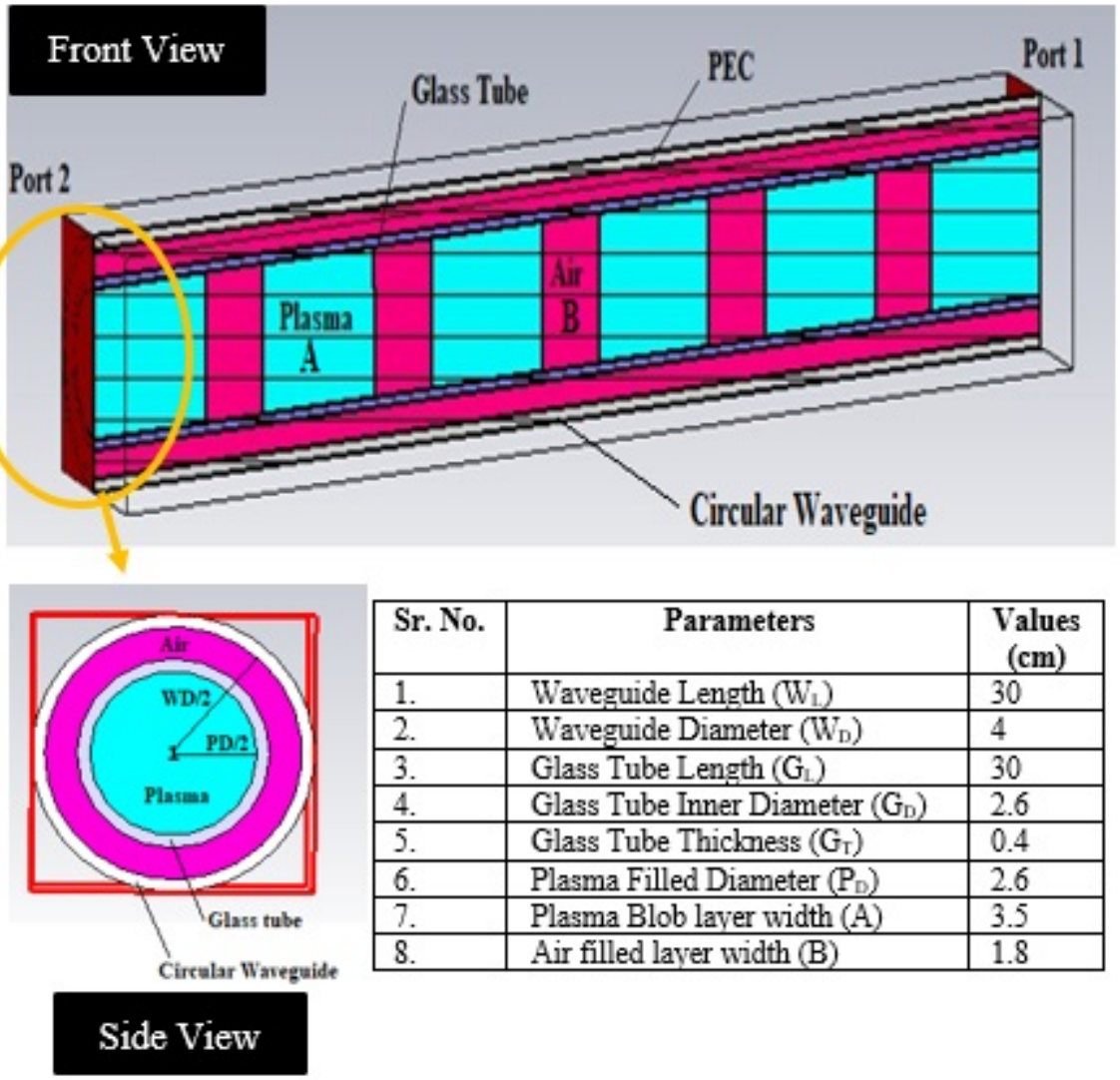

Sr. No.	Parameters	Values (cm)
1.	Waveguide Length (W_L)	30
2.	Waveguide Diameter (W_D)	4
3.	Glass Tube Length (G_L)	30
4.	Glass Tube Inner Diameter (G_D)	2.6
5.	Glass Tube Thickness (G_T)	0.4
6.	Plasma Filled Diameter (P_D)	2.6
7.	Plasma Blob layer width (A)	3.5
8.	Air filled layer width (B)	1.8

Figure 5.7: Cross-section view of the simulated model of $1-D$ SC-PPC structure and its designing parameters extracted from experimental data

variable plasma density obtained from experimental data, where the cut-off frequency ($\frac{\omega_p}{2\pi}$) are marked as $1.0GHz$, $2.01GHz$ and $2.7GHz$ for three plasma densities cases respectively. The cut off frequency is defined for the physical property of the plasma medium where the permittivity of plasma is zero.

Based on the cut off frequency, when $\omega < \omega_p$ the plasma dielectric constant is negative, whereas for $\omega > \omega_p$ plasma dielectric constant is positive. In the negative region where permittivity is negative, few TE waves of certain frequencies is able to propagate in the photonic crystal structure because of the local resonance which is associated with the surface plasmon wave. In positive permittivity region, some waves of certain frequency will not able to travel in the PPCs structure due to the periodic scattering of EM waves on the plasma surface[87]-[94]. The result of two region is considered as PBG structure which will be produced in the region of the negative and positive permittivity respectively. The

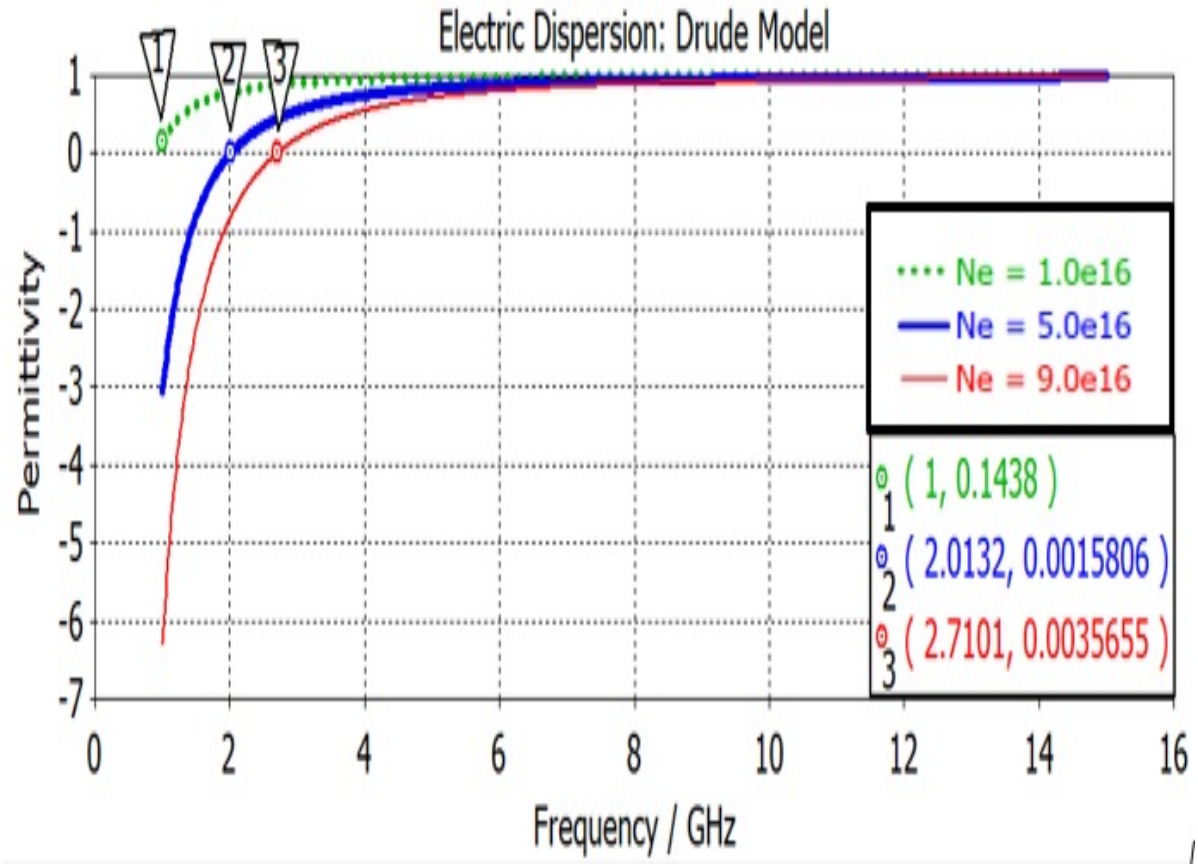

Figure 5.8: Real components of relative permittivity of the plasma for three cases of plasma densities

propagation of EM waves in the PPC is explained in below subsection.

5.3.2 Propagation of EM waves in SC-PPC

The SC-PPC is aligned in $x-$direction where $y-$axis is the direction of $E-$field polarization. The propagation of EM waves in SC-PPC follows the Helmholtz equation[63, 91] which is given as following,

$$\bigtriangledown \times \left(\frac{1}{\mu_r(r)} \bigtriangledown \times E_y(r) \right) - k_0^2 \left(\epsilon_r(r) - \frac{j\sigma}{\omega \epsilon_0} \right) E_y(r) = 0 \tag{5.8}$$

where $\epsilon_r(r)$ and $\mu_r(r)$ are the relative permittivity and permeability of the medium, σ is dielectric conductivity of the medium. $E_y(r)$ is the electric field at r, ϵ_0 is the dielectric constant of the vacuum which is 1. The term $k_0 = \frac{\omega}{c}$ is the wave vector, which is related to the angular frequency ω and c is the speed of light.

According to Bloch's theorem, the electric field can be expressed as a product of periodic functions and natural exponential products. Solution of eq. 5.8 presents the electric and

magnetic field as a function of time and space are given in eq. 5.9 and eq. 5.10.

$$E(r,t) = E_y(r)e^{i(\omega t - kr)} \tag{5.9}$$

$$H(r,t) = -\frac{i}{k_0\epsilon(r)} \bigtriangledown \times E(r,t) \tag{5.10}$$

The propagation of wave in SC-PPC structure depends on the physical properties of plasma and air medium which may able to formed the photonic bandgaps. For the analysis of PBG, the transmission of wave in SC-PPC is analysed which is explained in next section.

5.4 Simulation Outcomes and Discussion

To investigate the plasma photonic bandgap, SC-PPC simulation outcomes have been analysed. In the simulation, both ends of the SC-PPC are excited with waveguide ports which are named port-1 and port-2 respectively. Software excites any one of the ports at a time and solves it for the transmission and reflection parameters based on power transferred in between the ports. The S_{21} represents the transmission S-parameter which is the ratio of power at output and input ports. The transmission parameter, S_{21} is investigated for variable plasma permittivity and nos. of blobs over the 1-16GHz frequency range which are explained in the following subsections.

5.4.1 For Variable Plasma Permittivity

The PBG in $1D$ SC-PPC is the function of positive and negative plasma permittivity which directly depends on the values of plasma density. The modelling and simulation of SC-PPC have been carried out for the variable plasma density to investigate its effect on the PBG. Simulation outcome in terms of transmission S_{21} parameter is presented in Fig. 5.9.

The Fig. 5.9 shows the transmission parameters at plasma densities ($n_e = 5 \times 10^{16} m^{-3}$ and $n_e = 9 \times 10^{16} m^{-3}$) for 6 plasma blobs where the cut off frequency corresponding to these densities, $2.01GHz$ and $2.7GHz$ which is presented in Fig. 5.8. The brief discussion about the obtained results are given as follow,

- Change in plasma density reconfigures the PBG. It can be verified with the prospective comparison of PBG 3, PBG 4 and PBG 5 at $n_e = 5 \times 10^{16} m^{-3}$ and $n_e = 9 \times 10^{16} m^{-3}$ where the PBGs becomes more prominent and widened with slight shift towards the higher frequency.
- New PBGs have been also appeared as the plasma density is increased. It is marked as PBG 1 and PBG 2 in Fig. 5.9. Moreover, a significant change in PBG 3 can be observed against the $n_e = 9 \times 10^{16} m^{-3}$.

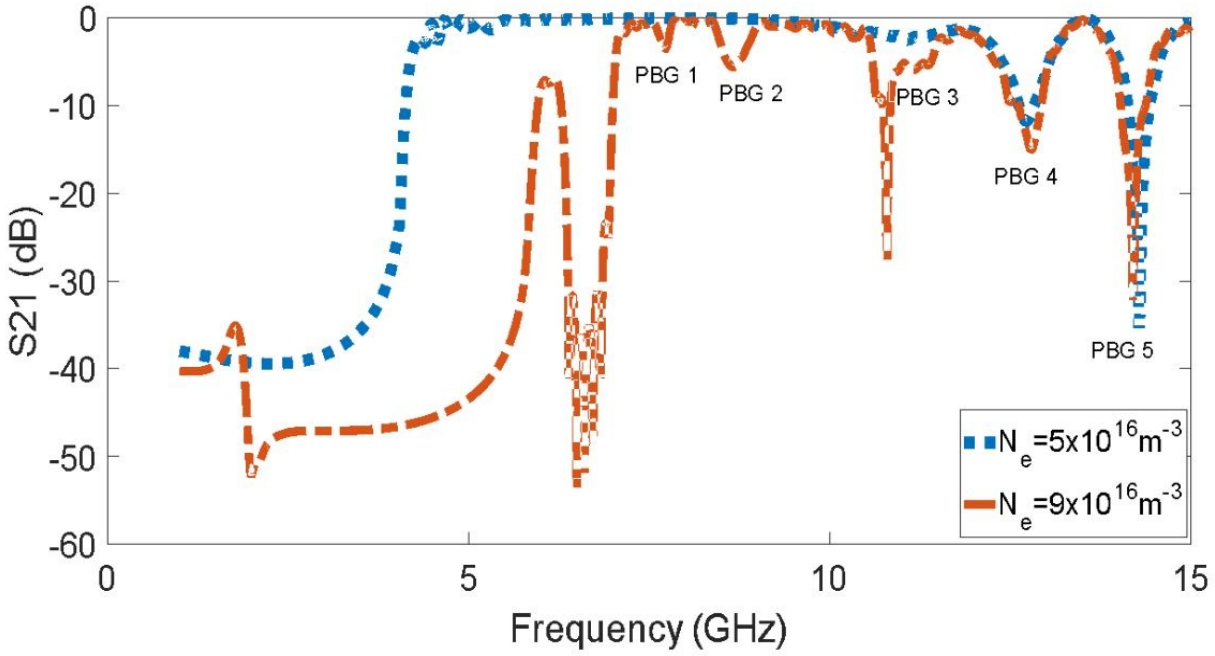

Figure 5.9: Transmission S_{21} parameter vs Frequency of $1D$ SC-PPC for the variable plasma density for 6 plasma blobs

- The change in plasma density significantly shifts the transmission of a wave toward the higher side. From Fig. 5.9, it can be seen that the transmission starts from $4.7GHz$ in case $n_e = 5 \times 10^{16} m^{-3}$ and it starts from $7.2GHz$ for $n_e = 9 \times 10^{16} m^{-3}$.

5.4.2 For Variable Plasma Blobs Numbers

Further, the SC-PPC is simulated by changing the plasma blobs numbers from 5 to 6 with change in a plasma density ($n_e = 2.45 \times 10^{16} m^{-3}$ in case 5 blobs, $n_e = 5 \times 10^{16} m^{-3}$ in case 6 blobs). The transmission S_{21} spectra for both of the cases are shown in Fig. 5.10. It can be observed that the PBG is also affected by the variation in the number of blobs and its positions. With the increase in the number of blobs from 5 to 6, the negative PBG is shifted towards the higher frequency whereas the bandgap is wider and deeper. A similar effect is observed in the case of variation of plasma density.

5.4.3 Analysis of Different Modes in SC-PPC

The SC-PPC model excited with TE_{11} mode at waveguide port 1 in $y - z$ which is shown in Fig. 5.11a. The Fig. 5.11b - 5.11g represent the electric field distribution (E_y) in $x - y$ plane across the column at variable frequencies.

In general, the EM waves having frequency which is below the cutoff frequency will not able to propagate in PPC. In SC-PPC for 6 blobs at $n_e = 5 \times 10^{16} m^{-3}$, negative region is

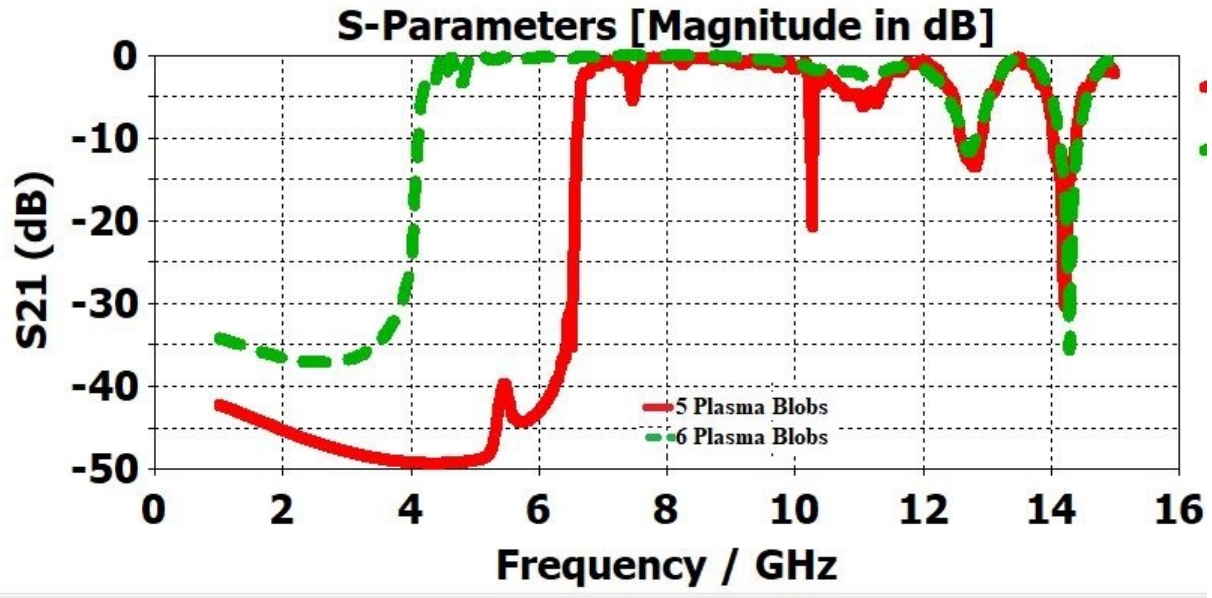

Figure 5.10: Simulated S_{21} parameter of $1D$ SC-PPC with various plasma blobs Structure

lied below the cutoff frequency i.e. $2.01GHz$ where the Fig. 5.9 shows a passband in the range of $4 - 6.45GHz$. The frequency of the surface wave is depending on the frequency of plasma ω_p and the dielectric constant of the air ϵ_r. As plasma frequency increases, surface modes will be shifted to the higher frequency range.

In the frequency range of $1 - 2.01GHz$, the electric fields in these modes is intended to concentrate their energy evenly on the medium surrounded the plasma. The modes which appear below the flat band zone are considered as Fano mode which can be seen in Fig. 5.11b. Above the cut off frequency, plasma work as a scattering medium. Like the conventional PCs, the positive PBG of the $1D$ PPCs is the result of the periodic scattering of waves on the surface of the scattering medium, in which the variable permittivity plays an important role. It can be seen from Fig.5.9, three PBG at frequency $11.2GHz$, $12.7GHz$ and $14.2GHz$ for PBG 3, PBG 4 and PBG 5 respectively. The electric field distribution at these bandgap are shown in Fig. 5.11d, 5.11e,and 5.11g. The Fig. 5.11c-5.11f are presenting the passband at $8GHz$ and $13.4GHz$ respectively where the electric field distribution presents the propagation of Electromagnetic waves in a plasma medium.

Summary

In this chapter, the design and simulation of $1D$ SC-PPCs are presented. SC-PPC is a standing plasma density pattern in a single plasma column. It has been comprehensively investigated as a reconfigurable PBG for the first time. Reconfigurability of SC-PPC is characterised using modelling and simulation where the plasma parameter has been received from the experimentation. The study outcomes show that the PBG of SC-PPC can

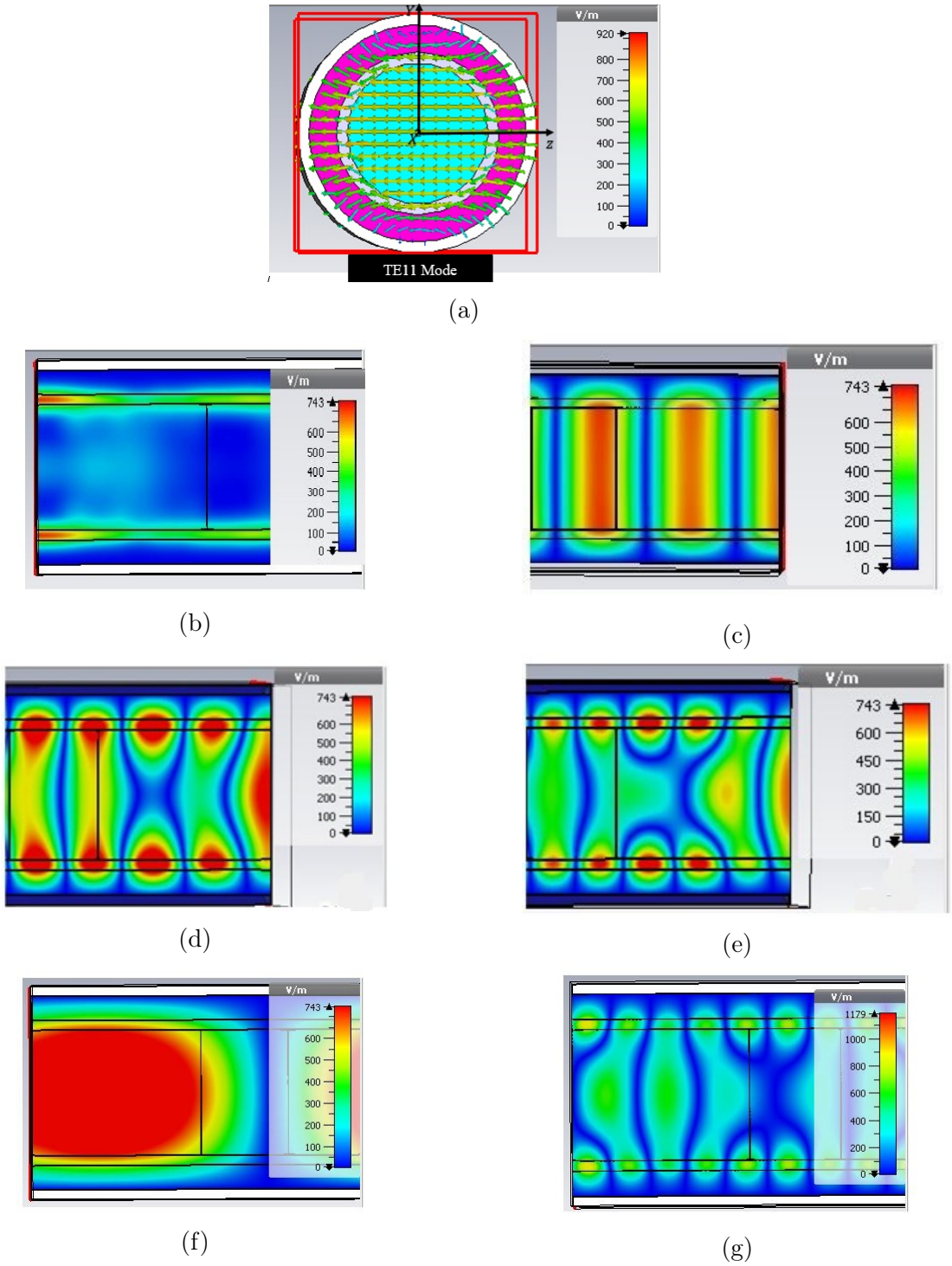

Figure 5.11: Electric field distribution for passband and bandgap across the negative and positive PBG of 1D SC-PPC for $Ne = 5 \times 10^{16} m^{-3}$ for 6 blobs (a) TE11 in y-z plane (b) Fano mode at 4GHz (c) Passband at 8GHz (d) Bandgap at 11.2GHz (e) Bandgap at 12.7GHz (f) Passband at 13.4GHz (g) Bandgap at 14.2GHz

be reconfigured by changing the plasma density and the standing plasma density pattern (plasma blobs). The structure of the $1D$ SC-PPC proposed is relatively convenient to rearrange the plasma properties by varying external parameters and provides an online option to control the propagation of the wave. The additional features of SC-PPC are its small in size, tunable lattice constant, and simple structure that can enable wide application scope in various fields ranging from communication to defence.

Chapter 6

DESIGN AND DEVELOPMENT OF RECONFIGURABLE PLASMA PHOTONIC CRYSTAL USING FLUORESCENT TUBES

6.1 Overview

This chapter describes the modelling and implementation of a two dimensional reconfigurable photonic bandgap (PBG) structure using low-pressure fluorescent tubes. The proposed $2D$ PPC model mainly consists of square lattice of 3×3 tubes array placed in free space. The dispersion relation of the PPC has been optimized by using mathematical modelling for the variable plasma density. Modelling of $2D$ PPC incorporates the actual plasma parameters which have been extracted from the experimental setup, where the variable plasma density is created by changing the applied AC potential. The developed PPC setup is implemented on test bench as per the mathematical modelling outcomes and tested using VNA (Vector Network Analyzer) for investigation of photonic bandgaps for variable plasma density. The main objective of the work is to conceptualize a reliable plasma-based structure for the development of microwave reflectors, filters, absorbers etc. which can have important applications in the field of radar, satellite and navigation.

6.2 Plasma Photonic Crystal (PPC) using Fluorescent Tubes

A two dimensional PPC is a periodic arrangement of fluorescent tubes aligned in free space where its schematic is shown in Fig. 6.1. In schematic, top and side view of PPC are shown which present a square lattice of 3×3 plasma tubes in the air. The permittivity of the fluorescent tube and air are presented with ϵ_t and ϵ_r. Similarly, the refractive indices are denoted as n_t and n_r respectively. Here, the lattice constant is denoted by Δ, which is the sum of tube diameter (d_t) and the distance between two consecutive tubes (d_r) i.e. $\Delta = d_t + d_r$.

Based on the proposed PPC structure, the modelling and theoretical analysis have been done by using MATLAB (MATrix LABoratory) programming language. In MATLAB, theoretical code has been written to analysis the dispersion characteristics of the $2D$ PPC

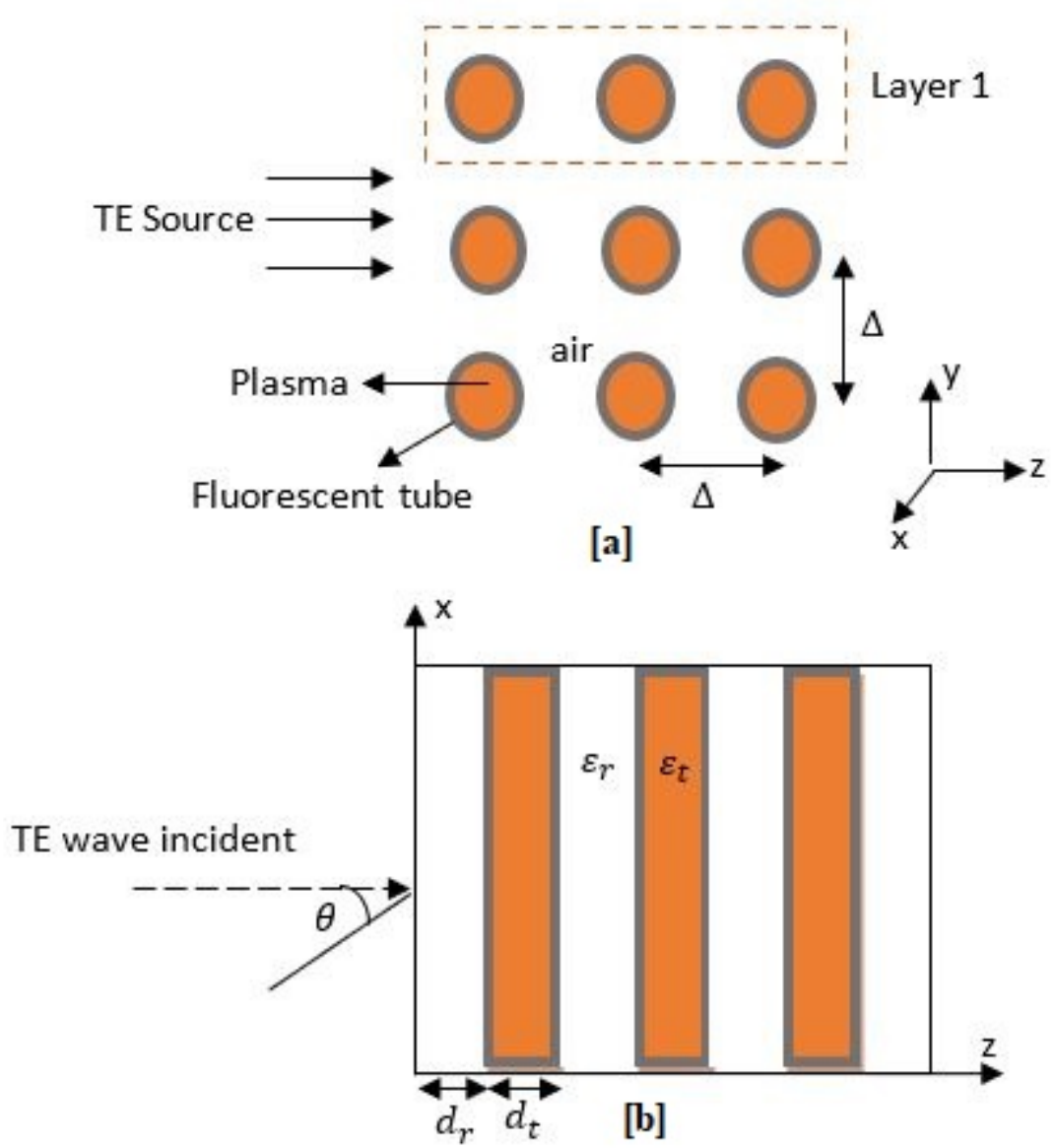

Figure 6.1: (a) Schematic of two-dimensional plasma photonic crystal (b) side view of PPC presents the plasma tubes placed in air.

structure. A modelling is done based on the formulation related to the dispersion relation which is presented in subsection.

6.2.1 Mathematical Modelling

In PPC structure, 3×3 array of fluorescent tubes of length $600mm$ with the diameter of $30mm$ are arranged in free space in x-direction with the periodicity $\Delta = 39mm$. The TE wave is incident on PPC structure from one side which propagate along the z-direction. A wave is incident with the angle θ to the boundary of the PPC at $z = 0$ and satisfies the

Helmholtz equation, i.e., given by [71]

$$\left[\frac{d^2}{dz^2} + (k_0^2\epsilon(z) - \beta_i^2)\right] E(z) = 0 \tag{6.1}$$

where, $k_0 = \omega/c$ is wave factor of free space where c is speed of light. The term $\beta_i = (n_i\omega/c)\sin\theta_i$ is the propagation constant in different layers of plasma, n_i is the refractive index of each layer and θ_i is the angle of propagation direction of the wave in any layer with normal direction. Here, EM wave frequency is below the plasma frequency. Therefore, solutions of eq. 6.1 for two different regions of the PPC can be written as follows [63, 70]:

$$E(z) = a_m e^{ik_1 z} + b_m e^{-ik_1 z}, m\Delta < z < m\Delta + d_r \tag{6.2}$$

$$c_m e^{ik_2 z} + d_m e^{-ik_2 z}, m\Delta + d_r < z < (m+1)\Delta$$

where a_m, b_m, c_m and d_m are the amplitudes of waves in forward and backward direction, respectively. The terms k_1 and k_2 are the wave component in air and plasma regions that can be expressed as,

$$k_1 = \frac{\omega}{c\sqrt{\epsilon_r}}\cos(\theta_r) \tag{6.3}$$

$$k_2 = \frac{\omega}{c\sqrt{\epsilon_t}}\cos(\theta_t) \tag{6.4}$$

The terms θ_r and θ_t presents the incidence angle of the wave in the air and plasma layer, respectively. The terms n_r and n_t are refractive index of region air and plasma,

$$n_t = \sqrt{\epsilon_t}\sqrt{\frac{\epsilon_0}{\mu_0}}\frac{1}{cos\theta_t} \tag{6.5}$$

$$n_r = \sqrt{\epsilon_r}\sqrt{\frac{\epsilon_0}{\mu_0}}\frac{1}{cos\theta_r} \tag{6.6}$$

For evaluating the optical properties of the proposed structure, the Transfer Matrix Method (TMM) has been used [76, 88]. Each layer i.e. air and plasma can be represented with transmission matrix parameter i.e. M_r and M_t as given below:

$$M_r = \begin{pmatrix} \cos(k_1 d_r) & \frac{-j}{n_r} sin(k_1 d_r) \\ -jn_t \sin(k_1 d_r) & \cos(k_1 d_r) \end{pmatrix} \tag{6.7}$$

$$M_t = \begin{pmatrix} \cos(K_2 d_t) + \epsilon_2 1 \tan\theta_t \sin(k_2 d_t) & -\frac{j}{n_t}[1 + (\epsilon_{21}\tan\theta_p)^2] \\ -jn_t \sin(k_2 d_t) & \cos(k_2 d_t) - \epsilon_{21}\tan\theta_t \sin(k_2 d_t) \end{pmatrix} \tag{6.8}$$

The term ϵ_{21} is the relative permittivity from dielectric to plasma medium. Now, transmis-

sion of wave through lattice can be written as,

$$\begin{bmatrix} a_{m-1} \\ b_{m-1} \end{bmatrix} = M \begin{bmatrix} a_m \\ b_m \end{bmatrix} \tag{6.9}$$

where, b_{m-1} and a_{m-1} are forward and reflected amplitude of wave at left boundary of the lattice whereas b_m and a_m are forward and reflected amplitude of the transmitted wave. The term M is the transmission matrix and given by the multiplication of transfer matrices of the two cascaded layers of plasma and air. It is evaluated in terms of the $ABCD$ parameters as:

$$M = M_r M_t = \begin{bmatrix} A & B \\ C & D \end{bmatrix} \tag{6.10}$$

The dispersion relation can be evaluated by considering the half trace of the transfer matrix M which is given by

$$\cos(k\Delta) = 1/2(A + D) \tag{6.11}$$

where, k is the Bloch wave vector which is basically described the conduction of an electron in the PPC structure. The terms A and D are the diagonal elements of transmission matrix and obtained from the matrix multiplication,

$$A = \cos(k_1 d_r)\cos(k_2 d_t) + \epsilon_{21}\tan\theta_t \cos(k_1 d_r)\sin(k_2 d_t) - \frac{n_t}{n_r}\sin(k_1 d_r)\sin(k_2 d_t) \tag{6.12}$$

$$D = \cos(k_1 d_r)\cos(k_2 d_t) - \epsilon_{21}\tan\theta_t \cos(k_1 d_r)\sin(k_2 d_t) - \frac{n_r}{n_t}[1 + (\epsilon_{21}\tan\theta_t)^2]\sin(k_1 d_r)\sin(k_2 d_t) \tag{6.13}$$

Putting the value of A and D in eq. 6.11, we get

$$\cos(k\Delta) = \cos(k_1 d_r)\cos(k_2 d_t) - \frac{1}{2}\left(\frac{n_r}{n_t} + \frac{n_t}{n_r}[1 + (\epsilon_{21}\tan\theta_t)^2]\right)\sin(k_1 d_r)\sin(k_2 d_t) \tag{6.14}$$

$$k = \frac{1}{\Delta}\cos^{-1}\left[\cos(k_1 d_r)\cos(k_2 d_t) - \frac{1}{2}\left(\frac{n_r}{n_t} + \frac{n_t}{n_r}[1 + (\epsilon_{21}\tan\theta_t)^2]\right)\sin(k_1 d_r)\sin(k_2 d_t)\right] \tag{6.15}$$

For analysis of dispersion relation of $2D$ PPC, variable operating plasma parameters and lattice constant of the structure have been calculated numerically and experimentally which are explained in next subsection.

6.2.2 Plasma Parametric Analysis

In PPCs, plasma is a variable medium, whose physical property mainly depends on the plasma density (n_e), plasma frequency (ω_p) and collision frequency (v_c). The plasma permittivity (ϵ_t) is given by [65, 72, 77],

$$\epsilon_t = 1 - \frac{\omega_p^2}{\omega^2 + v_c^2} \tag{6.16}$$

$$\omega_p = \sqrt{\frac{n_e e^2}{m\epsilon_0}} \tag{6.17}$$

The plasma density of the tube for different excitations has been measured using an interferometry technique which is detailed discussed in chapter 5. A schematic of a typical interferometer setup is shown in Fig. 6.2. It mainly consists of a pair of Vivaldi antennas connected with VNA and placed across the plasma tube. It measures the transmission scattering parameters with and without plasma inside the tube which is utilized further to calculate plasma density[80] based on the attenuation and phase shift of an electromagnetic wave which are given as follow,

$$\alpha(dB) = 10log_{10}(e^{-2d\omega/c}) = f(n_e, v_c, \omega, d) \tag{6.18}$$

$$\Delta\phi = \phi = \phi_f = ((\omega/c)\mu - 2\pi/\lambda)d = g(n_e, v_c, \omega, d) \tag{6.19}$$

To evaluate plasma density, 15 nos. of data samples measuring the transmission S-parameters has been taken with the delay of $10ns$ time interval for each excitation. Based on received data, plasma density has been calculated for all 15 samples using interferometer techniques. A plasma density plot for all samples with different excitations varying in the range of $100 - 240V$ is shown in Fig. 6.3. The average density for a single excitation can be considered as final plasma density.

A significant change in plasma density with applied voltage can be observed from the plot. The plasma density is also calculated as approximately zero for no excitation to the tube. In our experiment, plasma density is measured as $0.4 \times 10^{17}m^{-3}$, $1.3 \times 10^{17}m^{-3}$, $2.4 \times 10^{17}m^{-3}$, $3.7 \times 10^{17}m^{-3}$ and $5.3 \times 10^{17}m^{-3}$ at $100V$, $150V$, $200V$, $220V$ and $240V$ respectively.

Plasma permittivity is mainly a function of plasma density (n_e) and is also variable with wave frequency (ω) which is passing through PPC. Plasma permittivity is characterized in the range of $0.1 - 10GHz$ using measured plasma density and its plot is shown in Fig. 6.4.

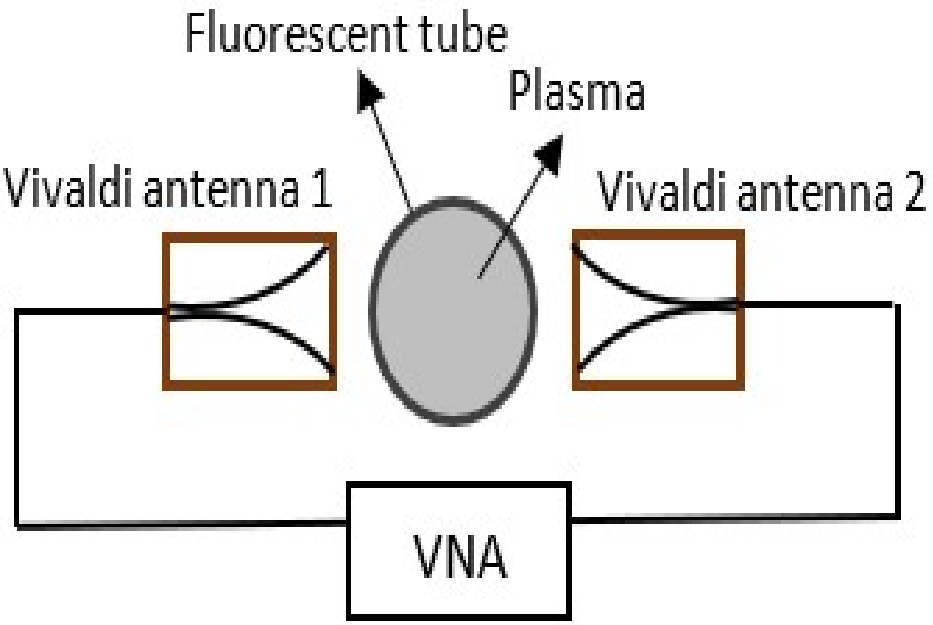

Figure 6.2: Schematic of interferometry for plasma density evaluation

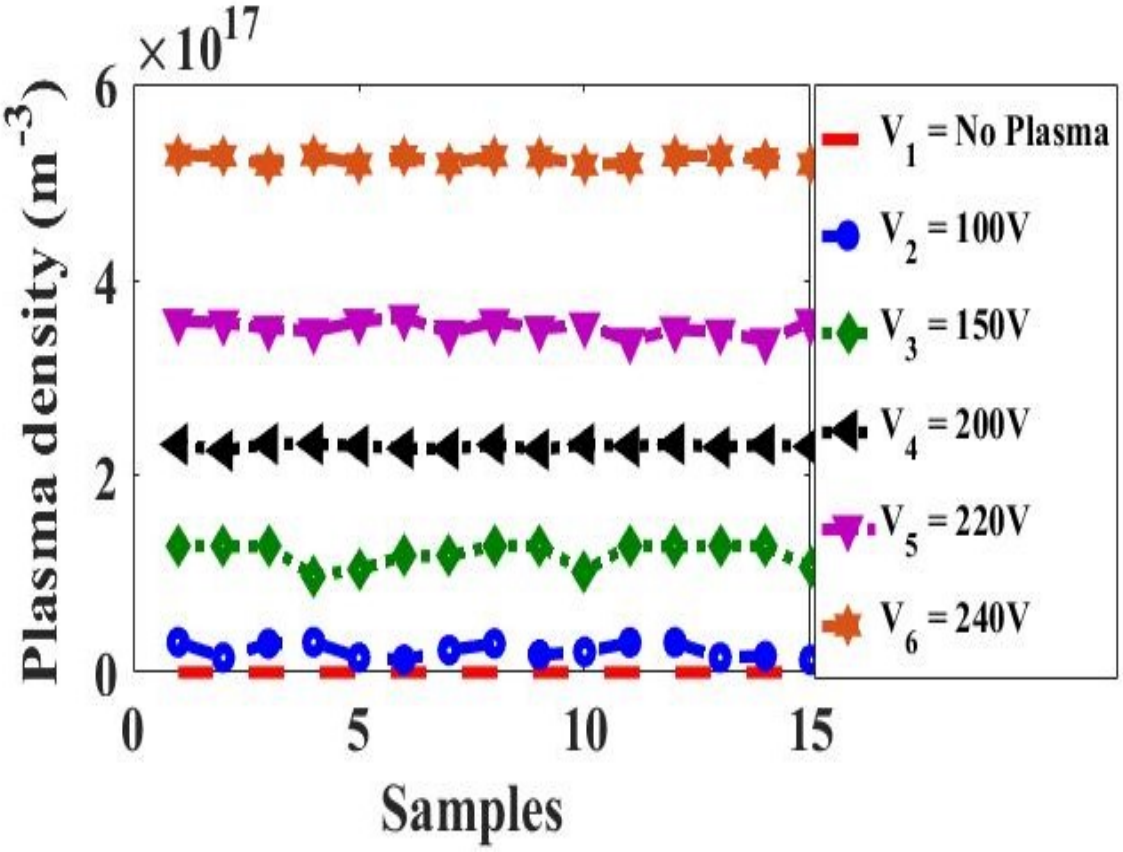

Figure 6.3: Plot of plasma density of fluorescent tube for variable voltage supply.

Permittivity below the cut-off frequency, $f_c = \frac{\omega_p}{2\pi}$ is negative. The f_c is variable with plasma density which is given as $1.8 \times 10^9 GHz$, $3.2 \times 10^9 GHz$, $4.4 \times 10^9 GHz$, $5.4 \times 10^9 GHz$ and

$6.7 \times 10^9 GHz$ for the measured plasma densities.

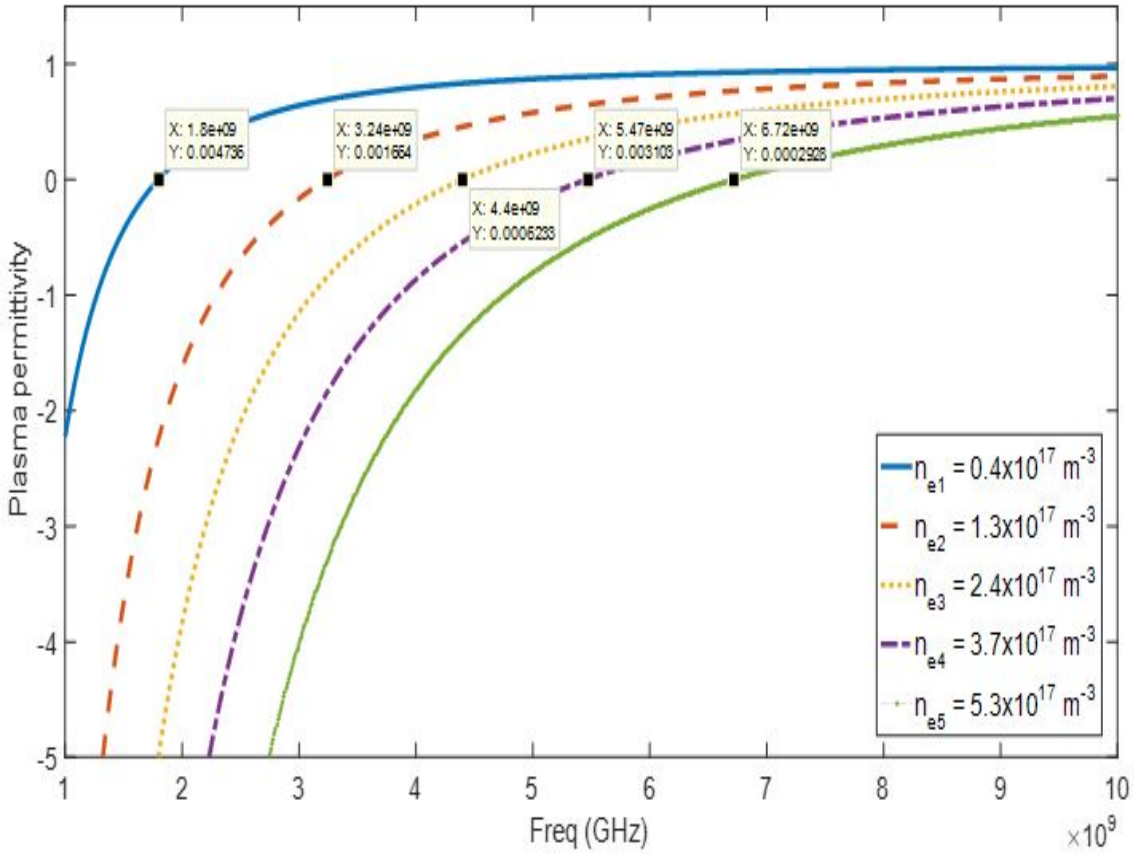

Figure 6.4: Real part of plasma permittivity for variable plasma density

In the negative region, waves in plasma do not propagate. However, waves with certain frequencies can propagate in the PPCs due to the local resonance associated with the surface plasmon wave called Fano-mode [62, 64, 67]. The bandgap is mainly observed in the positive region where the waves in a certain frequency range are forbidden to propagate through the PPCs due to the periodic scattering from the plasma surface[63, 71, 74].

6.2.3 Dispersion Relation of PPC

The bandgap of the PPC structure has been analysed using the dispersion relation given by eq. 6.15. The dispersion relation is simply presenting a plot between the wavenumber ($kd/2\pi$) and frequency. Fig. 6.5 and Fig. 6.6, show the dispersion characteristics of developed PPC which have been characterised with variable plasma density and lattice constant respectively. Photonic Bandgaps (PBG) obtained from the mathematical analysis for different plasma densities and lattice constants are given in Table-6.1

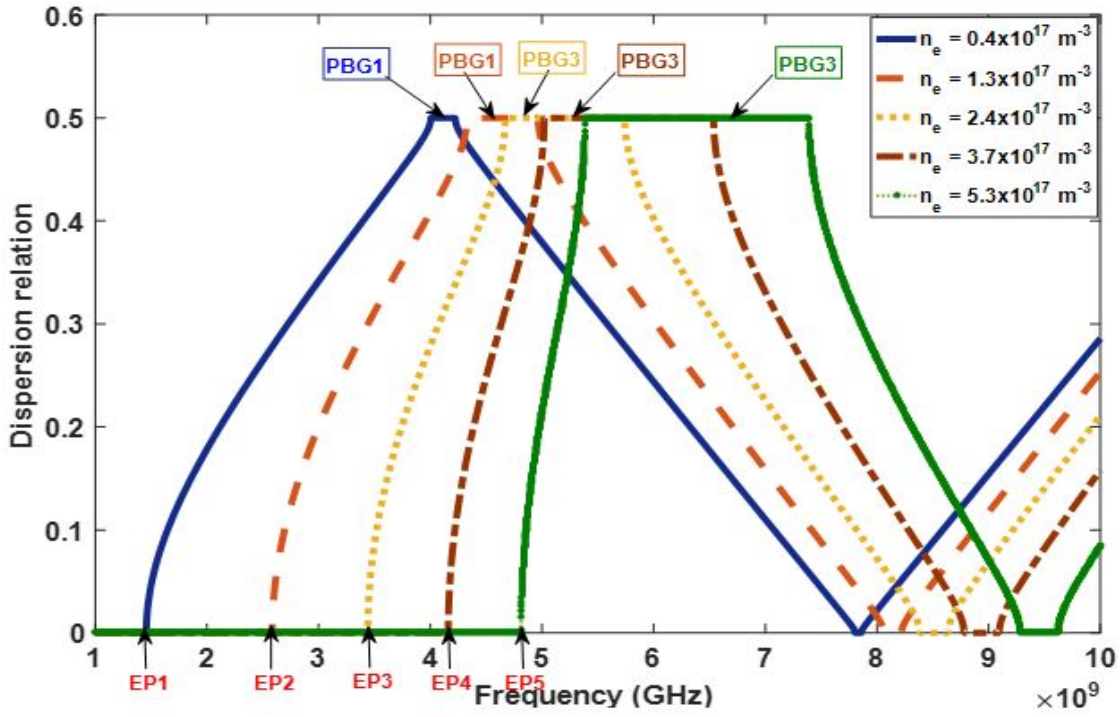

Figure 6.5: Dispersion relation of PPC with variable plasma density ($\epsilon_r = 1$,$d_r = 13mm$,$d_t = 26mm, \Delta = 39mm$)

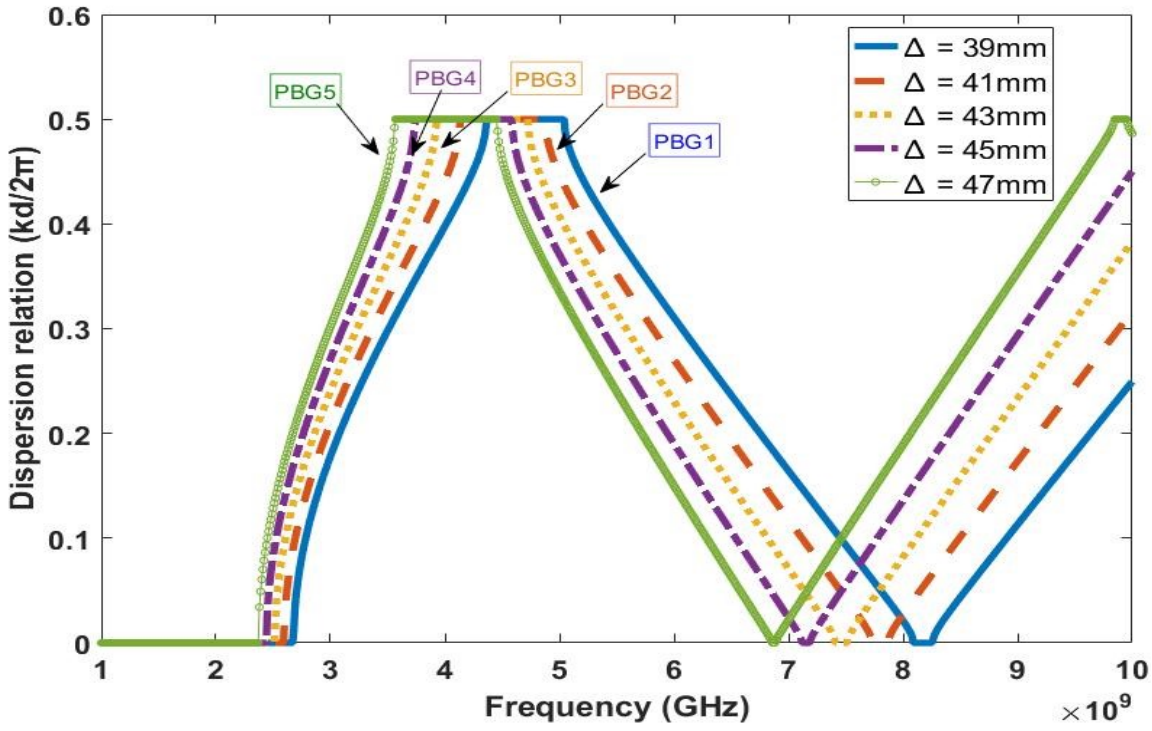

Figure 6.6: Dispersion relation characteristics of PPC for variable lattice constant($\epsilon_r = 1$,$d_r = (13 - 21mm)$,$d_t = 26mm$)

Sr. No.	n_e	PBG	Δ	PBG
1.	$0.4 \times 10^{17} m^{-3}$	0.3GHz	39mm	0.4GHz
2.	$1.3 \times 10^{17} m^{-3}$	0.8GHz	41mm	0.6GHz
3.	$2.4 \times 10^{17} m^{-3}$	1.6GHz	43mm	0.8GHz
4.	$3.7 \times 10^{17} m^{-3}$	2.4GHz	45mm	1.1GHz
5.	$5.3 \times 10^{17} m^{-3}$	2.7GHz	47mm	1.4GHz

Table 6.1: PBG for plasma density and lattice constant

It can be observed from the measured value presented in Table 6.1 that the bandgap is tunable with plasma density as well as lattice constant in a similar manner. At plasma density $0.4 \times 10^{17} m^{-3}$ for fixed lattice constant $\Delta = 39mm$, the photonic bandgap of $0.3GHz$ is obtained. As plasma density increases to $5.3 \times 10^{17} m^{-3}$, PBGs are shifted towards higher frequencies and photonic bandgap of $2.7GHz$ has been obtained.

On other hand, in the case of lattice constant the photonic bandgap is shifted towards lower frequency with the increase in spacing between tubes. For instant, at $\Delta = 39mm$, the photonic bandgap of $0.4GHz$ is observed in the frequency range $4.6GHz$ - $5.0GHz$ whereas at $\Delta = 47mm$, the bandgap is shifted to lower frequency where $1.4GHz$ of bandgap is obtained in the $3.5GHz - 4.4GHz$. It is difficult to change the lattice constant because we have to change the physical structure whether plasma density is electrically reconfigurable. Hence, we reconfigure the photonic bandgap with the applied potential $(100 - 240V)$ at fluorescent tube input. The theoretically analysis of PPC has been verified by implementing the structure and measured its bandgap characteristics which are explained in next section.

6.3 Experimental Setup and Test Results

6.3.1 Experimental Setup

The schematic of the experimental setup of PPC is shown in Fig. 6.7. It consists a square lattice of a 3 × 3 array of fluorescent tubes periodically placed with a lattice constant, $\Delta = 39mm$. Tube array utilizes the $600mm$ long $TD-8$ Philips's tubes with inner diameter and outer diameter of $26mm$ and $30mm$ respectively.

Two linearly polarised array (LPDA) antennas operating in the range of $2 - 18GHz$ are placed across the PPC, which are terminated with VNA for the measurement of the scattering parameters. To avoid external interference, the setup is completely shielded using pyramid shaped absorbers. To get the variable plasma density, tubes are supplied with a variable voltage AC power supply $(10V - 240V)$. A photograph of the developed experimental setup is shown in Fig. 6.8. The figure shows the fluorescent tubes without plasma and with plasma PPC structure. The PPC structure is implemented on test bench.

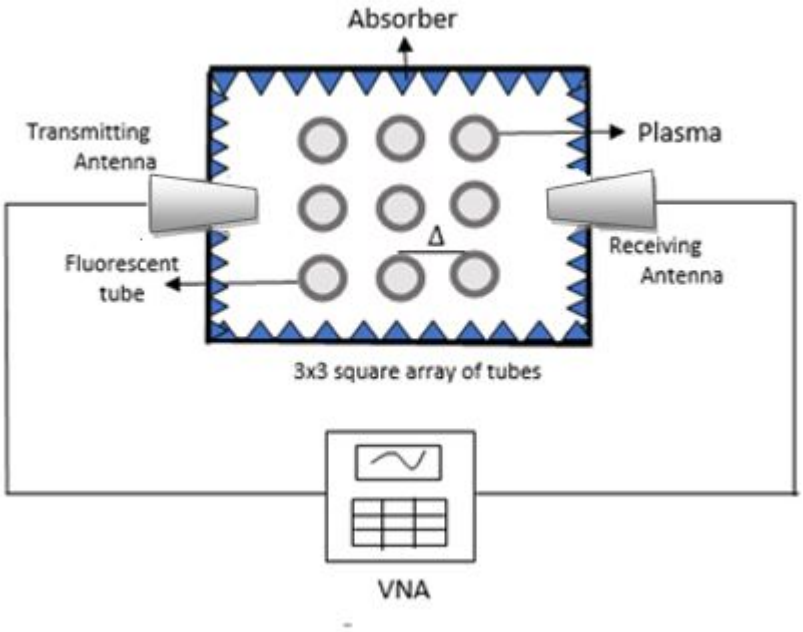

Figure 6.7: Schematic of experimental setup of plasma photonic crystal

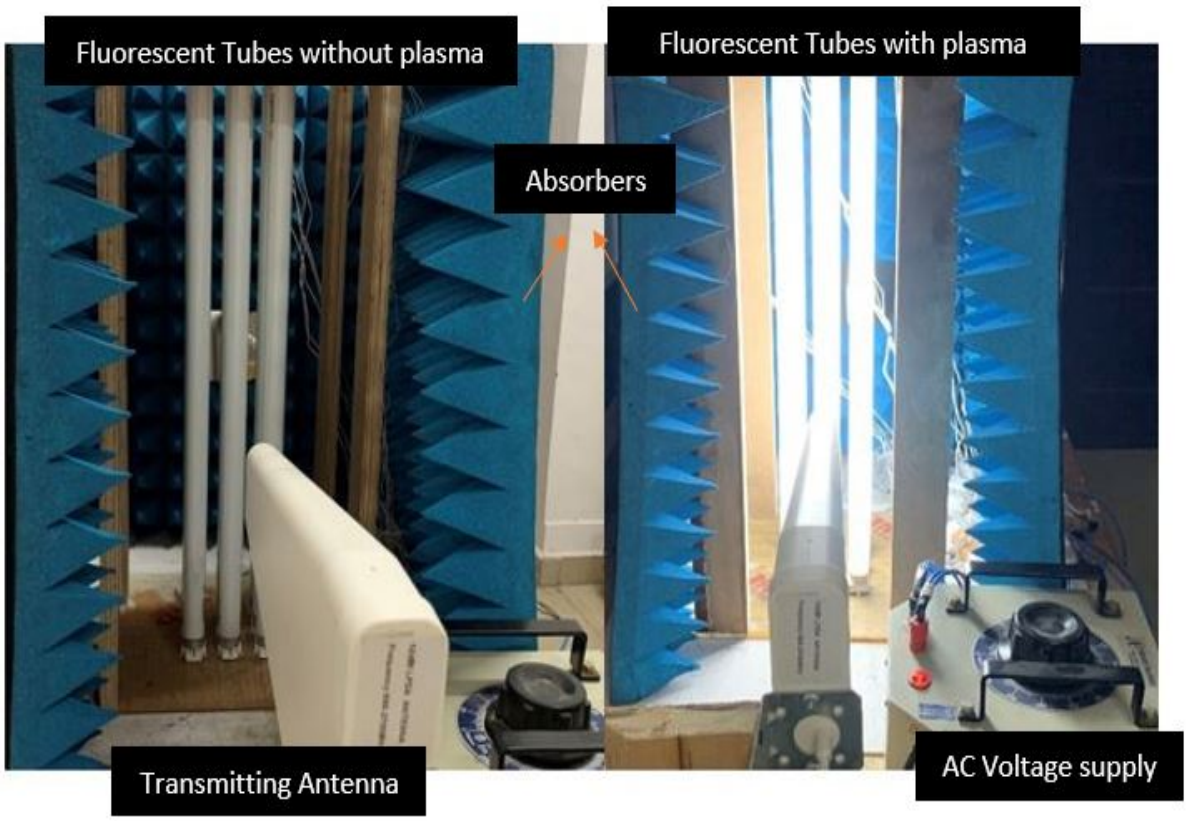

Figure 6.8: Photograph of the developed experimental setup of plasma photonic crystal using TD-8 fluorescent tubes

.

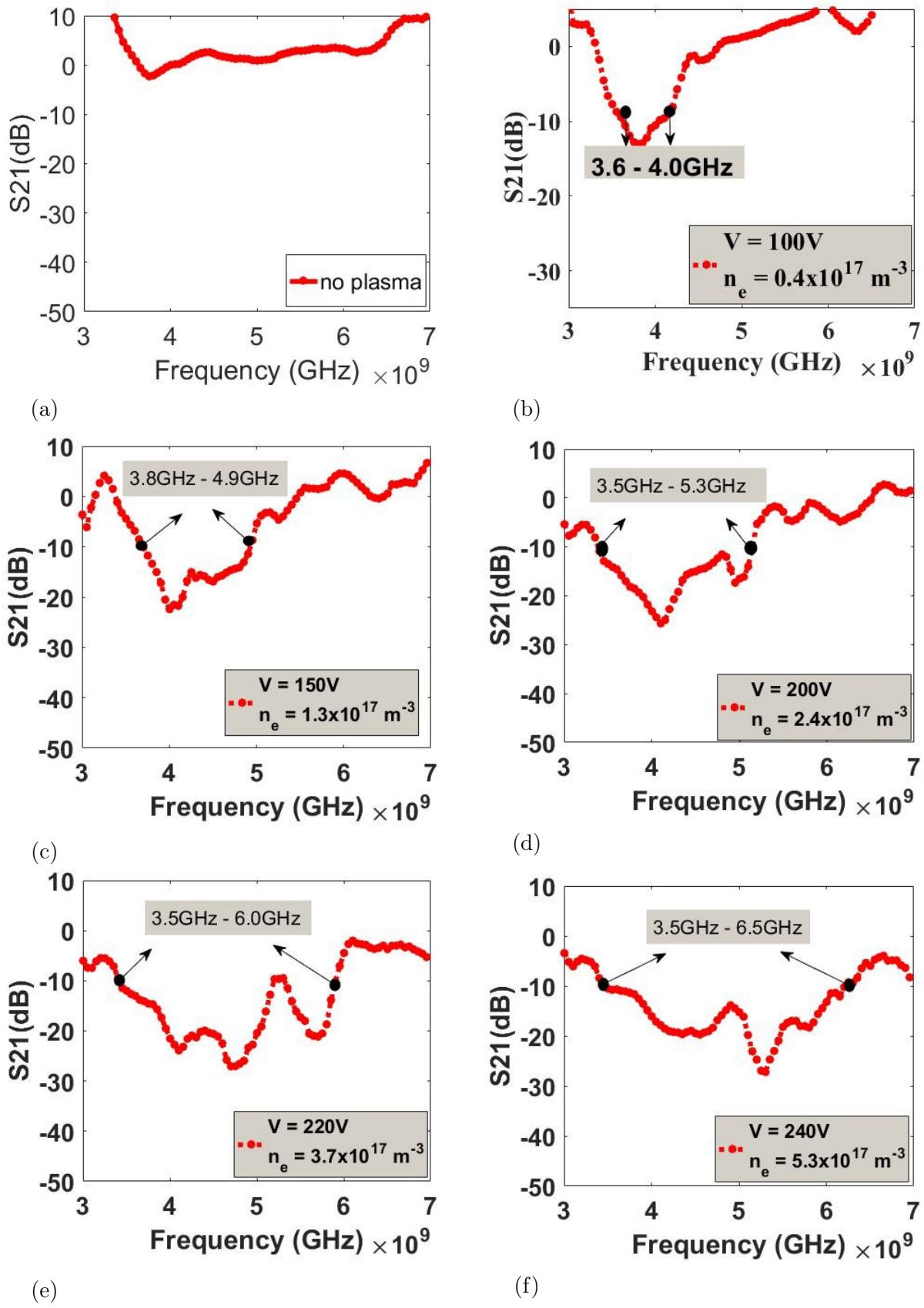

Figure 6.9: Photonic bandgaps of $2D$ PPC for variable parameters (a) V = no plasma (b)$V = 100V$, $ne = 0.4 \times 10^{17}m^{-3}$ (c) $V = 150V$, $ne = 1.3 \times 10^{17}m^{-3}$ (d) $V = 200V$, $ne = 2.4 \times 10^{17}m^{-3}$ (e) $V = 220V$, $ne = 3.7 \times 10^{17}m^{-3}$ (f) $V = 240V$, $ne = 5.3 \times 10^{17}m^{-3}$

6.3.2 Test Results

Transmission scattering parameters, S_{21} of PPC have been measured using VNA for different plasma densities across the variable voltage. The S_{21} for different plasma frequencies are shown in Fig. 6.9a-6.9f. The Fig. 6.9a presents S_{21} in case of no plasma means no voltage is provided to the tubes whereas Fig. 6.9b - 6.9f shows the S_{21} at plasma densities, $0.4 \times 10^{17}m^{-3}$, $1.3 \times 10^{17}m^{-3}$, $2.4 \times 10^{17}m^{-3}$, $3.7 \times 10^{17}m^{-3}$ and $5.3 \times 10^{17}m^{-3}$ for the voltage range $(100V - 240V)$ respectively. The bandgap along with the plasma density is given in Table 6.2.

Sr. No.	Input Voltage (V)	Plasma density (n_e)	Bandgap
1.	100	$0.4 \times 10^{17}m^{-3}$	0.4GHz
2.	150	$1.3 \times 10^{17}m^{-3}$	1.1GHz
3.	200	$2.4 \times 10^{17}m^{-3}$	1.8GHz
4.	220	$3.7 \times 10^{17}m^{-3}$	2.5GHz
5.	240	$5.3 \times 10^{17}m^{-3}$	3.1GHz

Table 6.2: PBG for different plasma densities

The transmission (S_{21}) below $-10dB$ can be considered as a band gap. Test results verify our estimated outcomes as per the Table-6.1. The plot shown in Fig. 6.9a the measured S_{21} parameter when no plasma is formed which is considered as a reference for the analysis. As shown in Fig. 6.9b, when the voltage source is set at $100V$ and tube lights glow with the density $n_e = 0.4 \times 10^{17}m^{-3}$, then a bandgap is formed in the range of $3.6GHz - 4GHz$. As the voltage increases to $200V$ density of tubes becomes double, $n_e = 2.4 \times 10^{17}m^{-3}$, the bandgap of $1.8GHz$ has appeared in the range of $3.5GHz - 5.3GHz$. In case voltages are increased to $240V$, and corresponding density changed up to $n_e = 5.3 \times 10^{17}m^{-3}$, then the bandgap becomes widened and shifted towards a higher side in the frequency range $3.5GHz - 6.5GHz$ which can be seen in Fig. 6.9f. The experimental measurement provides stopbands/bandgaps which are found in good agreement with the estimated outcomes as shown in Fig. 6.5. The tunability in photonic bandgaps for variable plasma density enables the structure as a reconfigurable 2D photonic crystal device.

summary

The design and development of $2D$ Plasma Photonic Crystal (PPC) are presented in this chapter. It is fabricated using a low-pressure fluorescent tube ($TD - 8$). Plasma density inside the tube is found to be variable ($0.4 \times 10^{17}m^{-3} - 5.3 \times 10^{17}m^{-3}$) with applied potential ($100 - 240V$) at tube input. It is measured using the interferometer technique. Based on the received plasma parameter, an experimental setup for PPC is designed. Photonic

Bandgaps (PBG) of the designed PPC has been investigated using mathematically modelling where reconfigurability of PBG with plasma density and lattice constant is estimated. The developed PPC is tested using VNA where results are found per the estimate. Our investigation characterised plasma-based structures for a photonic bandgap which can be useful for fabrication of reconfigurable $2D/3D$ microwave reflector, absorbers, filters etc.

Chapter 7

Conclusion and Future Scope

7.1 Conclusion

This thesis presents the design and development of plasma based antenna and photonic crystal device. Plasma is a kind of medium where its properties can be tuned by changing the operating input parameters. The usage of plasma in antenna and photonic crystal device enable the option to electronically reconfigurable the physical properties of the device. The developed 30cm long plasma antenna has been developed at given pressure $P_r = 0.03mbar$ and applied RF power $P_0 = 50Watts$ with plasma density profile $n_e = 2.7 \times 10^{16}m^{-3}$ inside the column. The plasma column antenna is investigated for its radiation characteristics at three resonant frequencies i.e. $112MHz$, $347MHz$ and $409MHz$. In lead to this, plasma based collinear antenna array has been developed using classical state of plasma called plasma blobs or striations. Two model of plasma antenna array is developed based on 4 and 5 blobs with plasma density profile, $n_e = 2.47 \times 10^{16}m^3$ and $5.85 \times 10^{16}m^3$ respectively. The radiation characteristics of the plasma antenna array having 4 and 5 plasma blobs have been investigated at resonant frequencies i.e. $56MHz, 73MHz, 178MHz$ and $390MHz$. The findings reveals that the radiation patterns show significant change for plasma properties. Moreover, study also explores that the classical state of plasma behaving as an antenna array which improves the radiation characteristics in terms of directivity, intensity and beamwidth of radiation in comparison with continues plasma column antenna. Additionally, radiation measurement system has been developed which is novel approach to measured the radiation pattern in elevation and azimuthal plane.

Further, a novel model of plasma photonic crystal using single column called SC-PPC has been developed which is presented in thesis for the very first time. The developed SC-PPC is formed by having 6 stationary Standing Plasma Density Patterns (SPDP) in a column called plasma blobs and investigated its photonic bandgaps for variable plasma density$(n_e) = 1 \times 10^{16}m^{-3}$, $5 \times 10^{16}m^{-3}$ and $9 \times 10^{16}m^{-3}$ shape and size of blobs. The reconfiguribility in photonic bandgaps have been observed which verify the SC-PPC structure as bandgap device. The additional features of SC-PPC over conventional PPC are its small in size, tunable lattice constant, and simple structure. Further, a two dimensional reconfigurable photonic bandgap (PBG) structure using 3×3 array of fluorescent tubes has been developed. The 2D PPC structure is tested for bandgap analysis by varying plasma densities ranging from $0.4 \times 10^{17}m^3 5.3 \times 10^{17}m^3$ and lattice constant $\Delta = 39mm - 47mm$. The study explore

that the photonic bandgap are the function of plasma properties which can been reconfigured as per desired.

The main objective of presented work in this thesis is to conceptualize a reliable plasma-based structure for the development of RF/microwave devices like antenna, photonic crystal which can have important applications in the field of ranging from communication, defence, homeland security etc.

7.2 Future Scope

- The study presented in this thesis is related to the design and development of plasma based antenna and photonic device. Plasma based technology is research interest due to its interesting and innovative properties. Applicability of plasma make the reconfigurable device by varying its plasma properties.
- In developing reconfigurable RF/microwave devices like filters, absorbers, amplifiers, switches etc., the developed experimental setup of plasma column can be used to explore more plasma properties and analyse its impact on the physical properties of the device.
- The Standing Plasma Density Pattern (SPDP) is a unique form of plasma. In this thesis, it has been utilised for the plasma antenna array and photonic crystal applications. Measuring the density of SPDP is a bit of a challenging task. To investigate the density profile, the advanced level of the interferometer system is required to be developed.
- For wave transmission in SC-PPC, a waveguide with different mode transitions is required to develop which is a challenging task. The setup of a plasma column having SPDP can be considered to develop the reconfigurable waveguide cavity for the SC-PPC.
- The developed setup of plasma blobs in a single column is a unique behaviour of plasma which can also be utilised to explore the blob properties for a wide range of applications in the field of optical communication.
- The developed setup of radiation measurement is a novel system which can also be used to measure elevation and azimuthal profile of other antenna radiation characteristics.
- The developed system can be considered for plasma-based devices in the field of ranging from communication to defence.

Bibliography

[1] R. Kumar, S. V. Kulkarni, D. Bora, "Experimental Study of Parameter of Plasma Antenna," *Plasma science and technology,* vol. no. 12, 2010.

[2] A. Zhu, Z. Chen, J. Lv, "Reconfigurable Characteristics of the Monopole Plasma Antenna and its Array Driven by Surface Wave," *WSEAS Transaction on Communications*, Issue 4, vol. 12, 2013.

[3] J. P. Rayner, A. P. Whichello, A. D. Cheetham, "Physical Characteristics of Plasma Antennas," *IEEE Transactions on Plasma Sciences,* vol. 32, no. 1, pp. 269–281, 2004.

[4] H. Ja'afar, M. T. Ali, N. A. Halili, H. M. Zali, A. N. Dagang, "Analysis and Design between Plasma Antenna and Monopole Antenna," *IEEE International Symposium on Telecommunication Technologies,* 2012.

[5] I. Alexeff, T. Anderson, S. Parameswaran, E. P. Pradeep, "Experimental and Theoretical Results with Plasma Antennas," *IEEE Transactions on Plasma Sciences,* vol. 34, no. 2, 2006.

[6] J. Hettinger, "Aerial Conductor for Wireless Signaling and Other Purposes," U.S patent number 1309031, 1919.

[7] H. Ja'afar, M. T. Ali, A. Dagang, H. M. Zali, N. A. Halili, "A Reconfigurable Monopole Antenna with Fluorescent Tubes Using Plasma Windowing Concepts for 4.9-GHz Application," *IEEE Transactions on Plasma Science*, vol. 43, no. 3, pp. 815-820, 2015.

[8] U. S. Inan, M. Gokowski, "Principles of Plasma Physics for Engineers and Scientists," *Cambridge University Press*, Dec. 2010

[9] F. F. chen, "Introduction to plasma physics and controlled fusion," *Plenum Press*, London, 1984.

[10] J. A. Bittencourt, "Fundamentals of plasma physics, Springer Science Business Media," 2013.

[11] Y. Lee, and S. Ganguly, "FDTD Analysis of a Plasma Column Antenna," IEEE, International Symposium on Antennas and Propagation Society, vol.1B, no., pp.430-433, 2005.

[12] P. Russo, G. Cerri, and E. Vecchioni, "Self-Consistent Analysis of Cylindrical Plasma Antennas," IEEE Transactions on Antennas and Propagation, vol. 59, no. 5, pp. 1503-1511, 2011.

[13] F. Sadeghikia, and F. Hodjat-Kashani, "A Two Element Plasma Array," ETASR, Engineering, Technology and Applied Science Research, vol. 3, 2013.

[14] G. G. Borg, J. H. Harris, N. M. Martin, D. Thorncraft, R. Milliken, D. G. Miljak, B. Kwan, T. Ng, and J. Kircher, "Plasmas as antennas: Theory, experiment and applications," Physic Plasmas, vol. 7, pp. 2198 -2202, 2000.

[15] S. Dine, J-P Booth, G. A Curly, C. S. Corr, J. Jolly and J. Guillon, "A Novel Technique for Plasma Density Measurement using Surface Wave Transmission Spectra," Plasma Sources Sciences Technologies, IOP Publication, vol. 14, pp. no. 777-786, 2005.

[16] G. Cerri, V. M. Primiani, P. Russo, and E. Vecchioni, "Measurement of the Properties of a Plasma Column used as a Radiating Element," IEEE Transactions on Instrumentation and Measurement, vol. no. 57, 2008.

[17] T. Natio, S. Yamaura, Y. Fukuma, and O. Sakai, "Radiation Characteristics of Input Power from Surface Wave Sustained Plasma Antenna," Physic of Plasma, AIP Publications, vol. no. 23, 2016.

[18] N. A. Halili, M. T. Ali, H. M. Zali, H. Ja'afar, and I. Pasya, "A Study on Plasma Antenna Characteristics with Different Gases," International Symposium on Telecommunication Technologies (ISTT), vol., no., pp. 56-59, 26-28 Nov. 2012.

[19] L. Zheng, L. Cao, and Z. Zhang, "Study on the Gain of Plasma Antenna," International Symposium on Antennas, Propagation and EM Theory, ISAPE pp. 222-224, Nov. 2008.

[20] J. Zhou, J. Fang, Q. Lu, and F. Liu, "Research on Radiation Characteristic of Plasma Antenna through FDTD Method," The Scientific World Journal, vol. no. 290148, 2014.

[21] Z. H. Qian, R. S. Chen, H. W. Yang, K. W. Leung, and K. N. Yung, "FDTD Analysis of a Plasma Whip Antenna," IEEE, International Symposium on Antennas and Propagation Society, vol. 2B, pp. 166-169, 2005.

[22] L. Chao, X. Yue-Min, and W. Zhi-Jiang, "Numerical Simulation of Plasma Antenna using FDTD Method," Chinese Physics Lett. vol. 25, no. 10, pp. 3712, 2008.

[23] F. Luo, and B. J. Hu, "FDTD Analysis for Radiated Performance of a Cylinder Plasma Antenna," International Symposium on Antennas, Propagation and EM Theory, ISAPE, pp.803-806, 2 Nov. 2008.

[24] H. M. Zali, M. T. Ali, N. A. Halili, H. Ja'afar, and I. Pasya, "Design of a Cylindrical Parabolic Reflector on Monopole Plasma Antenna," IEEE Transactions International RF and Microwave Conference, Dec. 2013.

[25] P. Darvish, A. B. Gorji, and B. Zakeri, "Design, Simulation and Implementation of a Pre-ionized Coupled Plasma Antenna at VHF Band," Proceedings of 2013 URSI International Symposium on Electromagnetic Theory (EMTS), vol., no., pp.452-455, 20-24 May 2013.

[26] D. C. Jenn, "Plasma Antennas: Survey of Techniques and the Current State of the Art," NPS, California, Sep 2003.

[27] G. G. Borg, J. H. Harris, D. G. Miljak, and N. M. Martin, "Application of plasma columns to radiofrequency antennas," Applied Physics Letters, vol. 74, no. 22, p. 3272, 1999.

[28] C. A. Balanis, "Antenna Theory: Analysis and Design," 2nd ed. Hoboken, NJ, USA: Wiley, pp. 772–776,1999.

[29] A. Taflove, "Computational electrodynamics: The finite-difference time-domain method," Artech House, Boston, 1995.

[30] T. Anderson, "Plasma Antenna," Artech House, Boston, 2011.

[31] ASI Technology Corporation web page: http://www.asiplasma.com.

[32] https://www.scribd.com/doc/63560119/Plasma-Antenna.

[33] http://www.slideshare.net/aijazgr/plasma-antenna-report.

[34] A. Aurius, "The fourth state of matter" [Online]. Available: http://cidocido.hubpages.com/hub/They-taught-you-wrong-theres-way-more than-solid-liquid-gas.

[35] Z. Zakrzewski, M. Moisan, V. M. M. Glade, C. Beaudry and P. Leprince, "Attenuation of a surface wave in an unmagnetized RF plasma column," Plasma Physics, vol. 19, pp. 77, 1977.

[36] K. Hanada, H. Zushi, N. Yoshida, N. Yugami, T. Honda, M. Hasegawa, K. Mishra, A. Kuzmin, K. Nakamura, A. Fujisawa, H. Idei, Y. Nagashima, O. Watanabe, T. Onchi, H. Watanabe, K. Tokunaga, A. Higashijima, S. Kawasaki, H. Nakashima, Y. Takase, A. Fukuyama, O. Mitarai, Y.K.M. Peng, Particle balance in long duration RF driven plasmas on QUEST, Journal of Nuclear Materials, Volume 463, 2015, Pages 1084-1086,

[37] C. M. Ferreira, and J. Loureiro, "Electron energy distributions and excitation rates in high-frequency argon discharges" Journal of Physics D:Applied Physics, vol. 16, pp. 2471 (1983).

[38] M. Moisen and Z. Zakrzewski, "New surface wave launchers for sustaining plasma columns at submicrowave frequencies (1–300 MHz)" Rev. Sci. Instrum., vol. 58, pp. 1895, 1987.

[39] M. Moisan and Z. J. Zakrzewski, "Plasma sources based on the propagation of electromagnetic surface waves" J. Phys. D:Appli. Phys., vol. 24, pp. 1025, 1991.

[40] D. Melazzi, P. D. Carlo, F. Trezzolani, M. Manente, A. D. Capobianco, and S. Boscolo, "Beamforming capabilities of a plasma circular reflector antenna," IET Microwave Antenna Propagation, pp. 1-7, 2018.

[41] M. Laroussi and J. R. Roth, "Numerical calculation of the reection, absorption, and transmission of microwaves by a nonuniform plasma slab," IEEE Transactions on Plasma Science, vol. 21, no. 4, pp. 366-372, 1993.

[42] R. Kumar, S. V. Kulkarni, and D. Bora, "Study of array plasma antenna parameters," AIP ADVANCES,American Institute of Physics, vol. no. 8, 2018.

[43] M. T. J. Tajudin, "Study and design of recongurable antennas using plasma medium," Ph.D. dissertation, Universite Rennes 1, 2014. [Online]. Available: https://hal-univ-rennes1.archives-ouvertes.fr/tel-01060295/

[44] F. Sadeghikia, M. T. Noghani, and M. R. Simard, "Experimental study on the surface wave driven plasma antenna," International Journal of Electronics and Communications, pp. 652-656, 2016.

[45] A. N. Dagang, C. X. Lei, and H. Jaafar, "Study on the effect of a variation types of gas, pressure and coupling sleeves on the performance of monopole plasma antenna," ARPN Journal of Engineering and Applied Sciences, vol. 12 No. 23 pp. 6649-6656, 2017.

[46] H. Jaafar, S. Omar, R. Shafie, R. Abdullah, and N. Ismail, "Simulation study of monopole plasma antenna for 2.4GHz application," Proc. of IEEE Region 10 Conference, Malaysia, pp. 2927-2930, 2017.

[47] T. Anderson, I. Alexe, E. Farshi, N. Karnam, E. P. Pradeep, N. R. Pulasani, and J. Peck, "An operating intelligent plasma antenna," in 2007 16th IEEE International Pulsed Power Conference, vol. 1, pp. 353-356, 2007.

[48] L. Norberti, R. Nebuloni and M. Magarini, "Characterization of the Indoor-to-Outdoor Wireless Channel in Air-to-Ground Communication Systems," 2020 16th International Conference on Wireless and Mobile Computing, Networking and Communications (WiMob), pp. 1-6, 2020.

[49] T. Anderson and I. Alexe, "Theory of plasma antenna windowing," in The 31st IEEE International Conference on Plasma Science, 2004. ICOPS 2004, pp. 328, Jul. 2004.

[50] A. K. Pandey and S. K. Pathak, "Investigation of Dispersion and Radiation Characteristics of Plasma Loaded Helical Antenna," 2021 15th European Conference on Antennas and Propagation (EuCAP), pp. 1-4, 2021.

[51] A. V. Krasavin, P. Segovia, P. Ginzburg and A. V. Zayats, "Surface nonlinearities in plasmonics," 2014 Conference on Lasers and Electro-Optics (CLEO) - Laser Science to Photonic Applications, pp. 1-2, 2014.

[52] R. A. Goldstein, M. A. Huerta, and J. C. Nearing, “Stationary striations in an argon plasma as a bifurcation phenomenon,” AIP Physics of Fluids, vol. 22, 1979.

[53] T. Yamamoto and T. Kobayashi, "A recongurable antenna using fluorescent lamps," in Antennas and Propagation (ISAP), 2014 International Symposium on. IEEE, pp. 89-90, 2014.

[54] H. Ja’afar, M. T. Ali, H. M. Zali, N. A. Halili, and A. N. Dagang, "A monopole fluorescent tube antenna in wireless communication application," in 2013 10th International Conference on Electrical Engineering/Electronics, Computer, Telecommunications and Information Technology (ECTI-CON), pp. 1-5, May 2013.

[55] H. M. Zali, M. T. Ali, N. A. Halili, H. Ja’afar, and I. Pasya, "Study of monopole plasma antenna using fluorescent tube in wireless transmission experiments," in 2012 International Symposium on Telecommunication Technologies (ISTT), pp. 52-55, Nov. 2012.

[56] G. Cerri, R. D. Leo, V. M. Primiani, P. Russo, and E. Vecchioni, "2.45 GHz waveguide plasma generation in cylindrical structures," in Microwave Symposium Digest (MTT), 2010 IEEE MTT-S International, pp. 1032-1035, May 2010.

[57] A. Dounavis, R. Achar and M. Nakhla “Efficient Sensitivity Analysis of Lossy Multiconductor Transmission Lines with Nonlinear Terminations”, IEEE Transactions on Microwave Theory and Techniques, vol. 49, no. 12, pp. 2292-2299, Dec 2001.

[58] A. Patel and S. K. Pathak, "Numerical Study on the Effect of Plasma Density on Runaway Electron Suppression in the ADITYA-U Tokamak," in IEEE Transactions on Plasma Science, doi: 10.1109/TPS.2022.3152082.

[59] M. T. Jusoh, O. Lafond, F. Colombel, and M. Himdi, "Performance of a Recongurable Re ector Antenna with Scanning Capability Using Low Cost Plasma Elements," Microwave and Optical Technology Letters, vol. 55, no. 12, pp. 2869-2874, 2013.

[60] O. A. Barro, "Design and manufacturing reconfigurable antennas using plasma," Ph.D. dissertation, Universite Rennes 1, 2016.

[61] H. Jaafar, M. T. Ali, A. N. Dagang, I. P. Ibrahim, N. A. Halili, and H. M. Zali, "Recongurable Plasma Antenna Array by Using Fluorescent Tube for Wi-Fi Application," Radioengineering, vol. 25, no. 2, pp. 275-282, 2016.

[62] L. Zhang and J. T. Ouyang, "Experiment and simulation on one-dimensional plasma photonic crystals," AIP Physics of plasma, vol. 21, no. 10, Oct. 2014.

[63] H. Tan, C. Jin, L. Zhuge, and X. Wu, "Simulation on the Photonic Bandgap of 1-D Plasma Photonic Crystals," IEEE Transactions on plasma science, vol. 46, no. 3, 2018.

[64] H. Hojo and A. Mase, "Dispersion relation of electromagnetic waves in one-dimensional plasma photonic crystals," J. Plasma Fusion Res., vol. 80, no. 2, pp. 89–90, 2004.

[65] H. Hojo and A. Mase, "Electromagnetic-wave transmittance characteristics in one-dimensional plasma photonic crystals," J. Plasma Fusion Res., vol. 8, pp. 477–479, 2009.

[66] B. Guo, M. Q. Xie, X. M. Qiu, and L. Peng, "Photonic band structures of 1-D plasma photonic crystal with time-variation plasma density," Phys. Plasmas, vol. 19, no. 4, 2012.

[67] L. Qi, L. Shang, and S. Zhang, "One-dimensional plasma photonic crystals with sinusoidal densities," Phys. Plasmas, vol. 21, no. 1, 2014.

[68] S. Prasad, V. Singh, and A. K. Singh, "Effect of inhomogeneous plasma density on the reflectivity in one dimensional plasma photonic crystal," Progr. Electromagn. Res. M, vol. 21, pp. 211–222, 2011.

[69] O. Sakai and K. Tachibana, "Plasmas as metamaterials": A review, Plasma Sources Sci. Technol, vol. 21, no. 2, 2012.

[70] A. Jafari and A. Rahmat, "Band structure of one-dimensional plasma photonic crystals using the Fresnel coefficients method," Indian J. Phys., vol. 91, no. 4, pp. 453–460, 2017.

[71] T. Mittal, R. P. Yadav, D. Bora, "Analysis of trapped oscillation modes in magnetized PPC and its tunability for variable plasma parameters," Optics Communications 382, pp. 7–12, 2017.

[72] P. Ginzburg, P. V. Kapitanova, G. Marino "Near-field interference in optics and RF," 2014 Conference on Lasers and Electro-Optics (CLEO) - Laser Science to Photonic Applications, pp. 1-2, 2014.

[73] B. Wang and M. A. Cappelli, "A tunable microwave plasma photonic crystal filter," Appl. Phys. Lett., vol. 107, no. 17, 2015.

[74] B. Guo, M. Q. Xie, and L. Peng, "Photonic band structures of one dimensional photonic crystals doped with plasma," Phys. Plasmas, vol. 19, no. 7, 2012.

[75] B. Wang and M. A. Cappelli, "A plasma photonic crystal bandgap device," Appl. Phys. Lett., vol. 108, no. 16, 2016.

[76] X. k. Kong, S. b. Liu, H. F.Zhang, H. l. Guan, "The effect of random variations of structure parameters on photonic band gaps of one-dimensional plasma photonic crystals," Optics Communications, 284, pp. 2915-2918, 2011.

[77] H. F. Zhang, S. B. Liu X. k. Kong, B. Bian, H. Zhao, "Properties of omnidirectional photonic bandgap in one-dimensional staggered plasma photonic crystals," Optics Communications 285, pp. 5235-5241, 2012.

[78] Y. Yin, H. Xu, M. Y. Yu, Y. y. Ma, H. B. Zhuo, C. l. Tian, "Bandgap characteristics of one-dimensional plasma photonic crystal," Physics of plasma vol. 16, pp. 102-103, 2009.

[79] J. C. Knight, "Photonic crystal fibres," Nature, vol. 424, no. 6950, pp. 847–851, 2003.

[80] M. K. Howlader, Yunqiang Yang and J. R. Roth, "Time-resolved measurements of electron number density and collision frequency for a fluorescent lamp plasma using microwave diagnostics," IEEE Transactions on Plasma Science, vol. 33, no. 3, pp. 1093-1099, June 2005.

[81] Z. Yao, J. Luo, and Y. Lai, "Photonic crystals with broadband, wideangle, and polarization-insensitive transparency," Opt. Lett., vol. 41, no. 21, pp. 5106–5109, 2016.

[82] I. Andonegui and A. J. Garciaadeva, "The finite element method applied to the study of two-dimensional photonic crystals and resonant cavities," Opt. Exp., vol. 21, no. 4, pp. 4072–4092, 2013.

[83] V. I Kolobov, "Striations in rare gas plasmas," Journal of Physics D: Applied Physics, vol. no. 39, pp. no. R487–R506, Dec. 2006.

[84] L. Shiveshwari and P. Mahto, "Photonic band gap effect in one-dimensional plasma dielectric photonic crystals," Solid State Commun., vol. 138, no. 3, pp. 160–164, 2006.

[85] T. Sakaguchi, O. Sakai, and K. Tachibana, "Photonic bands in two-dimensional microplasma arrays. II. Band gaps observed in millimeter and subterahertz ranges," J. Appl. Phys., vol. 101, no. 7, p. 073305, 2007.

[86] B. Guo and X.-M. Qiu, "Formation of a plasma photonic crystal by selfinduced quasi periodic plasma density grating," J. Electromagn. Waves Appl., vol. 25, nos. 5–6, pp. 785–794, 2011.

[87] S. Liu, W. Hong, and N. Yuan, “Finite-difference time-domain analysis of unmagnetized plasma photonic crystals,” Int. J. Infr. Millim. Waves, vol. 27, no. 3, pp. 403–423, 2006.

[88] B. Guo and X.-M. Qiu, “Differential transfer matrix method for photonic band structure of one dimensional non-uniform distribution plasma photonic crysta,” Optik-Int. J. Light Electron Opt., vol. 123, no. 15, pp. 1390–1392, 2012.

[89] O. Sakai, T. Sakaguchi, and K. Tachibana, “Photonic bands in two-dimensional microplasma arrays. I. Theoretical derivation of band structures of electromagnetic waves,” J. Appl. Phys., vol. 101, no. 7, pp. 073304, 2007.

[90] O. Sakai, T. Sakaguchi, and K. Tachibana, “Plasma photonic crystals in two-dimensional arrays of microplasmas,” Contrib. Plasma Phys., vol. 47, nos. 1–2, pp. 96–102, 2007.

[91] F. Righetti, B. Wang, and M. A. Cappelli , "Enhanced attenuation due to lattice resonances in a two-dimensional plasma photonic crystal," Physics of Plasmas, vol. 25, pp. 124502, 2018.

[92] O. Sakai, T. Sakaguchi, and K. Tachibana , "Verification of a plasma photonic crystal for microwaves of millimeter wavelength range using two-dimensional array of columnar microplasmas," Appl. Phys. Lett., vol. 87, pp. 241505, 2005.

[93] V. Kumar and M. Kumar, "Photonic crystal assisted multiband compact terahertz antenna on engineered silicon-on-insulator", IEEE-IET Optoelectronics 10 (2016) 7 - 10.

[94] D. Nobahar, K. Hajisharifi, and H. Mehdian , "Twisted beam shaping by plasma photonic crystal," Journal of Applied Physics, vol. 124, pp. 213102, 2018.

[95] M. C. Paliwoda and Joshua L. Rovey , "Multiple parameter space bandgap control of reconfigurable atmospheric plasma photonic crystal," Physics of Plasmas, vol. 27, pp. 023516, 2020.

[96] D. Bora, and R. Kumar, " Design and Development of Plasma Antenna," PhD Thesis, 2010.